INVESTIGATION OF THE DIMER INTERFACE OF CTP:PHOSPHOCHOLINE CYTIDYLYLTRANSFERASE AND ITS MODULATION BY LIPIDS

by

Jillian Smith
B.Sc. (Hon.), Simon Fraser University, 2001

THESIS SUBMITTED IN PARTIAL FULFILLMENT OF
THE REQUIREMENTS FOR THE DEGREE OF

MASTER OF SCIENCE

In the
Department
of
Molecular Biology and Biochemistry

SIMON FRASER UNIVERSITY

Fall 2005

APPROVAL

Name: Jillian Smith

Degree: Master of Science

Title of Thesis: Investigation of the Dimer Interface of CTP: Phosphocholine Cytidylyltransferase and its Modulation by Lipids

Examining Committee:

Chair: **Dr. Nancy Hawkins**
Assistant Professor, Department of Molecular Biology and Biochemistry

---

Dr. Rosemary Cornell
Senior Supervisor
Professor, Department of Molecular Biology and Biochemistry

Dr. Mark Paetzel
Supervisor
Assistant Professor, Department of Molecular Biology and Biochemistry

---

Dr. Frederic Pio
Supervisor
Assistant Professor, Department of Molecular Biology and Biochemistry

---

Dr. Lisa Craig
Internal Examiner
Assistant Professor, Department of Molecular Biology and Biochemistry

Date Defended/Approved: December 1, 2005

ABSTRACT

CTP:phosphocholine cytidylyltransferase (CCT) is the rate-limiting enzyme in phosphatidylcholine synthesis. CCT is an amphipathic homodimer, whose activity is regulated by membrane binding – a process resulting in conformational restructuring of the dimer interface. I used site-directed mutagenesis of domain N lysines in CCT, followed by lysine specific chemical cross-linking in the presence and absence of activating lipids, to locate sites of dimer interactions and to pinpoint where conformational rearrangement occurs. Analysis revealed that none of the lysines in the N-terminus are required for cross-linking. Thus lysine-mediated cross-links involve other CCT domains. I found that CCT 236, despite lacking a membrane-binding domain, appears to undergo conformational changes that disrupt the dimer interface in the presence of activating lipids. The mechanism causing lipid-induced rearrangements of both CCT 367 and CCT 236 dimer interfaces remains unknown, but appear to be different. Moreover, the two CCTs are activated by different lipids suggesting different activation mechanisms.

KEYWORDS: CTP:phosphocholine cytidylyltransferase, dimer interface, lysine, cross-linking

For Bernie and my Family

Thank you for all your love and support

ACKNOWLEDGEMENTS

Above all, I would like to thank my senior supervisor, Rosemary Cornell, for her continued assistance and enthusiasm. Such zest and zeal are potent motivators. Thanks also to my committee members, Drs. Mark Paetzel and Frederic Pio for their time, help and suggestions.

Thanks to all my lab mates, past and present, for being such a great group of people to work with. Special thanks to Theresa Kitos and Joanne Johnson for teaching me so much, and to Melissa Dennis who went from being a good undergrad assistant to a good friend. Thanks also to Becky Thorne, Hani Zaher, Wendy Lee, Kristin McKnight, Laila Singh, Jim Stewart and all of the many friends I made at SFU.

Thanks to all the MBB labs for sharing reagents, equipment and ideas, especially the Paetzel and Verheyen labs. Thanks also to the department staff for their assistance, particularly Duncan Napier.

Finally, thanks to my family, my mom, dad and sister, for their unwavering encouragement and belief in me. Special thanks to my husband Bernie who supported me in every way possible during my studies.

TABLE OF CONTENTS

LIST OF FIGURES

LIST OF TABLES

GLOSSARY

ATP:	adenosine 5'-triphosphate
βME:	β-mercaptoethanol
bp:	base pair
BS^3:	bis[sulfosuccinimidyl] suberate
CCT:	CTP:phosphocholine cytidylyltransferase
CDP:	cytidine 5'-diphosphate
CMP:	cytidine 5'-monophosphate
$Cu(Phe)_3$:	copper $^{2+}$ phenanthroline
CTP:	cytidine 5'-triphosphate
CTAB:	cetyltrimethylammonium bromide
DAG:	diacylglycerol
DEAE:	diethylaminoethyl
DMEM:	Dulbecco's Modified Eagle Medium
DMSO:	dimethyl sulphoxide
DSP:	dithiobis[succinimidylpropionate]
DSS:	disuccinimidyl suberate
DTT:	dithiothreitol
EDTA:	ethylenediaminetetraacetic acid
ER:	endoplasmic reticulum
FBS:	fetal bovine serum
GAR-HRP:	goat anti-rabbit horseradish peroxidase
GCT:	glycerol-phosphate cytidylyltransferase
NEM:	*N*-ethylmaleimide

O or O/A	oleic acid
P:	phosphate
PA:	phosphatidic acid
PAG(E):	polyacrylamide gel (electrophoresis)
PBS:	phosphate buffered saline
PC:	phosphatidylcholine
PG:	phosphatidylglycerol
PCR:	polymerase chain reaction
PE:	phosphatidylethanolamine
PI:	phosphatidylinositol
PMSF:	phenylmethylsulphonylfluoride
PS:	phosphatidylserine
PVDF:	poly(vinylidine difluoride)
SDS:	sodium dodecyl sulphate
Tris:	Tris(hydroxymethyl)methylamine
WT:	wild-type

1 INTRODUCTION

1.1 Phosphatidylcholine, And The Role Of CTP:Phosphocholine Cytidylyltransferase In PC Metabolism

Phosphatidylcholine (PC) is the most abundant phospholipid in mammalian cells. As there are no known diseases caused by defects in PC metabolism,[1] and experiments with a defective PC biosynthetic pathway resulted in apoptosis in CHO cells,[2] it can be concluded that PC is an essential phospholipid. PC has many functions in the cell, such as maintaining the bilayer structure in membranes, aiding in the transport of non-soluble lipids through blood in a lipoprotein complex, and is the main component of pulmonary surfactant, a protein/lipid mixture that reduces surface tension in air:liquid interfaces in the lung. The catabolism of PC by phospholipases yields such products as diacylglycerol (DAG), phosphatidic acid and arachidonic acid, which are important lipid second messengers and function in the transduction of intracellular signals[3,4].

In higher eukaryotic organisms, PC is most commonly biosynthesised via the CDP-choline pathway[5], but can also be synthesized in the liver by the methylation of phosphatidylethanolamine (PE)[6]. PC can be reformed by the recycling of its breakdown products, such as the acylation of lyso PC (Figure 1.1). In bacteria, the methylation of PE is the sole means of PC production, while both pathways exist in yeast.

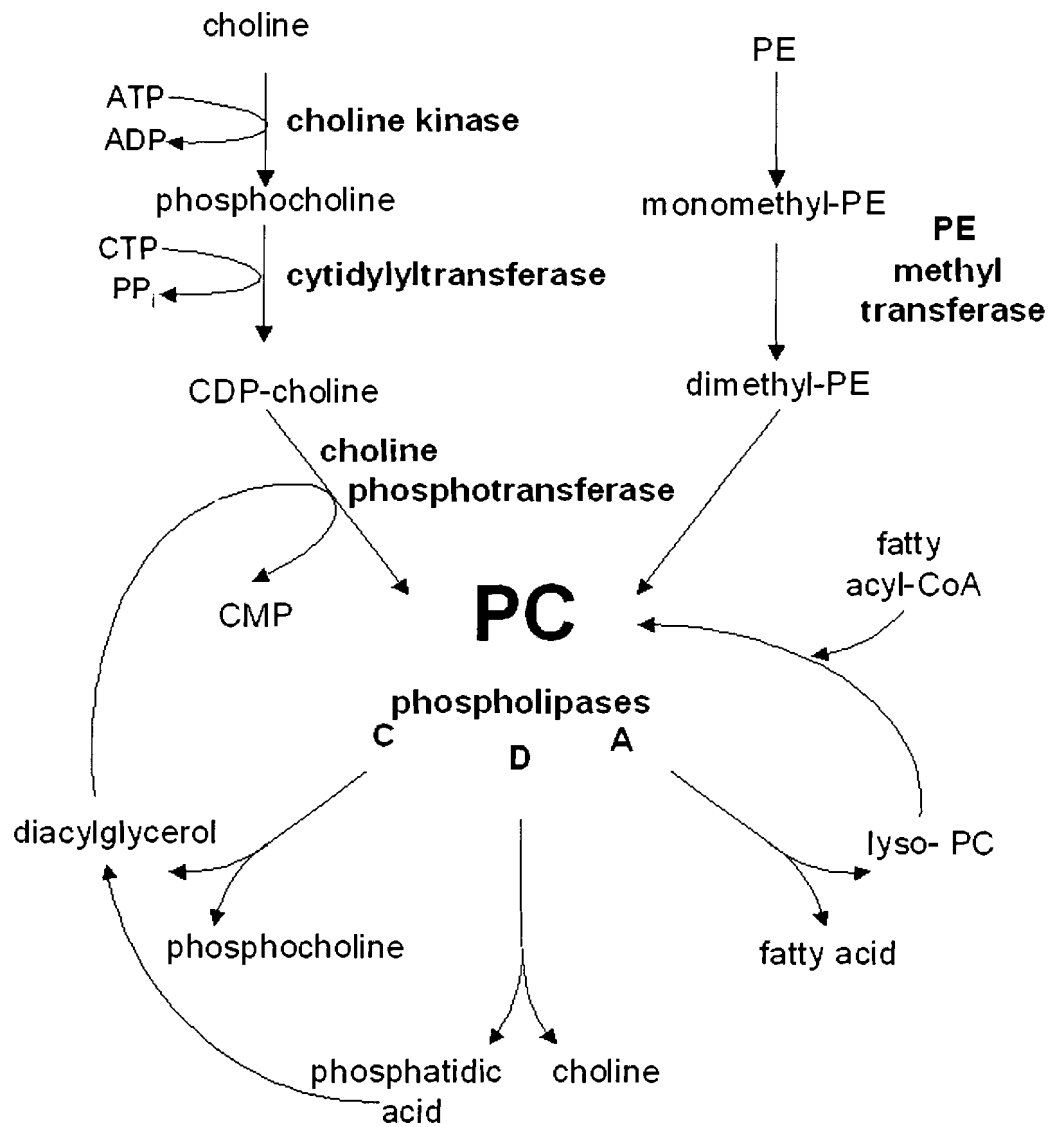

Figure 1.1 PC metabolic pathways

CTP:phosphocholine cytidylyltransferase (CCT) is the rate-limiting enzyme in the CDP-choline pathway for the production of PC. Choline, taken up into the cell by facilitated transport, is immediately phosphorylated by choline kinase to form phosphocholine. CCT then catalyses the transfer of cytidine 5'-mono-phosphate (CMP), from CTP to phosphocholine to produce CDP-choline and pyrophosphate (Figure1.2). Choline phosphotransferase facilitates the condensation of CDP-choline with DAG to generate PC. There is no direct evidence demonstrating protein-protein interactions between the enzymes in this pathway. However, as radiolabeled PC precursors were not incorporated into the synthesis of PC in electropermeabilized glioma cells, and only choline, but not phosphocholine or CDP-choline, was effective at chasing pre-labeled phosphatidylcholine PC in cells, it is supposed that channelling of the intermediates of PC biosynthesis occurs through a multi-enzyme complex of choline kinase, CTP:phosphocholine cytidylyltransferase and choline phosphotransferase[7].

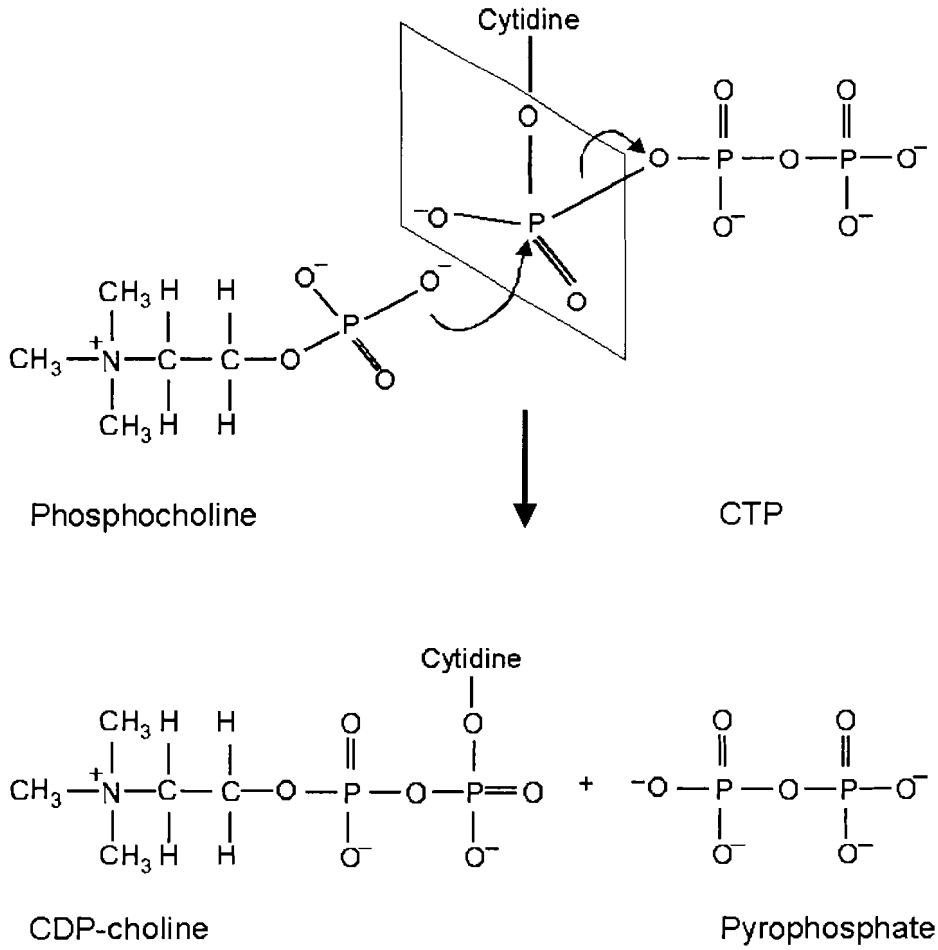

Figure 1.2 CTP:phosphocholine cytidylyltransferase catalysed reaction

1.2 CCT: Domains, Structure And Function

1.2.1 Characterization Of CCT

Kennedy and Weiss[5] first discovered CCT as they were studying the enzymatic synthesis of CDP-choline in rat liver. They noted that it was found in both soluble and membrane bound forms, a property that was later termed amphitropism – a characteristic of proteins whose activities are regulated by interconversion between an inactive soluble form and an active membrane bound

form. In the 1980s and 1990s many separate investigations led to a model for stimulation of PC synthesis in cells by induction of the translocation of CCT from a soluble to a particulate (membrane) compartment[8,9].

Due to its propensity to aggregate and lose activity, it was an additional thirty years before CCT was successfully purified. Weinhold et al.[10] finally purified mammalian CCT from rat liver by means of treating the soluble fraction of CCT as a membrane enzyme with the addition of lipids and detergent.

The gene for CCT was first cloned by complementation of a CCT-defective mutant in *Saccharomyces cerevisiae*[11] and the first mammalian cDNA was cloned from rat liver[12]. The information garnered revealed that CCT is an enzyme comprised of 367 amino acids, with a calculated molecular weight of 41,720 Daltons, which supports the estimation from SDS-PAGE gels of ~42,000 Daltons.

So far, cDNAs for CCT have been isolated in many mammals: human, mouse, rat, Chinese hamster[12-15], as well as some plants: *Arabidopsis thaliana*, rapeseed and pea[16,17] and invertebrates: *Drosophilae melanogaster* and *C. elegans*[18-20] (Figure 1.3).

There are two different isoforms of CCT: α and β. While the splice variants of β (β1, β2, and β3) are expressed mainly in gonadal and neuronal tissue, α is the ubiquitous and predominant form of CCT[21-23]. CCTα was the isoform used for all the experiments in this thesis.

Figure 1.3 Comparison of the amino acid sequences of several CCTs
Amino acids conserved in at least five of the six CCTs are bold. Amino acid residues proposed to be located within the dimer interface, as based on the crystal structure for glycerol 3-phosphate cytidylyltransferase, are boxed. CTP:phosphocholine cytidylyltransferases shown are: *R. norvegicus* CCT alpha (RatA, accession P19836), *R. norvegicus* CCT beta 2 (RatB2, accession Q9Y5K3), *C. elegans* CCT (Celeg, accession P49583), *D. melanogaster* CCT (Dros, accession NP_647622), *A. thaliana* CCT (Athal, accession NP_193249) and *S. cerevisiae* CCT (yeast, P13259). Sequence alignment was done using ClustalW.


RatA ----------MDAQSSAKVNSRKRRKEVPG-PNGATEEDGIPSKVQRC 37
RatB2 ----------MPVVTTDAESETGIPKSLSN-EPPSETMEEIEHTCPQP 37
Celeg ----------MFIHKQEKMPQRKRTMDSPQEEDVEVKKKATEVEYVVR 38
Dros ----------MDRMPKEDDESPVSTAPATPTSPMEFKMLPLFMDFE 36
Athal ----------MSVNGENKVSGGDSSS---------- 16
Yeast MANPTTGKSSIRAKLSNSSLSNLFKKNKNKRQREETEEQDNEDKDESKNQDENKDTQLTP 60
RatA AVGLRQPAPFSDEIEVDFSKP----YVRVTMEEACRGTPCERPVRVYADGIFDLFHSGHA 93
RatB2 RLTLTAPAPFADETNCQCQAP----HEKLTIAQARLGTPADRPVRVYADGIFDLFHSGHA 93
Celeg SLASDEPAPFSDEALAITTREAVDYSKKITLAMAEAN-EAGRPVRIYADGIYDLFHHGHA 97
Dros DFSICQPAPFSYDDKAMLELERCDYTQRITYHMARAG-KTTRRVRVYADGIYDLFHQGHA 95
Athal ----------SDRPVRVYADGIFDLFHFGHA 37
Yeast RKRRRLTKEFEEKEARYTNELPKELRKYRPKGFRFNLPPTDRPIRIYADGVFDLFHLGHM 120
RatA RALMQAKNLFPNTYLIVGVCSDELTHNFKGFTVMNENERYDAVQHCRYVDEVVRNAPWTL 153
RatB2 RALMQAKTLFPNSYLLVGVCSDDLTHKFKGFTVMNEAERYEALRHCRYVDEVIRDAPWTL 153
Celeg NQLRQVKKMFPNVYLIVGVCGDRDTHKYKGRTVTSEEERYDGVRHCRYVDEVYREAPWFC 157
Dros RQLMQAKNVFPNVYLIVGVCNDELTLRMKGRTVMNGFERYEAVRHCRYVDEIVPNAPWTL 155
Athal RAIEQAKKSFPNTYLLVGCCNDEITNKFKGKTVMTESERYESLRHCKWVDEVIPDAPWVL 97
Yeast KQLEQCKKAFPNVTLIVGVPSDKITHKLKGLTVLTDKQRCETLTHCRWVDEVVPNAPWCV 180
RatA TPEFLAEHRIDFVAHDDIPYS--SAGSDDVYKHIKEAGMFAPTQRTEGISTSDIITRIVR 211
RatB2 TPEFLEKHKIDFVAHDDIPYS--SAGSDDVYKHIKEAGMFVPTQRTEGISTSDIITRIVR 211
Celeg TVEFLKNLKVDFIAHDAIPYV--APGEEDLYEKFRREGMFLETERTEGVSTSDVVCRIIR 215
Dros NEEFIEEHKIDFVAHDDIPYG--AGGVNDIYAPLKAKGMFVATERTEGVSTSDIVARIVK 213
Athal TTEFLDKHKIDYVAHDALPYADTSGAGNDVYEFVKSIGKFKETKRTEGISTSDIIMRIVK 157
Yeast TPEFLLEHKIDYVAHDDIPYV--SADSDDIYKPIKEMGKFLTTQRTNGVSTSDIITKIIR 238
RatA DYDVYARRNLQRGYTAKELNVSFINEKKYHLQERVDKVKKKVKDVEEKSKEFVQKVEEKS 271
RatB2 DYDVYARRNLQRGYTAKELNVSFINEKRYRFQNQVDKMKEKVKNVEERSKEFVNRVEEKS 271
Celeg DYDKYVRRNLQRGYSPKELNVGFLAASKYQIQNKVDSLKSKG---------- 257
Dros DYDVYVRRNLARGYSAKELNVSFLSEKKFRLQNKMDELKTRGKRELTKVK---------- 263
Athal DYNQYVLRNPGPRYSREELSCQLE-EKRLRVNMRLKKLQEKVKEQQEKIQTVAKTAG--- 213
Yeast DYDKYLMRNFARGATRQELNVSWLKKNELEFKKHINEFRSYFKKNQTNLNNASRDLYFEV 298
RatA IDLIQKWEE---KSREFIGSFLEMFGPEGALKHMLKEGKGRMLQAISPKQSPSSSPTHER 328
RatB2 HDLIQKWEE---KSREFIGNFLELFGPDGAWKQMFQERSSRMLQALSPKQSPVSSPTRSR 328
Celeg IELLSTWKS---KSDDIIRDFIDTFHKDGGLNAFGGRLKGIMSMSRSPSPSPHEGSPTGI 314
Dros VDIITKWEE---KSREFIDAFLLLFGRER-LNTFWNESKGRIIQALSPPGSPN-GSVNGD 318
Athal -MHHDEWLE---NADRWVAGFLEMF--EEGCHKMGTAIRDGIQQRLMRQESEENRRLLQN 267
Yeast REILLKKTLGKKLYSKLIGNELKKQNQRQRKQNFLDDPFTRKLIREASPATEFANEFTGE 358
RatA SPS----PSFRWPFSGKTSPSSSPASLSRCKAVTCDISEDEED---------- 367
RatB2 SPSRSPSPTFSW-LPLKTSPPSSPKAASASISSMSEGDEDEK---------- 369
Celeg EHHLETQDEEEEEEALEEEKVVEQKIVEKKEVVKKRSSRNKAKTPLEY---------- 362
Dros DPD-ATDDLDSEDEYMELPPDYGSGSCVSLSRKQKRPDKVNASANLNYSEQPEHKDVVDE 377
Athal GLT---ISKDNDDEQMSDDNEFAEERLRQCEQQRD---------- 299
Yeast NSTAKSPDDNGNLFSQEDDEDTNSNNTNTNSDSDSNTNSTPPSEDDDDNDRLTLENLTQK 418
RatA ------
RatB2 ------
Celeg ------
Dros RRSD-- 381
Athal ------
Yeast KKQSAN 424

1.2.2 The Domain Structure Of CCT

Sequence homologies of the primary sequences for CCT from several organisms, secondary structure predictions, the crystal structure of the GCT (glycerol-phosphate cytidylyltransferase) catalytic domain, and numerous molecular and biochemical studies, have enabled a model to be proposed for the domain structure of CCT (Figure 1.4).

CCT is comprised of four domains: the N-terminal domain (amino acids 1-73), the catalytic domain (73-236), the membrane-binding domain (237-300) and the phosphorylation domain (315-367).

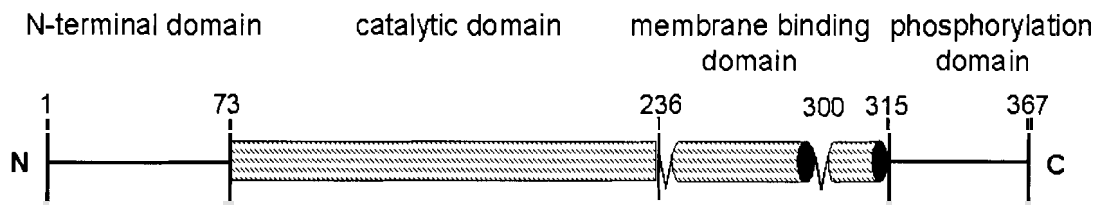

Figure 1.4 The domain structure of CCT

1.2.2.1 N-Terminal Domain

The N-terminal domain consists of amino acids 1 through 73. It contains a 21 residue nuclear localization signal (NLS) (^{8}KVNSRKRRKEVPGPNGATEED^{28}) that dictates the translocation of the enzyme to the nucleus[24].

The role for nuclear localization is unclear. Deletion of the NLS resulted in a higher proportion of CCT in the cytoplasm, but had no affect on the activity of

the enzyme, or on PC biosynthesis in CHO cells deficient in wild-type CCT at non-permissive temperatures[24].

The interdomain contacts of domain N are not known. Due to their proximity, it was postulated that there might be contacts between domain N and the catalytic domain. Recent evidence suggests that there may be interactions between domain N and the membrane-binding domain. Bogan *et al.*[25] showed with protease cleavage maps comparing soluble CCT, membrane bound CCT and CCT lacking the membrane binding and phosphorylation domains, that domain N is more available to chymotrypsin digestion in the membrane bound and truncated versions of CCT. Domain N is less accessible to proteases in the soluble form. This implies that there may be contacts between domains N and M when CCT is in its inactive form.

There is no known structure for the N-terminal domain. PROFsec, a secondary structure algorithm, predicts chiefly disordered conformations for this domain[26].

1.2.2.2 Catalytic Domain

On the strength of the sequence conservation between rat and yeast CCT, it was proposed that residues 72-235 form the catalytic domain in mammalian CCT[12]. It is now apparent that the catalytic domain is the most highly conserved domain across all proteins in the cytidylyltransferase family. There is up to 99% sequence identity between mammalian CCT catalytic domains[9], 75% sequence identity with the yeast CCT catalytic domain[12], 48% identity with *Plasmodium falciparum*[27] and 37% identity with GCT from *Bacillus subtilis*[28]. Because the

catalytic domain sequences are so similar between cytidylyltransferases, it is supposed that they all operate with the same catalytic mechanism.

There are three highly conserved motifs found within the catalytic domains of cytidylyltransferases: HXGH, RTXGISTT and RYVDEVI (Figure 1.5). The HXGH motif is also conserved in another nucleotidyltransferase family, the class I aminoacyl –tRNA synthetases, where it has been shown that the histidines in the motif bind to and stabilize the transition state. Mutagenesis of the glycine and histidines within the HXGH motif of CCT resulted in a 4-fold reduction in V_{max} and a 25-fold increase in the K_m for CTP[29,30]. Mutagenesis of the corresponding histidines in GCT[31] resulted in a decrease in k_{cat} by several orders of magnitude, thus lowering the efficiency of the enzyme. These results were experimental validation of the hypothesis that the HXGH motif in CCT is involved in catalysis, specifically in CTP binding and transition-state stabilization. The RTXGISTT motif is unique to cytidylyltransferases. The crystal structure of GCT tightly bound to CTP implicates both the HXGH and RTXGISTT motifs in substrate binding, as it shows they are involved in the formation of a CTP cradling cavity and forge numerous interactions with the substrate itself[32]. The GCT crystal structure also illustrates that the RYVDEVI sequence is partially found in the dimer interface, as are the two hydrophobic residues that precede the HXGH motif.

In addition to the histidines in the HXGH motif, lysine 122 and arginine 196 in CCT have been shown to participate in substrate binding. Arg 196 is part of the RTXGIST motif, and lys 122, not a conserved residue and therefore

previously overlooked as a candidate in catalysis, is thought to form contacts with phosphocholine and is located within the catalytic active site[33].

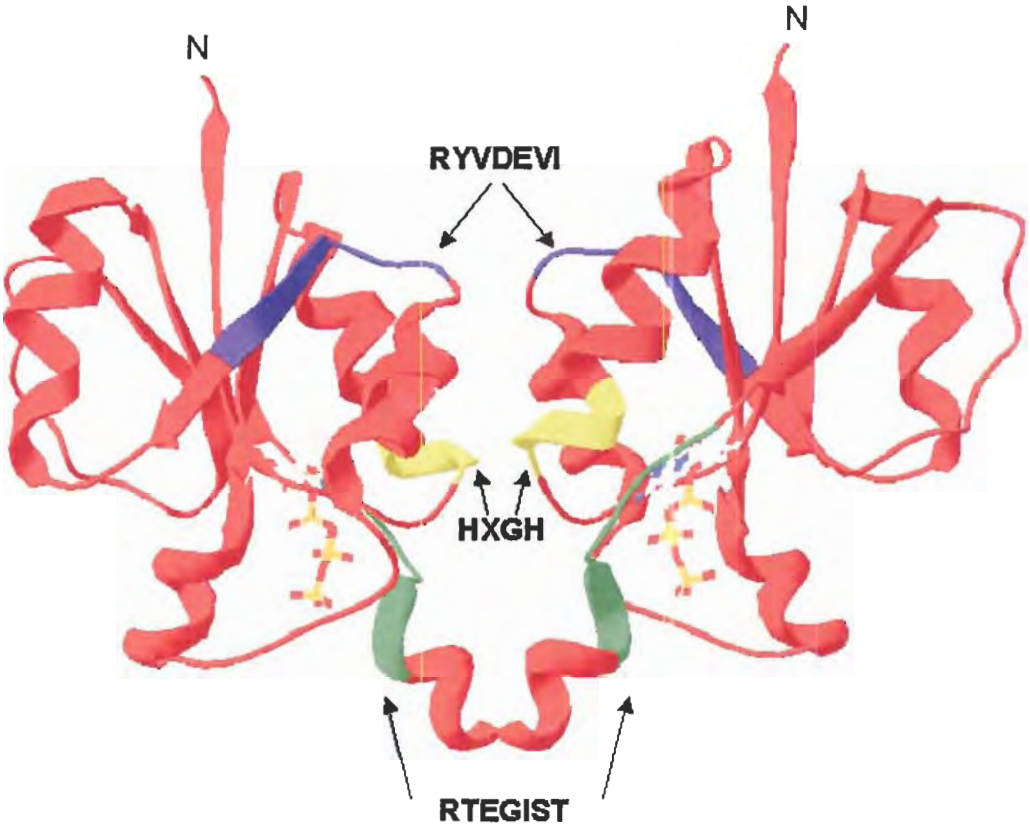

Figure 1.5 Conserved motifs with cytidylyltransferase catalytic domains
RTEGIST is green, HXGH is yellow, and RYVDEVI is blue. GCT image viewed using Swiss-PdbViewer DeepView using coordinates from accession number: 1coz.

1.2.2.3 Membrane Binding Domain

Located approximately from amino acids 237-300, domain M is the membrane-binding domain of CCT. Several secondary structure algorithms[12] predict the region to form either an unbroken α-helix or two helices interrupted briefly by a β-strand between residues 272-276. Within this domain there are three 11-mer tandem repeats (VEEKSKEFVQK VEEKSIDLIQK WEEKSREFIGS)

(residues 256-288). When this region was displayed as a helical wheel it was strikingly amphipathic, with an asymmetrical distribution of polar *vs.* hydrophobic residues (Figure1.6). Of the 47 amino acids on the polar face, there is a concentration of 26 charged residues, alternating between positively and negatively charged clusters that were thought to provide stabilization to the helix through salt bridging, however the NMR structure of the 2 helical peptides within domain M indicated that no oppositely charged residues are near enough for salt-bridge formation[34]. The non-polar face contains 18 hydrophobic residues, sufficient to drive hydrophobic interactions with the lipid bilayer and to promote membrane intercalation[12]. The interfacial zone of the helix is rich in basic residues that interact with the anionic phospholipid head groups of the target membrane. Since there is no long stretch of hydrophobic residues elsewhere on the enzyme, yet CCT was known to be associated with membranes, it was proposed that this section of the sequence constituted, in part or in whole, the membrane binding region, where the helix lies parallel to the plane of the membrane, with its hydrophobic face inserted into the non-polar core of the lipid bilayer[12]. Photolabelling of CCT with a hydrophobic [^{125}I]TID probe[35] revealed that CCT does intercalate into the membrane and, in conjunction with proteolysis and anti-domain M and anti-domain C antibody labelling[36], the putative α-helix was identified as the membrane binding site. Many subsequent studies involving mutagenesis[37-39] confirmed that domain M is the principle membrane-binding domain.

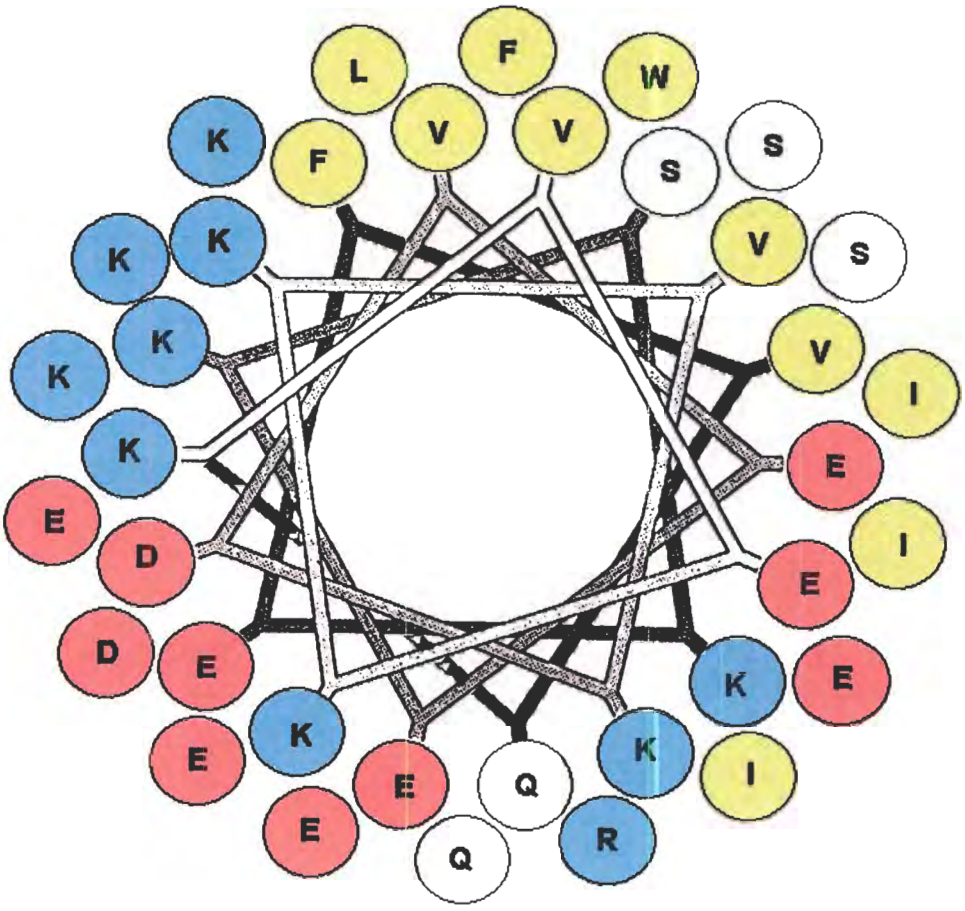

Figure 1.6 Helical wheel projection of domain M, residues 251-286.
Hydrophobic residues are yellow, acidic residues are red, basic residues are blue and neutral residues are white.

Circular dichroism studies with peptides derived from the three 11-mer repeats revealed that in the absence of lipids the conformation adopted by the peptide was random coil. The addition of anionic lipid vesicles resulted in a transition to α-helix, the secondary structure predicted for the peptide and corresponding region in CCT[40]. This finding was confirmed with CD analysis on whole CCT, where it was shown that lipids trigger a conformational change in

domain M from a mixed structure to an α-helix[26], which provides a hydrophobic face for membrane insertion.

1.2.2.4 Phosphorylation Domain

Watkins and Kent[41] first demonstrated CCT to be phosphorylated *in vivo*. They mapped the phosphorylation sites to serine residues in the C-terminal end of the enzyme. There are 16 serines located downstream of Ser 315 (inclusive) and all were shown to be phosphorylated to some extent. Of these 16 serines, seven are followed by prolines, leading to a hypothesis that a proline-directed kinase was responsible for CCT phosphorylation.

The highly disordered phosphorylation domain is comprised of the final 55 amino acids of CCT (315-367) and has many putative phosphorylation sites: primarily serine-proline motifs, which are targets for cyclin dependant kinases, as well as putative sites for casein kinase II and glycogen synthase kinase III. Despite several trials, attempts to phosphorylate pure CCT *in vitro* with these kinases have yielded very low stoichiometries: 0.1-0.2 mol P/mol CCT, and had no affect on activity[39,42]. It is proposed that the phosphorylation and dephosphorylation of these sites has a role in the regulation of CCT activity. In cells, the trend is that domain P is highly phosphorylated in the soluble inactive state and dephosphorylated in the active membrane bound state, although there are exceptions to this tendency.

The intersubunit contacts of the phosphorylation domain are not known. Its susceptibility to protease cleavage[36] suggests that it may be loosely folded and/or highly accessible. Based on an increase in membrane affinity upon

dephosphorylation *in vitro*, it was proposed by Arnold *et al.*, that the phosphates on phosphorylated CCT might forge electrostatic interactions with basic residues on the membrane-binding domain[43]. These interactions would be out competed by negative charges on the membrane bilayer.

1.2.3 Quaternary Structure Of CCT: A Homodimer

Evidence indicates that CCT is found as a homodimer within cells. Using CCT isolated from the cytosols of various types of cells, Weinhold *et al.*[44] performed both glycerol density centrifugation and gel filtration. The sedimentation coefficient obtained from glycerol density centrifugation (4.8S) indicated that the estimated molecular weight of the cytosolic (i.e. soluble) fraction of CCT was 90 000 Da. The Stokes radius obtained from gel filtration of the 4.8S fraction of CCT was 48 Å, which yielded a calculated molecular weight of 97 690 $\pm$ 10 175 Da. These two values are approximately double the molecular weight of ~45 000 Da for CCT seen on separating gels under reducing conditions, suggesting that in non-reducing conditions, CCT is a homodimer.

Cornell[45] found that when run on SDS-PAGE under reducing conditions, CCT appears as a 42 kDa band. However, in non-reducing conditions, another band was present at 84 kDa. 2D-gel electrophoresis (first in a non-reducing, then in a reducing environment) with a reversible chemical cross-linker revealed that the heavier species was in fact a dimer of the 42 kDa band. *In vitro*, a reducing or oxidizing environment can determine the oligomeric state of CCT, therefore it was hypothesized that within the dimer interface there is a pair of cysteines close

enough to form a disulphide bond. *In vivo* (i.e. in a reducing environment with the cell), all contacts between the surfaces of the two monomers are non-covalent.

Antibody identification of fragments produced by limited chymotrypsin proteolysis revealed that the N-terminal 26-30 kDa fragment could associate as a dimer[36]. Therefore, the dimerization interface includes, but may not be limited to, the first 230 amino acids of CCT.

A yeast two-hybrid was performed with various truncated constructs of CCT[46] in an attempt to further identify the location of the dimer interface. The strongest interaction was found to be between CCT 236 and CCT 236 (truncations of full length CCT consisting of only the N-terminal and catalytic domains). CCT 73-239 self-interactions were, by contrast, very weak. This further supports the premise that the N-terminal region of CCT is located in the dimer interface.

The crystal structure for GCT from *Bacillus subtilis* has been determined to 2 Å resolution[32]. GCT lacks the N-terminal, membrane binding and phosphorylation domains of CCT, yet was crystallized as a homodimer. This implies that the catalytic domain of CCT may also participate in CCT dimerization. The key sites of dimer contact in GCT were Arg 63 from the conserved RYVDEVI motif, as well as Trp 15 of the HXGH motif and two leucines, Leu 12 and Leu 13, which precede this motif. Dr. Frederic Pio modelled the CCT catalytic domain, residues 78-211, based upon the GCT structure coordinates, to elucidate the dimer interface of CCT (Figure 1.7). A look at the model showed that a single cysteine, Cys 139, was the most likely candidate to

form a disulfide bond with its counterpart on the opposing subunit, as the SH groups appeared to be only ~10 Å apart. Mutagenesis of Cys 139 to serine, followed by cysteine specific cross-linking, resulted in trapped homodimer, ruling out the possibility that Cys 139 is situated in the dimer interface[46]. There were no further cysteine candidates in the catalytic domain, but glutaraldehyde and DSP cross-linking also covalently trapped the homodimer, signifying that there may be lysines in the dimer interface. Examination of the proposed CCT domain C structure revealed no lysines in close enough proximity to be cross-linked, therefore initiating the search for cross monomer contacts elsewhere in the enzyme.

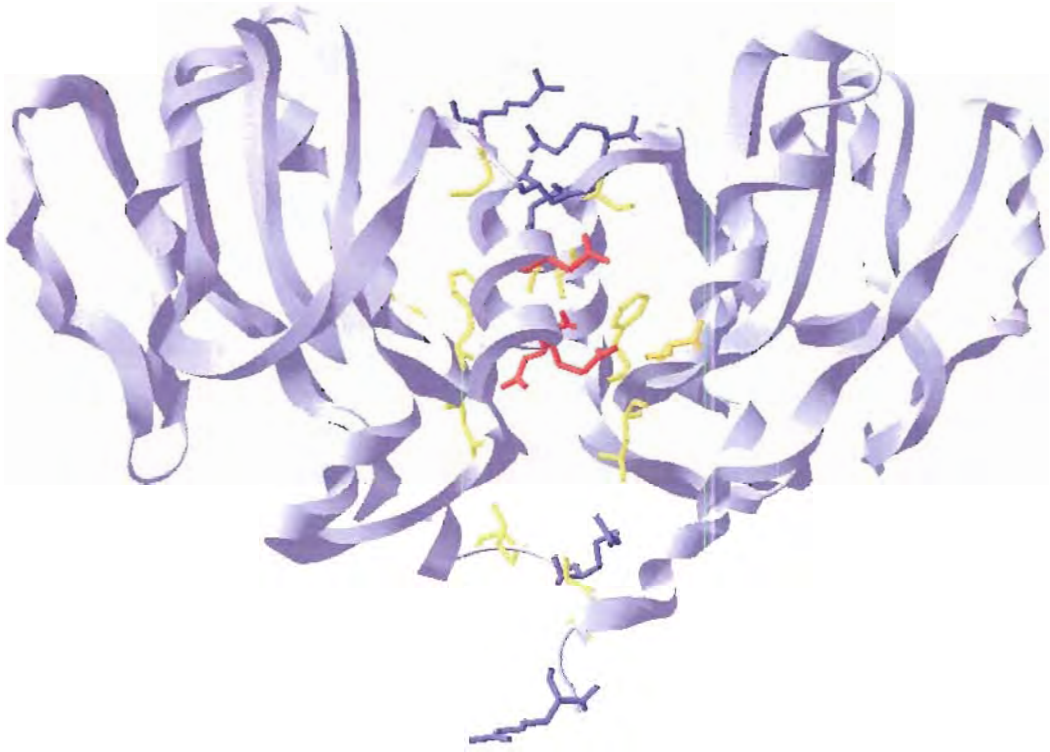

Figure 1.7 Model of CCT catalytic domain based on the structure of GCT
Model of CCT catalytic domain was made by Dr. Frederic Pio using Modeller, and is based on the crystal structure of GCT, pdb 1coz. Putative amino acid residues in the dimer interface are shown as sticks. Acidic residues are red, basic residues are blue and hydrophobic residues are yellow.

There are seven cysteines located throughout CCT (amino acids 37, 68, 73, 113, 139, 354, and 359). MT Xie substituted each one individually with serine and tested the ability of each construct to form a disulfide-bonded dimer after oxidation by copper phenanthroline. Only C37S resulted in a monomer after non-reducing SDS-PAGE. Engineering of C37 into a cys-free mutant of CCT restored the ability to form a disulphide bond after oxidation[46]. This substantiates the proposal that at least one cysteine (C37) is positioned in the dimer interface, and

its location is further evidence that the N-terminal domain is part of the dimer interface.

1.3 Regulation Of CCT Activity

Because CCT is an enzyme responsible for the control of the biosynthesis of PC, understanding its mechanisms of regulation is important. There is evidence for transcriptional and pre-translational regulation[47-49]. However, to meet the demands of regulating PC biosynthesis in the cell, more rapid and sensitive post-translational mechanisms for controlling CCT activity are required. Membrane binding is a quick mechanism for controlling the activity of CCT. According to current dogma, CCT picks up cues regarding the lipid composition of its target membrane, and responds by binding to the membrane and becoming active, consequently maintaining PC homeostasis.

1.3.1 Localization/Translocation Of CCT

CCT is distributed in both inactive/soluble and active/membrane bound forms and translocation between the two is controlled. It was originally thought that the soluble form was only found in the cytoplasm, while the membrane bound form was bound to the endoplasmic reticulum (ER). In most cells CCT is predominantly nuclear and its active form is bound to the nuclear envelope[50-52].

The nuclear localization signal located in the N-terminal domain of CCT directs its movement towards the nucleus[38]. The purpose for nuclear localization of CCT is not yet clear and somewhat perplexing; the enzyme preceding it in the CDP-choline pathway is cytosolic and the enzyme succeeding it seems to be ER

bound (although there is evidence that CPT is also associated with the nuclear membrane)[53]. Deletion of the NLS results in a primarily cytoplasmic location for CCT, yet its activity and its ability to promote PC biosynthesis were unaffected[24]. It has been proposed that the nucleus may function as a holding tank for an inactive CCT reserve[51].

There are two mechanisms proposed for the triggering of membrane binding *in vivo*: the first is the lipid composition of the target membrane; the second is the phosphorylation state of the C-terminal domain of CCT.

1.3.2 Membrane Binding Regulated By Lipid Composition

In vitro, domain M of CCT preferentially binds to two classes of lipids resulting in the catalytic activation of the protein. The first class contains the most potent activators of CCT, composed of phospholipids with anionic head groups such as PG (phosphatidylglycerol), PI (phosphatidylinositol), PS (phosphatidylserine) and PA (phosphatidic acid). The second class is comprised of Type II lipids with small head groups that impose negative curvature strain and packing defects in lipid bilayers, such as DAG and unsaturated phosphatidylethanolamine. A combination of these two classes of lipids results in a synergistic effect of CCT binding to membranes[54]. PC does not promote CCT activity, but decreased PC levels can result in CCT activation due to a destabilization of the membrane bilayer, which facilitates CCT insertion[55].

Binding to charged membranes appears to be a two-step process: electrostatic adsorption followed by hydrophobic interactions, which involve intercalation into the non-polar core of the bilayer.

Negatively charged phospholipid head groups attract basic amino acids situated on the interfacial boundary of domain M, which promotes surface localization of CCT thus facilitating the intercalation of the membrane-binding domain to the lipid bilayer. The degree of CCT binding to membranes is proportional to the net negative membrane surface charge: the greater the negative charge of the lipid, the lower the mol % required for CCT activation[54,56] An accumulation of negatively charged lipid head groups can also promote CCT insertion by contributing to the destabilization of the membrane bilayer through lipid-lipid charge repulsions.

Four membrane properties of class II lipids promote the insertion of CCT into the lipid bilayer: interfacial packing defects, low lateral pressure, acyl chain disorder and negative curvature strain. Lipids with small head groups create surface voids and cracks. Oxidized PC creates a disordering of acyl chains as observed with deuterium NMR[57] resulting in looser packing. Cone shaped lipids such as DAG and unsaturated PE create a tendency for the bilayer to curl and form a concave surface, causing negative curvature strain. This energetic tension is released when CCT inserts its membrane binding helix into the lipid bilayer.

It is the second process, bilayer insertion, which results in the activation of CCT. This was found when insertion was blocked by the use of viscous gel-

phase PG membranes, rather than fluid membranes. CCT bound electrostatically to the gel phase, but did not insert and was not active[54].

Although the details are not entirely clear, membrane insertion of CCT results in activation of the enzyme almost certainly by removing the auto inhibitory constraint on the catalytic site provided by the membrane-binding domain. The key evidence for domain M as an auto inhibitory domain was provided by Wang and Kent[38] who showed that deletion of domains M and P (but not P alone) renders the enzyme constitutively active. Both NMR and circular dichroism (CD) studies with peptides derived from the membrane binding domain[58] and CD studies with full length CCT[26] show that upon binding to lipid vesicles, there is a distinct change in the secondary structure of the membrane binding domain, which converts from an unstructured random coil to an α-helical conformation. This conformational change to the enzyme is translated to the catalytic site either through the displacement of a portion of domain M blocking and/or inhibiting the active site, or through a cascade of conformational changes which subtly affect the conformation of the catalytic site, rendering it active.

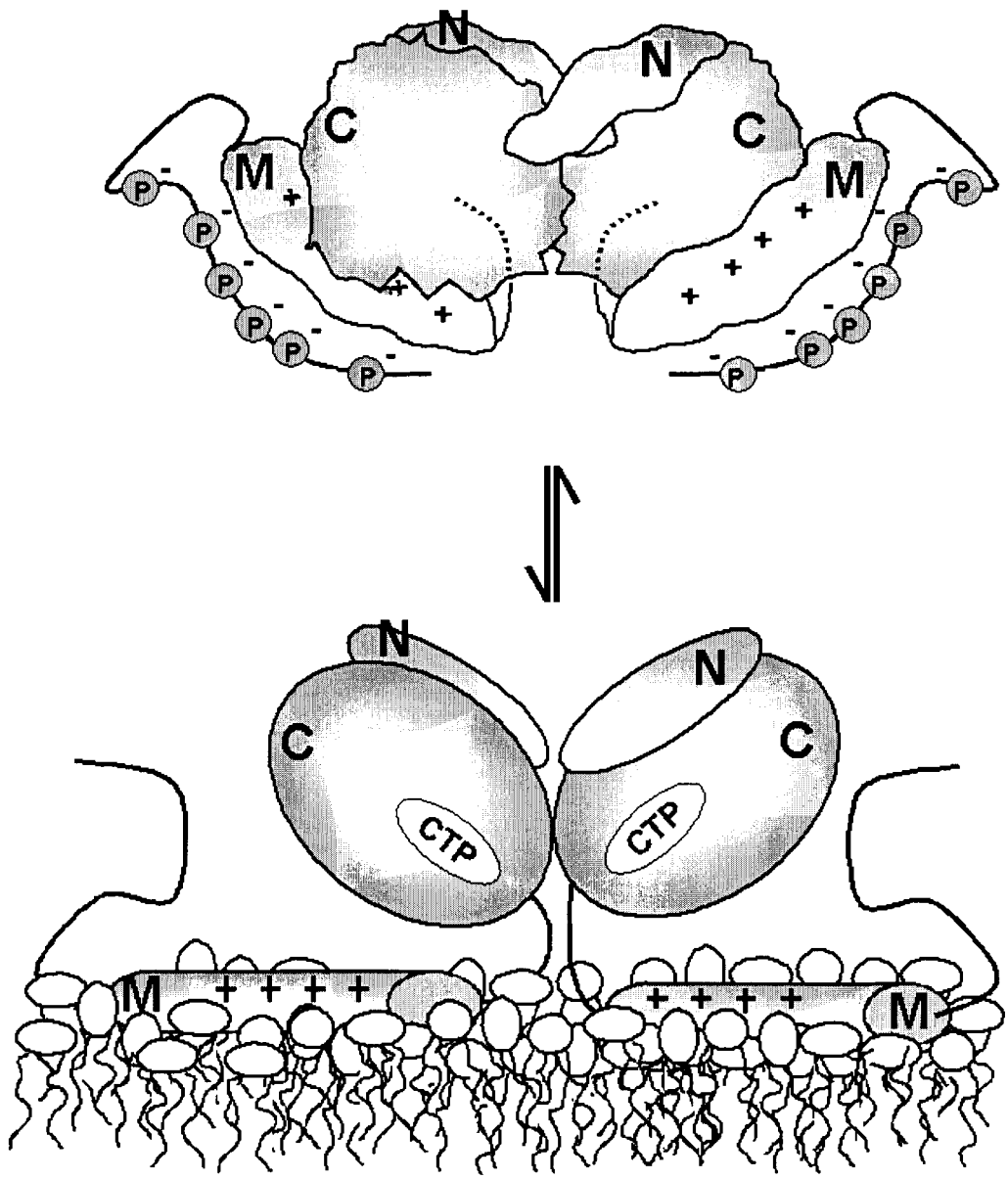

Figure 1.8 CCT in its soluble, inactive and membrane-bound, active states

1.3.3 Membrane Binding Regulated By Phosphorylation

There is a marked correlation between the degree of enzyme phosphorylation, and cell membrane association. Active CCT is significantly

dephosphorylated subsequent to membrane binding[59]. Okadaic acid, an inhibitor of protein phosphatase 1A and protein phosphatase B, inhibited PC synthesis, decreased CCT activity, and drove CCTs partitioning equilibrium to stabilize the soluble form[60]. When cells were treated with phospholipase C, which decreases membrane PC content and thus increases CCT activity, or with oleic acid, which enhances membrane binding and CCT activation, it was noted that CCT became dephosphorylated[59]. When serines were substituted with alanines to prevent phosphorylation, the membrane bound fraction of CCT increased as the alanine content increased. However, serines substituted with glutamic acid to preserve charge showed a wild-type distribution[61]. When the phosphorylation domain was entirely truncated however, there was no change in the cellular distribution of CCT[39].

The degree of domain P phosphorylation does not appear to have an effect on the catalytic function of CCT. Truncations of parts or the entire phosphorylation domain resulted in no change in activity[39,62]. Mutants in which phosphorylation was decreased or prevented by replacing some or all of the serines with alanines, were still able to support PC biosynthesis sufficient to sustain growth at non-permissive temperatures in CHO cells containing a temperature sensitive endogenous CCT[61].

All mutants with changes in the phosphorylation domain were activated by the same lipids as wild-type CCT, but the mol % anionic lipid required to initiate activation decreased as the negative charge on the phosphorylation domain decreased[43]. This observation led to the proposition that the phosphorylation

domain serves to modulate enzyme activation by lipid regulators. Arnold *et al.*[43] put forward that the phosphorylation domain may function as an electrostatic switch that fine-tunes the membrane affinity of the membrane-binding domain. It was proposed that the phosphates on domain P compete with the negatively charged phospholipid head groups for interactions with the basic lysines in domain M. Dephosphorylation would eliminate this competition and promote membrane binding.

As described above, domain P contains many potential sites for regulation by phosphorylation. However, it wasn't until just this year that extracellular signal-regulated kinase (ERK, p42/44 kinase) was found to be an *in vivo* regulator of CCT[63]. Agassandian *et al.* [63] also identified a putative ERK docking site (GSFLEMFGPEGALK) in the membrane-binding domain, as well as a physiologically relevant phosphorylation site at Ser 315.

1.4 Overview Of Objectives

A major goal of the Cornell lab is to elucidate the changes in the structure of CCT upon binding membranes: research has been ongoing to reveal changes at the secondary, tertiary and quaternary levels.

Some of the specific questions asked are:

(1) Does membrane binding alter the quaternary structure of CCT?

(2) Which residues are located in the dimer interface?

(3) Where are the lipid sensitive sites in the dimer interface?

(4) How do lipids affect the dimer interface of CCT-236?

I attempted to address these questions with the research presented in this thesis, largely using the approach of covalent chemical cross-linking. To test if membrane-binding alters the quaternary structure of CCT, specifically with respect to the dimer interface, I investigated the differences in the extent and efficiency of covalent cross-linking across the dimer interface in both the soluble, inactive and membrane-bound, active forms of the enzyme. To explore whether any of the lysines in the N-terminal domain are located within the lipid sensitive dimer interface, I selectively mutated each lysine and then cross-linked with lysine specific reagents in the absence and presence of lipids. The examination of the effect of lipids on CCT 236 was performed by a combination of cross-linking studies and enzyme activity assays, both in the absence of lipids and in the presence of activating and non-activating lipid vesicles, and single chained anionic or cationic amphiphiles in the monomer and micellar conformations.

1.5 Introduction To Chemical Cross-Linking

Non-covalent interactions that would usually hold spatially close regions of the protein together such as van der Waals interactions, salt-bridging *etc*, are destroyed when the protein is introduced to a denaturing environment, such as that found in SDS gel electrophoresis. Thus, proteins that would normally be found as dimers or multimers *in vivo* due to non-covalent interactions would appear as monomer bands on a gel. However, bifunctional chemical cross-linkers (cross-linkers with a reactive group on both ends) can be used to covalently trap these interactions by targeting and reacting with specific residues within the reach of the cross-linker (Figure 1.9).

The two aldehyde groups on glutaraldehyde principally react with the ϵ-amine on lysine residues, but can also partially conjugate with the phenolic and imidazole rings of tyrosine and histidine, as well as the sulfhydryl groups on cysteine, provided they are located within 7 Å of each other[64].

DSP, DSS and BS^3 all contain homobifunctional *N*-hydroxysuccinimide ester (NHS-ester) groups on either end of a 12 Å spacer that react selectively with primary amines such as the α-amine on the N-termini of proteins or the ϵ-amine group of lysine. DSP is non-sulfonated and is thiol-cleavable; therefore, it is not water-soluble and the cross-linker can be cleaved in a reducing environment. DSS is a non-thiol-cleavable form of DSP and cross-linking cannot be reversed. BS^3 is the sulfonated analogue of DSS and as a result is water-soluble. With the NHS-esters, a covalent amide bond is formed between the NHS-ester and primary amines, resulting in the release of *N*-hydroxysuccinimide (Figure 1.10).

Copper phenanthroline cross-linking does not introduce a linker to bridge targeted amino acids; rather the copper, by withdrawing electrons from the sulfhydryls on cysteine side chains, works by creating an oxidizing environment that favours the formation of disulfide bonds between sulfhydryl groups that are in immediate proximity to one another.

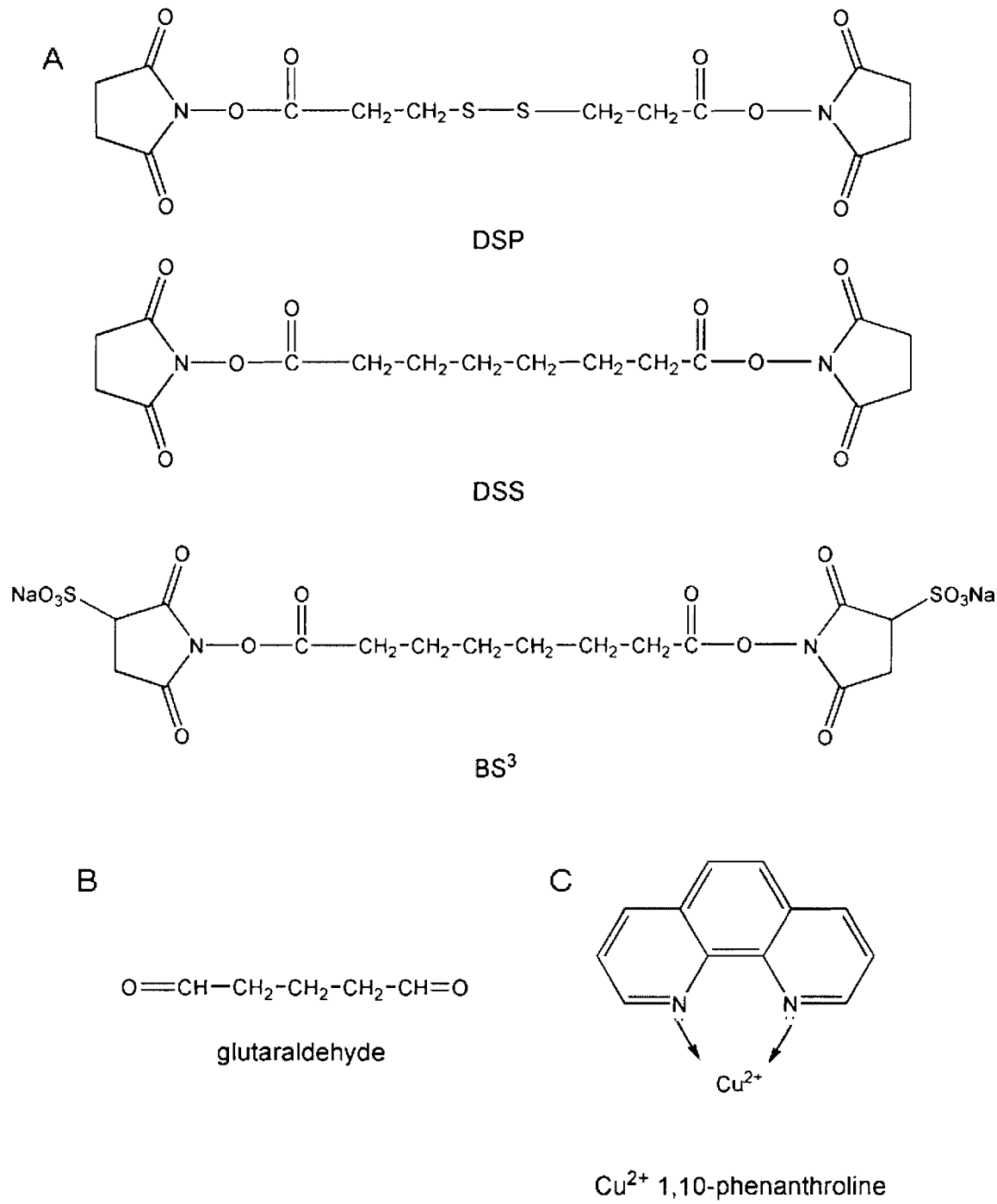

Figure 1.9 Cross-linkers
(A) *N*-hydroxysuccinimide esters (B) glutaraldehyde (C) copper phenanthroline

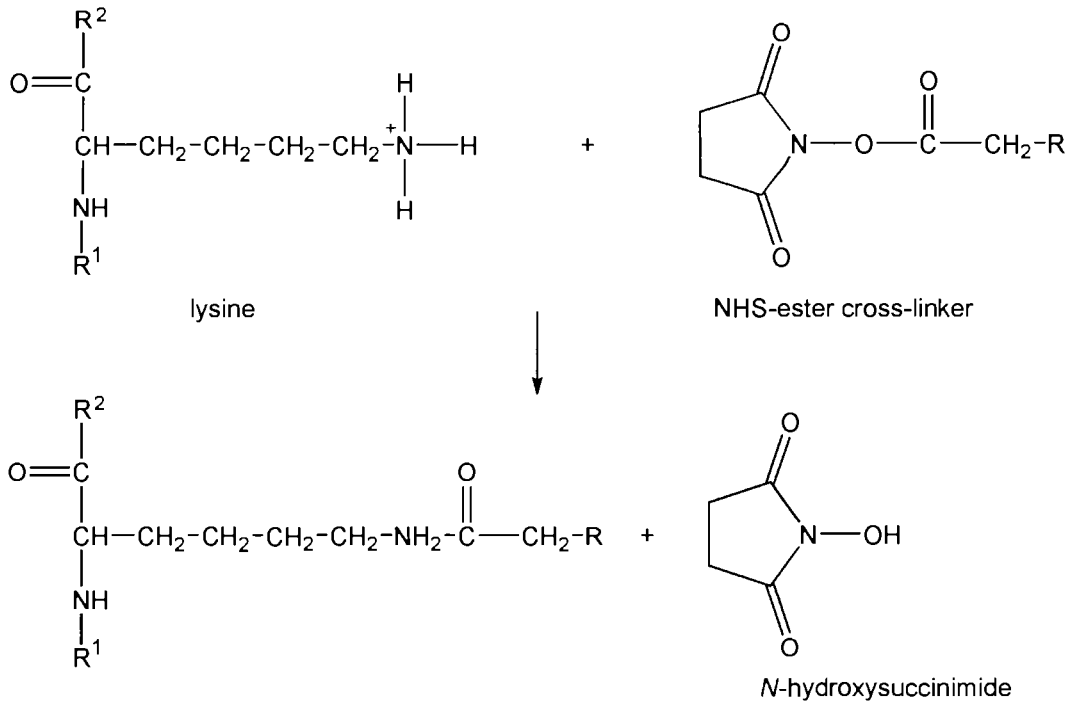

Figure 1.10 NHS-ester cross-linking
A covalent amide bond is formed between the carbonyl of the NHS-ester and the nitrogen of the ϵ amine of lysine.

2 MATERIALS AND METHODS

2.1 Materials

Restriction enzymes, oligonucleotide primers, T4 DNA ligase, Dulbecco's Modified Eagle Medium, fetal bovine serum, trypsin-EDTA and Penstrep were from Invitrogen. DNA ladder standards and Rapid Ligation kit were from Fermentas. dNTPs and ECL Western Blotting detection kit were from GE Healthcare (formerly Amersham Pharmacia). DpnI, *Pfu* Turbo and Epicurian Coli® XL1-Blue Supercompetent Cells were from Stratagene. Ampicillin, tetracycline, CTP, SDS, CTAB, oleic acid, 1,10-phenanthroline and Triton X-100 were from Sigma. Chemical cross-linkers DSP, DSS and BS^3 were from Pierce. Alexa Fluor 532 was from Molecular Probes. Glutaraldehyde was from Fisher. COS-1 cells and the pAX142 expression vector were gifts from Dr. Robert Kay (Terry Fox Laboratory, BC Cancer Research, UBC). Tissue culture flasks and supplies were from Falcon. [^{3}H]-phosphocholine was from PerkinElmer-NEN. Phosphatidylcholine and phosphatidylglycerol were from Northern Lipids. Lyso-PC and lyso PG were from Avanti Polar Lipids. NP40 was from Calbiochem. Gel purification kits, plasmid DNA extraction kits (Mini, Midi and Maxi) and Ni-NTA agarose beads were from Qiagen. Shrimp Alkaline Phosphatase was from Roche. Amicon Ultra centrifugal filter devices were from Millipore. Sequencing was done at the Nucleic Acid-Protein Service Unit, UBC.

2.2 Methods

2.2.1 Plasmids

2.2.1.1 pAX142

pAX142 is an expression vector derived from pAX114[65], but contains an elongation factor-1α promoter instead of a human cytomegalovirus promoter. pAX142 has an SV40 origin of replication to enable its massive replication within SV40 transformed COS cells. The SV40 provides initiation factors for replication of the pAX142 plasmid. This ultimately results in high levels of expression of the insert cDNA. The vector also contains a pUC19 origin of replication permitting the plasmid to be replicated in *E. coli*. Additionally, pAX142 contains a SupF suppressor tRNA for amber mutations in ampicillin and tetracycline resistance genes carried on the p3 single copy plasmid in *E. coli* p3 strains.

pAX142 was propagated in the DH5α p3 strain of *Escherichia coli* (*supE44*Δ*lac*U169[Φ80*lacZ*ΔM15]*hsdR*17*recA*1*endA*1 *gyrA*96thi-1*relA*1-Km^r amber Amp^r amber Tet^r), in LB media (10 g NaCl, 10 g bacto-tryptone, 5 g yeast extract/L, pH 7.0) supplemented with 100 μg/ml ampicillin and 5 μg/ml tetracycline.

2.2.1.2 pBS

The pBluescript II KS (-) phagemid is derived from the pUC19 phagemid.

pBS has a ColE1 origin of replication and T3 and T7 primer regions flanking the multiple cloning site, making it ideal for sequencing

pBS plasmids were propagated in the DH5α strain of *E. coli* (*supE44*Δ*lac*U169[Φ80*lacZ*ΔM15]*hsdR*17*recA*1*endA*1 *gyrA*96thi-1*relA*1) in LB media supplemented with 100 μg/ml ampicillin.

2.2.2 Cloning Techniques

2.2.2.1 PCR

Polymerase chain reaction fragments were generated with *Pfu* polymerase, following Stratagene's recommendations for reaction conditions, using a Biometra T3000 Thermocycler. (See Appendix A for details on PCR reactions).

2.2.2.2 QuikChange Site-Directed Mutagenesis

The Stratagene QuikChange site-directed mutagenesis kit employs a non-PCR based method of amplification that replicates only the original template DNA using a high fidelity polymerase, which results in high mutation efficiency and low formation of random mutations.

Double-stranded DNA plasmid with an appropriate insert is used as a template along with two complementary oligonucleotide primers containing the desired mutation. The primers are extended during thermocycling using *PfuTurbo* DNA polymerase, which has very high fidelity and does not strand-displace the primers. The result is a nicked circular daughter plasmid containing the incorporated mutation. DpnI is used to digest the methylated, non-mutated parental plasmid leaving only the transcribed daughter DNA which is transformed

into XL1-Blue supercompetent cells (*recA1 endA1 gyrA96 thi-1 hsdR17 supE44 relA1 lac* [F' *proAB lacI*^{q}*ZΔM15* Tn *10* (tet^{r})] that repair the nicks.

Site directed mutagenesis was performed as per the manufacturers instructions, with the following exceptions: 1) the dNTP mix for thermocycling was a 10 mM mix, each dNTP having a final concentration of 2.5 mM, 2) the XL1-Blue cells transformed with the mutated daughter DNA was grown in SOC (LB with 40 mM glucose, 10 mM $MgCl_2$, and 10 mM $MgSO_4$) media rather than NZY^+ broth.

All mutations were confirmed by sequencing, as well as by diagnostic digests using restriction enzymes for sites silently mutated near the location of the substitution mutation (See Appendix B for oligonucleotide primer sequences).

2.2.2.3 Plasmid DNA Preparations

Small and large scale plasmid isolations from bacterial cells, using a kit employing the alkaline lysis method ,were performed as per Qiagens instructions.

2.2.2.4 Restriction Digests

One μg of plasmid DNA was mixed with a variety of nucleases in the corresponding buffer and incubated at 37° for 1-2 hours. For sequential digests in non-compatible buffers, the DNA was EtOH precipitated prior to the second digest.

2.2.2.5 Agarose Gels And Plasmid DNA Purification

One μg of nuclease-digested plasmid DNA was run on 1% agarose gel (0.5 g agarose in 50 ml Tris-acetate buffer (40 mM Tris, 0.1% (v/v) glacial acetic acid, 1 mM EDTA, pH 8.0) 0.5 μg/ml ethidium bromide) at 125 volts on a BRL Model 4000 power supply for approximately 45 minutes, to separate fragments of different sizes. Gels were visualized on a 305 nm short-wave or 360 nm long wave UV box, or on a Typhoon 9410 Variable Mode Imager with a 532 nm green laser and a 610 nm filter.

Fragments of digested plasmid DNA were excised from agarose gels and purified according to instructions provided with the QIAquick Gel Extraction kit. .

2.2.2.6 Ethanol Precipitation Of DNA

Sample size 100-200 μl: 120 μl of 8 M NH_4Ac and 1 ml of 95% EtOH were added to the sample on ice, quickly vortexed and incubated at -20°C for 5 minutes. Samples were centrifuged at 13 000 rpm, at 4°C for 30 minutes. The supernatant was carefully aspirated from the sample and discarded. The DNA pellet was washed with ice cold 75% EtOH and centrifuged for 5 minutes, in the same conditions as above. The supernatant was discarded and the pellet washed with ice cold anhydrous EtOH before centrifuging for 5 more minutes. The supernatant was discarded and the pellet allowed to air dry at room temperature until all traces of EtOH had evaporated. The DNA pellet was then resuspended in 10 mM Tris pH 7.4 or ddH_2O; the buffer and its volume were decided depending on the subsequent steps to be performed.

Sample size <100 µl: Smaller samples were ethanol precipitated as above, but with half the volumes of 8 M NH_4Ac and 95% EtOH.

2.2.2.7 Phosphatase Treatment Of Vector

The digested vector was mixed with one unit of Shrimp Alkaline Phosphatase (SAP) per picomole of 5' ends in dephosphorylation buffer (50 mM Tris-HCl, 5 mM $MgCl_2$, pH 8.5) in a final volume of 10 μl. The reaction was allowed to proceed for 10 minutes at 37°C, before the phosphatase was heat killed by incubation at 65°C for 15 minutes.

2.2.2.8 Ligations

Initially ligation reactions were performed with a 3:1 molar ratio of insert to vector in ligation buffer (50 mM Tris-HCl pH 7.6, 10 mM $MgCl_2$, 1mM ATP, 1 mM DTT, 5% (w/v) polyethylene glycol-8000) with 1.5 units of T4 DNA ligase, in a final volume of 20 µl, with 30 fmol of vector. The ligation reaction was incubated overnight at 15°C.

For subcloning the CCT-236Δ12-16 and CCT Δ12-16 constructs into pAX142, the Fermentas Rapid Ligation Kit was used as per the manufacturers instructions, with a 1h incubation period.

2.2.2.9 Competent Cells

DH5*α*: 5 ml of LB media was inoculated with a single colony of DH5*α* *E. coli* and grown overnight with shaking at 250 rpm at 37°C. One ml of the overnight culture was used to start growth in 250 ml pre-warmed LB, and was grown with shaking (250 rpm) at 37°C until the optical density of the culture

reached 0.6 at 600 nm. Cultures were spun at 3700 rpm for 10 minutes at 4°C. The cell pellet was resuspended in cold 10 mM $MgCl_2$. and respun for an additional 10 minutes. The resulting cell pellet was resuspended in cold 50 mM $MgCl_2$ and incubated on ice for 30 minutes before a third 10 minute centrifugation. The cells were resuspended in cold 50 mM $MgCl_2$, 20 % (v/v) glycerol and incubated on ice for at least one hour before aliquoting into 100 μl volumes and flash freezing in a dry ice/ethanol bath. Competent cells were stored at –80°C.

DH5α p3: Competent cells for this strain of *E. coli* were made using a Mg-free protocol to prevent the Mg from inhibiting the tetracycline at later steps. A fresh colony of DH5α p3 was used to inoculate 1 ml of TY (5 g NaCl, 20 g bacto-tryptone, 5 g yeast extract/L), which was grown overnight at 37°C with shaking (250 rpm). This culture was added to 20 ml pre-warmed TY and grown to mid log phase, at which point it was added to 200 ml pre-warmed TY and grown to $O.D._{600}$ = 0.6. The culture was chilled on ice and centrifuged for 15 minutes at 3500 rpm at 4°C. The cell pellet was resuspended in cold TfBI (30 mM KOAc, 50 mM $MnCl_2$, 100 mM KCl, 10 mM $CaCl_2$, 15% (v/v) glycerol, pH7.0) and re-centrifuged as before. The cell pellet was resuspended in cold TfBII (10 mM Na-MOPS pH 7.0, 75 mM $CaCl_2$, 10 mM KCl, 15% (v/v) glycerol). Cells were aliquoted, frozen and stored in the same manner as the DH5α competent cells.

Competent cell transformation: Competent cells were allowed to thaw on ice for 10 minutes prior to the gentle addition of 1.0 μg of plasmid DNA or 5 μl ligation product, and were then incubated on ice for 20 minutes. Next, the cells

were heat-shocked in a 40°C water bath for 3 minutes then transferred to ice for 2 minutes. 0.5 ml of prewarmed LB was added and the culture was shaken at 250 rpm for one hour at 37°C. 100 and 500 μls of transfected cells were plated on LB plates containing the appropriate antibiotics, and grown overnight (a maximum of 16 hours) at 37°C.

2.2.3 Construction Of CCT Mutants

CCT mutants were engineered using CCT inserted into pBluescript KS (-) vectors to facilitate sequencing. The mutant CCT constructs were then spliced into pAX142 for expression in COS cells.

2.2.3.1 pAX-His CCT K8R/K13R/K16R

pBS-His WT CCT was amplified by PCR using an oligonucleotide primer containing lysine to arginine mutations at positions 8,13 and 16, and a primer complementary to the T7 primer region of pBS (See Appendix B). The PCR product was digested with SacI and KpnI to form a fragment 481 bp long, and was ligated into pBS KS (-) empty vector opened with SacI and KpnI (2859 bp). The pBS vector then contained His-tagged CCT with the desired mutations, but only up to Gly 20, the KpnI site. The remainder of the CCT sequence (1225 bp) was cleaved from pBS-WT CCT with KpnI and ligated into pBS-His CCT K8R/K13R/K16R (3340 bp), which was linearized with KpnI. The correct orientation of the insert was confirmed by diagnostic digest with XhoI. pAX142 empty vector was cleaved with MluI and SalI and the 2745 bp fragment was

ligated with the 1311 bp fragment of pBS-His CCT K8R/K13R/K16R, which was also digested with MluI and SalI (Figure 2.1).

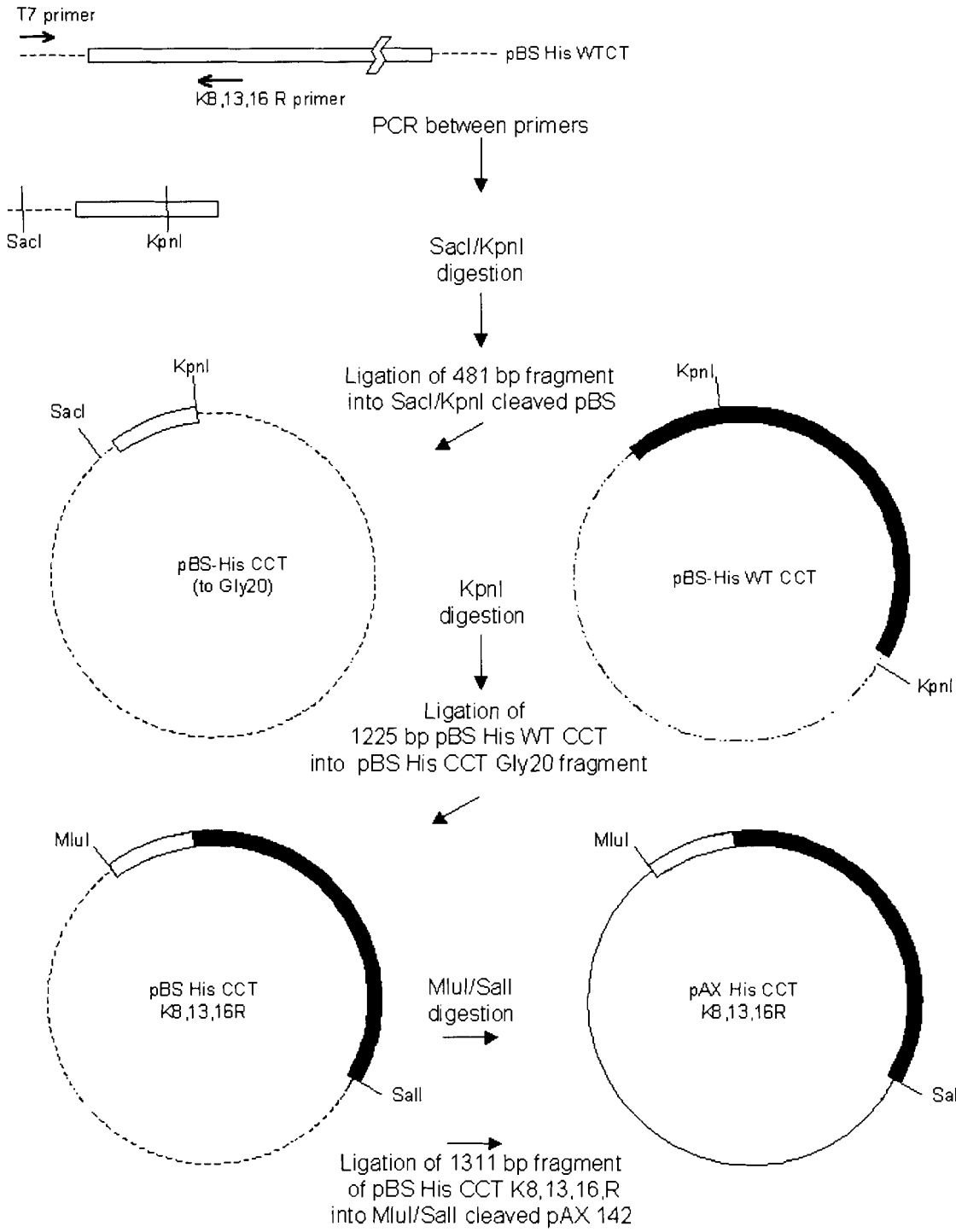

Figure 2.1 Construction of pAX-His CCT K8R/K13R/K16R

2.2.3.2 pAX-His CCT K33R

This mutation was made using the QuikChange Site-Directed Mutagenesis protocol (Stratagene) using pBS-His WT CCT as a template. pBS-His CCT K33R was digested with MluI and EcoRV and the 566 bp fragment was ligated into the 3600 bp fragment of pAX-CCT C354,359S, which had also been digested with MluI and EcoRV (Figure 2.2). Using CCT with the C-terminal cysteines mutated to serine was intended to minimize the amount of aggregation due to auto-oxidation, as suggested by a previous lab member. As it happens, these mutations did little or nothing to prevent the aggregation of the protein.

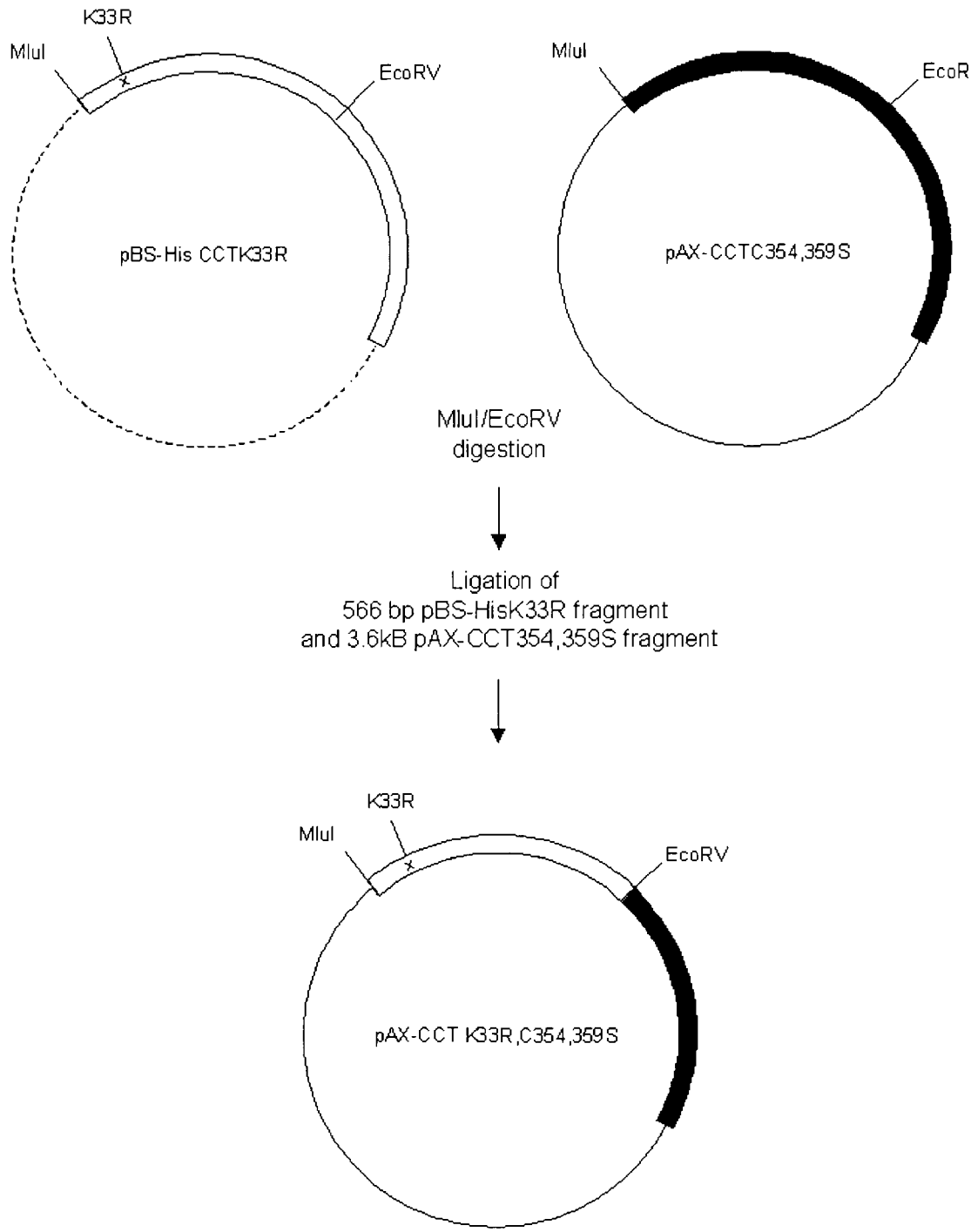

Figure 2.2 Construction of pAX-His CCT K33R

2.2.3.3 pAX-His CCT K57Q

This mutation was made using the QuikChange Site-Directed Mutagenesis protocol using pBS-His WT CCT as a template. PBS-His CCT K57Q was digested with MluI and SspI and the 307 bp fragment was ligated into the 3849 bp fragment of pAX-His WT CCT, which had also been digested with MluI and SspI (Figure2.3).

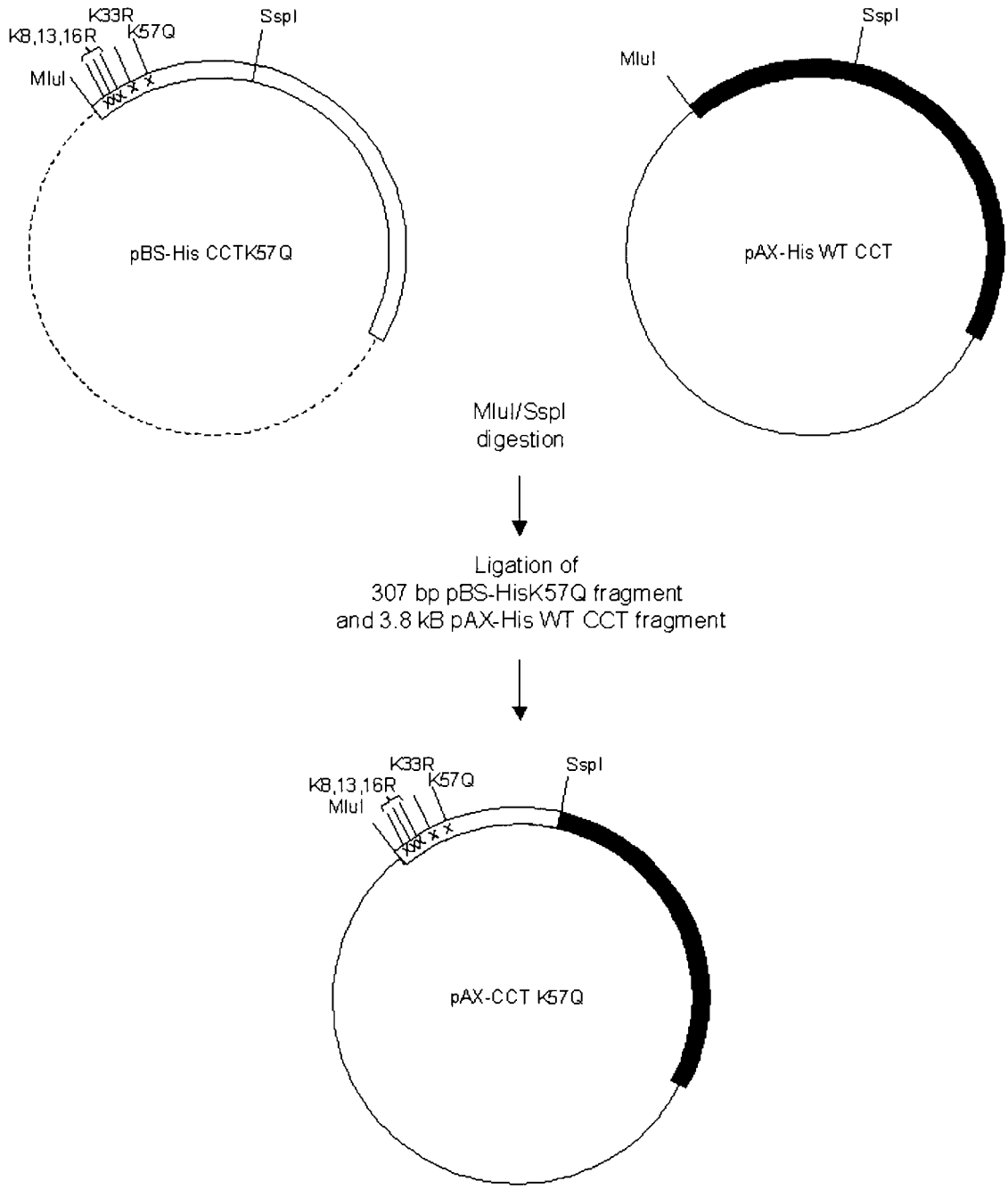

Figure 2.3 Construction of pAX-His CCT K57Q

2.2.3.4 pAX-His CCT K8R/K13R/K16R, K33R, K57Q (K free N-terminal CCT)

The lysine-free N-terminus of CCT was made with two rounds of mutagenesis using the QuikChange Site Directed Mutagenesis protocol. First, using pBS-His CCT K8R/K13R/K16R as a template, the lysine at position 33 was mutated to arginine with the same primer used above to make the single mutation. Once the sequence was confirmed, the product, pBS-His CCT K8R/K13R/K16R, K33R was then used as the template for a second round of mutagenesis to incorporate the K57Q mutation, again using the primer previously used to make the single K57Q mutation. pBS-His CCT K8R/K13R/K16R, K33R, K57Q was digested with MluI and SspI and the 307 bp fragment was ligated into the 3849 bp fragment of pAX-His WT CCT, which had also been cleaved with MluI and SspI (Figure 2.4).

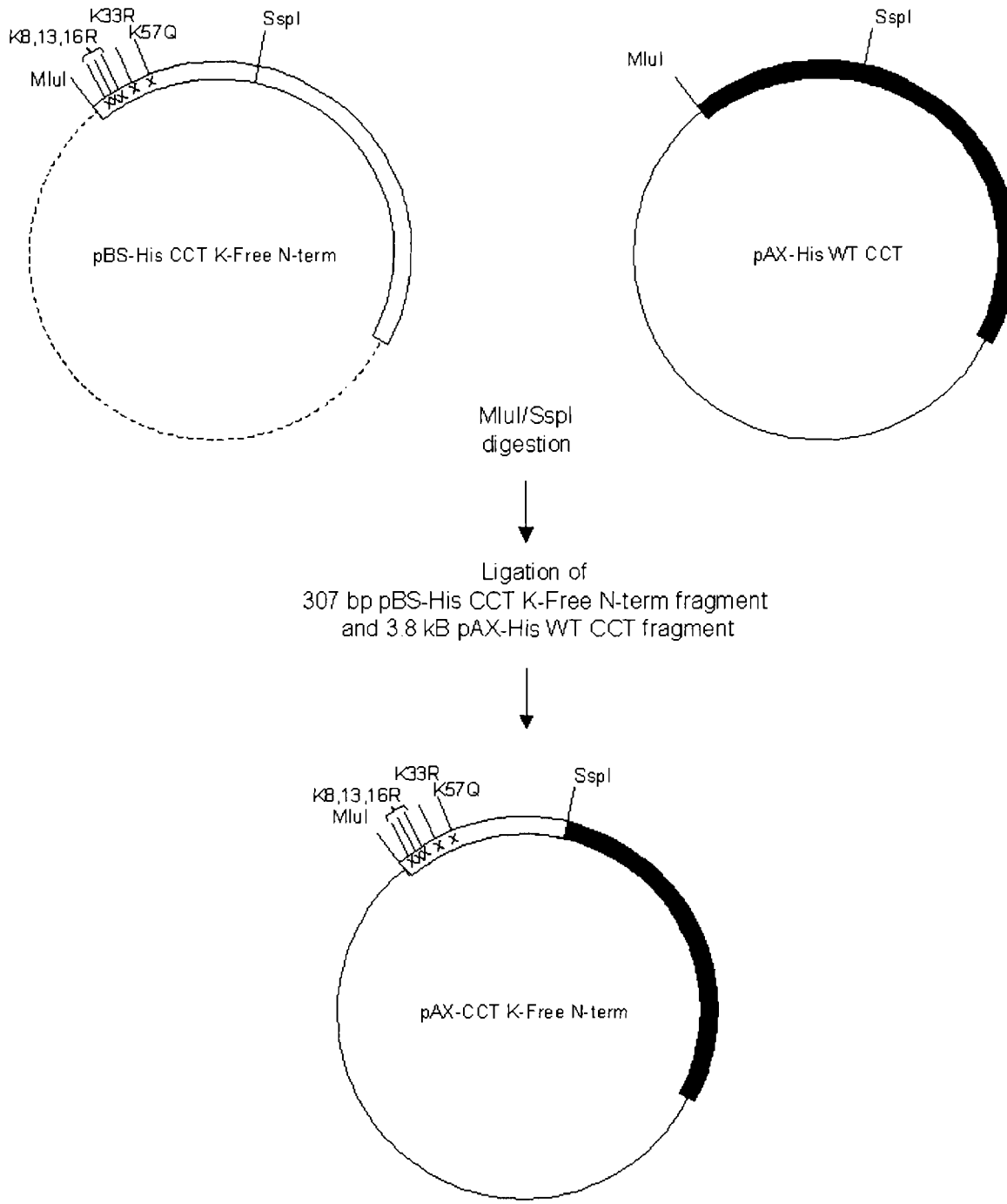

Figure 2.4 Construction of pAX-His CCT K free N-term

2.2.3.5 pAX-His CCT 236

The truncated form of CCT, CCT 236, was in the vector pCTV, which was unsuitable for our needs. pBS-His WT CCT and pCTV83.G2 (CCT 236) were both digested with AccI, which cuts at codon 142, as well as at the SalI site that follows the C-terminal stop codon of both versions of CCT. The 288 bp fragment of CCT 236 was ligated into the 3389 bp fragment of pBS-His WT CCT, to make pBS-His CCT 236. pBS-His CCT 236 and empty vector pAX142 were digested with MluI and SalI, and the 769 bp fragment of His CCT 236 was ligated into the 2845 bp fragment of pAX, to make pAX-His CCT 236 (Figure 2.5).

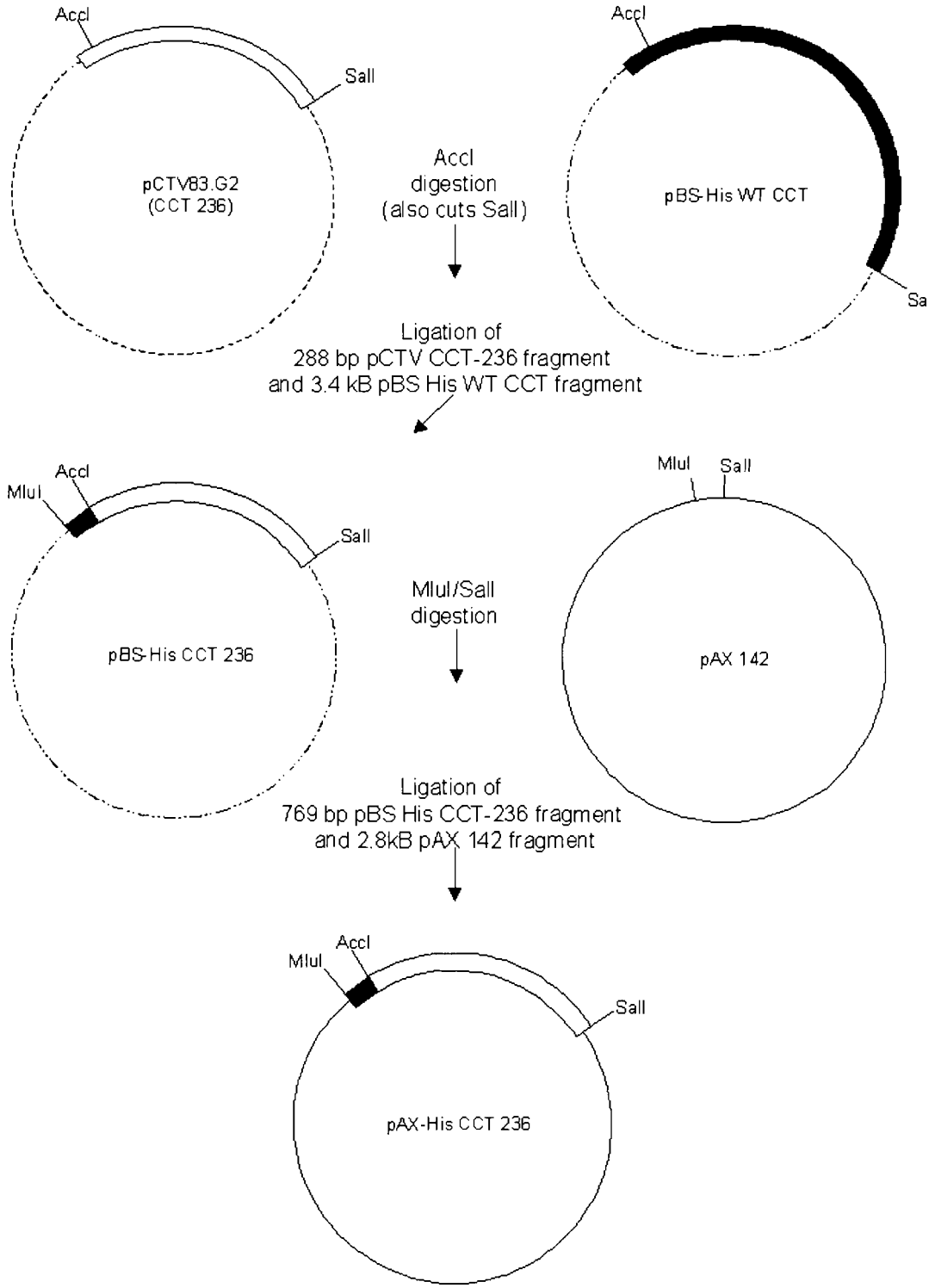

Figure 2.5 Construction of pAX-His CCT 236

2.2.3.6 pAX-His CCT 236 Δ12-16

Deletion mutations were also made using the QuikChange Site Directed Mutagenesis protocol, using pBS-His CCT 236 as a template. pBS-His CCT 236 Δ12-16 and empty pAX vector were digested with MluI and SalI, and the 754 bp fragment of CCT 236 Δ12-16 was ligated into the 2845 bp fragment of the pAX vector (Figure 2.6).

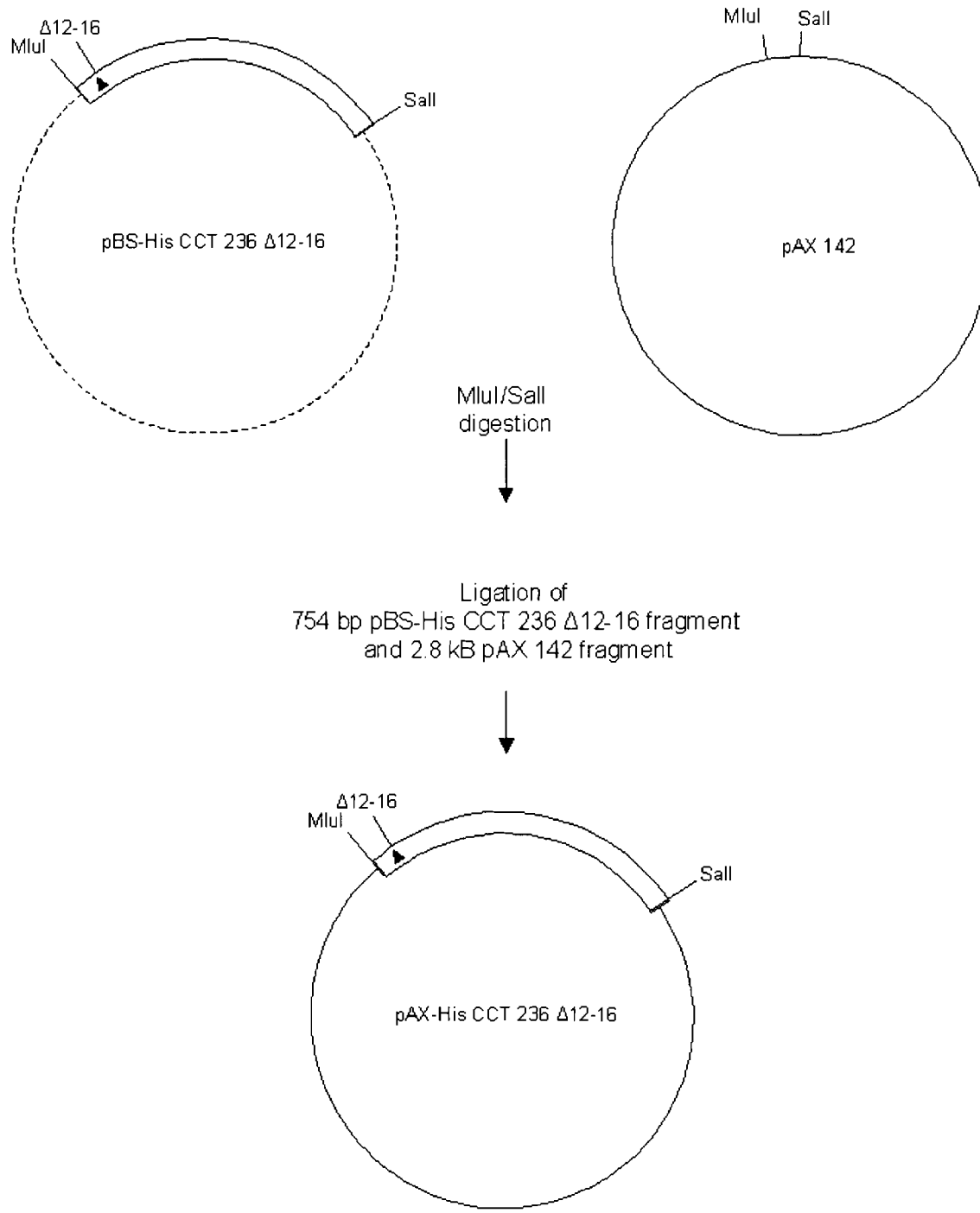

Figure 2.6 Construction of pAX-His CCT 236 Δ12-16

2.2.3.7 pAX-His CCT Δ12-16

pBS-His CCT 236 Δ12-16 was digested with MluI and SspI. The 292 bp fragment was ligated into the 3849 bp fragment of pAX-His WT CCT, which had also been digested with MluI and SspI (Figure 2.7).

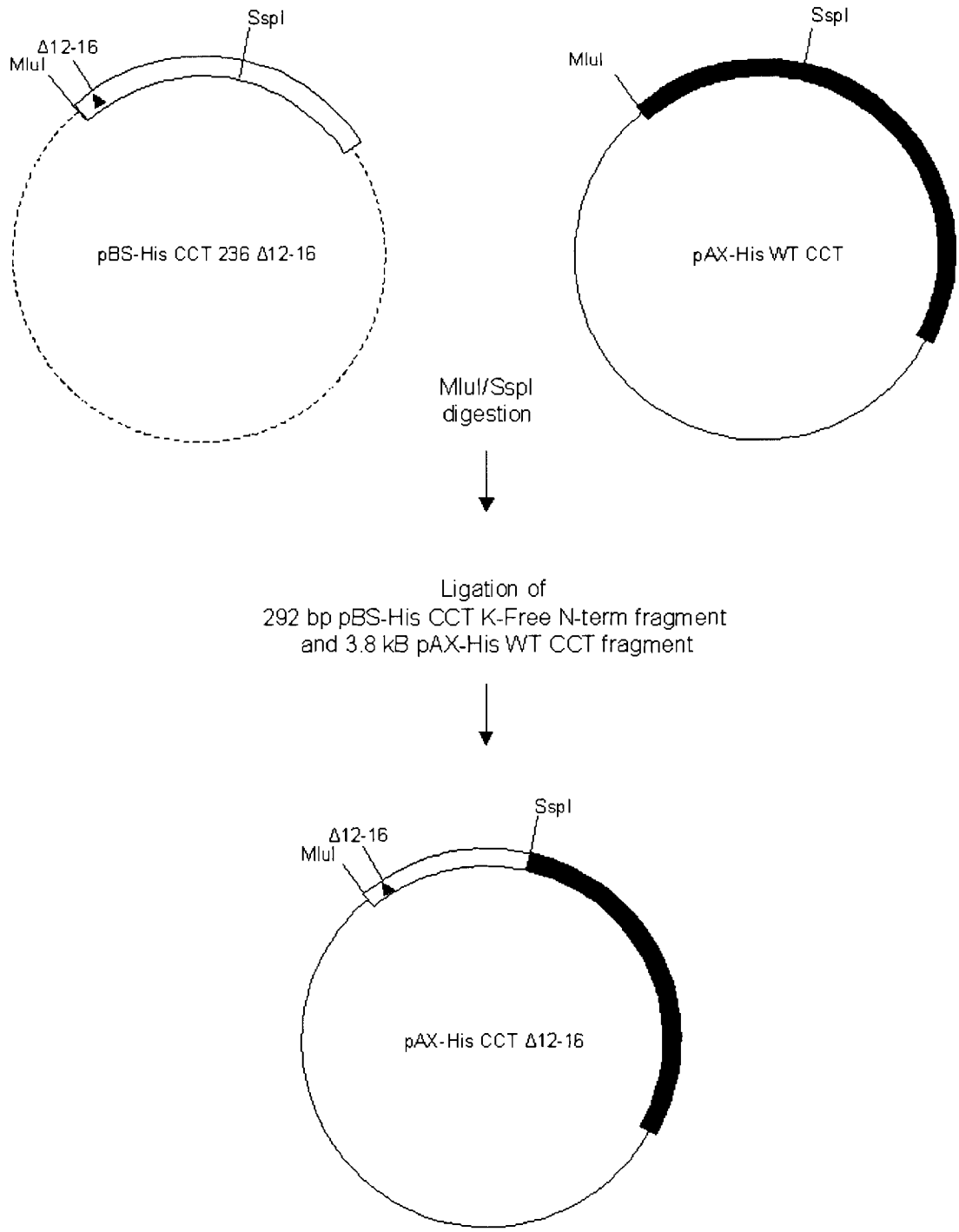

Figure 2.7 Construction of pAX-His CCT Δ12-16

2.2.4 COS-1 Cells

COS-1 cells are fibroblast-like cells derived from the African green monkey kidney. Permissive to lytic growth, COS cells are transformed with an origin-defective mutant of simian virus 40 (SV40) to drive the rapid replication of transfected plasmids containing the SV40 origin of replication,[66] to the order of several hundred thousand copies per cell over the 64 hour transfection incubation period[65]. They are used for high-level expression of mammalian proteins that require post-translational modifications not performed in the more commonly used bacterial expression systems.

2.2.4.1 Cell Line Maintenance

COS-1 cells are adherent cells that will replicate until a monolayer of cells covers the surface of the dish, at which point cells must be diluted and passaged. COS cells were grown in 10 cm dishes with 10 ml of Dulbecco's Modified Eagle Medium supplemented with 5% (v/v) Fetal Bovine Serum, 0.37% (w/v) $NaHCO_3$, 10 U/ml penicillin and 10 μg/ml streptomycin (complete media) at 37°C, under 5% CO_2. Plates seeded with cells thawed from stock cultures were grown to 80-90% confluence and the cells were detached from the plates by incubation with 0.05% (w/v) trypsin and 0.02% (w/v) EDTA for 2 minutes at 37°C, 5% CO_2, diluted 10-fold with the addition of fresh media and transferred to new plates. Cells were passaged every three days.

2.2.4.2 COS-1 Cell Transfection

The transfection protocol uses endocytosis of DEAE-dextran-conjugated DNA, lysosome poisoning with chloroquine and a glycerol shock of the cells.

Cells were subcultured 24 hours preceding transfection, and plated at a density of 1.0 x 10^6 cells/10 cm dish or 2.5 x 10^6 cells/15 cm dish. At the time of transfection, plates were ~80% confluent. Plates were washed with TS (140 mM NaCl, 25 mM Tris pH 7.5, 5 mM KCl, 0.5 mM Na_2HPO_4, 1 mM $MgCl_2$, 1 mM $CaCl_2$) prior to the addition of either the empty pAX142 vector or pAX-CCT DNA (10 µg/10 cm dish or 25 µg/15 cm dish, in 0.5 mg/ml DEAE-Dextran in TS) and were then incubated for 40 minutes at 37°C, 5% CO_2. The unattached DNA solution was aspirated off and replaced with Special Media (DMEM, 0.37 % (w/v) $NaHCO_3$, 10 mM Hepes pH 7.4,100 µM chloroquine, 5% (v/v) FBS), followed by a three hour incubation at 37°C, 5% CO_2. The Special Media was aspirated from the plates. The cells were washed with TS and then shocked for 2 minutes with TS/20% (v/v) glycerol at room temperature. Complete media replaced the glycerol solution after two washes with TS, and cells were incubated for ~64 hours at 37°C, 5% CO_2.

2.2.4.3 Harvesting Of Transfected COS-1 Cells

10 cm plates of transfected COS-1 cells were washed with prewarmed (37°C) phosphate buffered saline (PBS) (15 mM KH_2PO_4, 8 mM Na_2PO_4, 14 mM NaCl, 2.7 mM KCl, pH 7.4) then incubated for 5 minutes, with pre-warmed PBS/2.5 mM EDTA, at 37°C, 5% CO_2. Cells were either dislodged by repeated pipeting or gently scraped off the plate with a rubber policeman. Plates were

washed again with PBS and the wash was combined with the first cell suspension, and centrifuged at 2000 rpm for 3 minutes. All of the supernatant was aspirated and the cell pellet was resuspended in 0.5 ml of homogenization buffer (10 mM Tris pH 7.4, 1 mM EDTA, 1 mM PMSF, 2 mM DTT) and sonicated on ice for 30 seconds with a Fisher Sonic Dismembrator Model 300 at 30% output, to completely lyse the cells. NaCl was added, with immediate vortexing, to a final concentration of 0.1 M. This whole cell homogenate was aliquoted and stored at -70°C or processed to isolate the CCT.

2.2.5 Protein Purification

2.2.5.1 Batch Method For His-tagged Protein Purification

COS cells from fifteen 10 cm plates were harvested from the dishes as described above and pooled. The cell pellet was washed several times with chilled PBS and centrifuged at 1200 rpm for 4 minutes. The volume of the cell pellet was measured and 0.3 ml hypotonic buffer (20 mM KPi, pH 7.4) containing protease inhibitors (2.5 µg/ml leupeptin, 2 µg/ml chymostatin, 1 µg/ml antipain, 2 µg/ml pepstatin, 10 µg/ml p-amino-benzadine, 10 µg/ml benzamidine, 2 mM PMSF) was added per plate of cells. This homogenate was sonicated on ice until the cells were completely lysed, approximately three 30s bursts of the Fisher Sonic Dismembrator at 30% output. 10X binding buffer (50 mM NaPi, 5M NaCl, 150 mM imidazole, pH 8.0) was added to 1X and gently mixed on a slow vortex. The homogenate was equally divided amongst 1.5 ml Beckman centrifuge tubes and centrifuged for one hour at 45 000 RPM at 4° C in a Beckman Optima TLX Ultracentrifuge. The resulting supernatant (or cytosol) was transferred to 1.5 ml

Eppindorf tubes. The pellet (or microsome) was resuspended (in the same volume as supernatant removed) in hypotonic buffer/binding buffer, and sonicated until resuspended. A 1/8 volume of a 50% slurry of Ni-NTA Agarose beads was added to each Eppindorf tube containing supernatant. The remaining steps took place in a 4°C cold room. The resulting mixture was rotated for 1h to ensure complete binding of His-tagged protein to the nickel-charged beads, then centrifuged at 13 000 rpm for 2 minutes. The supernatant was removed and saved at -80°C. The beads were washed for 15 minutes with rotation, 3 times, in wash buffer 1 (50 mM NaPi, 0.5 M NaCl, 25 mM imidazole, 1% (v/v) NP-40, pH 8.0) and twice with wash buffer 2 (50 mM NaPi, 100 mM NaCl, 25 mM imidazole, pH 8.0) before pooling the beads in one tube for a final wash with wash buffer 2. All wash fractions were kept at -80°C. Bound His-tagged protein was eluted from the Ni-NTA Agarose beads by the addition of 200 µl elution buffer (50 mM NaPi, 100 mM NaCl, 350 mM imidazole, pH 8.0) followed by rotation for 15 minutes, centrifugation at 13 000 rpm for 2 minutes and careful removal of the supernatant. This was repeated twice more, and all supernatants were pooled. Triton X-100 was added to the pooled protein to a final concentration of 0.15 mM, followed by dialysis overnight in > 500 ml dialysis buffer (20 mM KPi, 100 mM NaCl, 0.15 mM Triton X-100, pH 7.4). Dialysis was necessary because imidazole, while not containing a primary amine, interferes with NHS-ester cross-linking. Dialyzed protein was aliquoted in 50 µl fractions and stored at -80°C.

2.2.5.2 Column Method For His-tagged Protein Purification

COS cells from six 15 cm plates were harvested from the dishes as described above and pooled. The cell pellet was washed several times with chilled PBS and centrifuged at 1200 rpm for 4 minutes. The volume of the cell pellet was measured and 0.75 ml of hypotonic buffer (with protease inhibitors) was added per plate harvested. The homogenate was sonicated as described in the Batch Method to lyse the cells. A 1:10 volume of 10X binding buffer was added and gently vortexed to mix. The homogenate was transferred to 1.5 ml Eppindorf tubes and centrifuged at 12 000 rpm for 10 min at 4°C. The pellets of cellular debris were floated (in the same volume as supernatant removed) in hypotonic buffer/binding buffer, pooled and sonicated briefly to resuspend. The supernatants (or cytosols) were transferred and pooled in a 15 ml Falcon tube to which was added a 1/8 volume of a 50% slurry of Ni-NTA Agarose beads. The resulting mixture was rotated for 2 hours at 4°C to ensure complete binding of His-tagged protein to the nickel-charged beads. After binding, the bead/supernatant mixture was poured into a 1 cm x 10 cm column fitted with a stopcock and left to settle at 4°C. The sample was passed through the column and the flow through was collected and passed over the column again. The column was washed twice: first with wash buffer 1, then with wash buffer 2. His-tagged protein was eluted from the column with the addition of elution buffer and collected in approximately 300 µl fractions. A sample of each fraction was run on a 10% SDS-PAG to determine the fractions with the highest protein concentration. Those fractions were then pooled and Triton X-100 was added to a final concentration of 0.15 mM. The pooled protein was then dialyzed overnight

at 4°C against > 500 ml dialysis buffer. Triton (0.15 mM) is required to prevent the formation of an insoluble protein aggregate. Dialyzed protein was aliquoted in 50 µl fractions and stored at -80°C. All flow-throughs, washes and fractions of the purification process were saved at -80°C.

2.2.5.3 Untagged Protein Purification

Untagged WT CCT and CCT 236 were expressed using the baculovirus expression system and were purified as described in [26].

2.2.6 CCT Activity Assay

2.2.6.1 Preparation Of Materials

Sonicated phospholipid vesicles: Appropriate volumes of phospholipids and oleic acid to give equimolar ratios were aliquoted from chloroform stocks to a 5 ml round bottom flask. The lipid mixture was evaporated to dryness for 15 minutes at 37°C, using a rotary evaporator. The dried lipids were resuspended in 1 ml liposome buffer (10 mM Tris, 1 mM EDTA, pH 7.4) and vortexed to resuspend. The suspension was sonicated with a Heat Systems Ultrasonic Processor W-375 set at 30% duty cycle, on ice for 5 minutes until the solution became clear, and was then centrifuged for 3 minutes at 13 000 rpm to remove any titanium debris sloughed from the sonicator probe. Lyso phospholipids were prepared in the same manner as the diacyl lipid vesicles.

SDS and CTAB detergents were prepared by dissolving powder stocks in water and vortexing.

[^{3}H]-phosphocholine was prepared from [^{3}H]-choline, ATP and choline kinase. The tritiated phosphocholine was separated on a Dowex-1 column and supplemented with non-radioactive phosphocholine to a final concentration of 10 mM and a specific activity of about 10 Ci/mol. CTP stocks were made in 100 mM Tris, pH 7.4 and the pH adjusted to pH 7.4 with 1 N NaOH.

2.2.6.2 Standard Assay

The CCT activity assay measures the amount of labelled CDP-choline produced by CCT using [^{3}H]-phosphocholine as a substrate. To start the reaction, [^{3}H]-phosphocholine was added to 1.5 ml microfuge tubes containing 20 mM Tris pH 7.4, 12 mM $MgCl_2$, 8 mM CTP, 88 mM NaCl, 100 µM PC/O (1:1) vesicles, 20 mM DTT and ~0.1 μg enzyme for a final volume of 50 µl and a final [^{3}H]-phosphocholine concentration of ~1.0 mM. The reaction was allowed to proceed for 15 minutes in a 37°C shaking water bath, and was stopped with the addition of 30 µl of 9:1 MeOH:NH_3. Samples were centrifuged briefly and [^{3}H]-CDP-choline was separated from the mixture via thin layer chromatography on plastic backed silica plates in a solvent of MeOH:0.6% (w/v) NaCl:NH_4OH, 5:5:1. [^{3}H]-CDP-choline was visualized on the TLC plate by spraying with 0.02% (w/v) dichlorofluoresceine and exposing it to short-wave UV light. The labelled product was scraped from the TLC plate and quantitated by liquid scintillation counting.

The activity of CCT was determined from either whole cell homogenates or purified protein and all fractions associated with purification. Standard conditions were used for full-length wild-type CCT and all CCT mutants that were of full-length.

2.2.6.3 Assay Under Non-Standard Conditions

CCT truncated after amino acid 236 is constitutively active. In the absence of lipid CCT 236 has a CTP K_m of ~3.2 mM compared to the CTP K_m of WT CCT which is ~1.7 mM[67] . Thus, CCT 236 and all CCT 236 mutants were assayed in the presence of 10 mM CTP.

2.2.7 Electrophoresis And Western Blotting

2.2.7.1 Protein Determination

The concentration of protein samples was determined using the Bradford method[68]. Standard (0-24 µg ovalbumin) and sample volumes were adjusted to 100 µl to which 1 ml of Bradford Dye Reagent (0.005% (w/v) Coomassie Brilliant Blue R, 5% (v/v) EtOH, 10% (v/v) H_3PO_4) was added while vortexing. Samples and standards were incubated for 15 minutes in a 37°C water bath, and the absorbance was read at 595 nm on a Beckman DU 640 Spectrophotometer.

2.2.7.2 Gel Electrophoresis

Proteins were separated on either 10 or 11% SDS-polyacrylamide gels using Bio-Rad's Mini-PROTEAN II gel apparatus[69] at a constant current of 30 mA, for ~45 minutes in Running Buffer (25 mM Tris pH 8.3, 192 mM glycine, 0.1% (w/v) SDS).

2.2.7.3 SDS-PAG Staining

Coomassie Staining: After electrophoresis, gels were fixed in Coomassie stain (0.3% (w/v) Coomassie Brilliant Blue R, 45% (v/v) MeOH, 10% (v/v) HAc) for at least one hour, destained for 10-15 minutes in Fast Destain (40% (v/v)

MeOH, 10% (v/v) HAc) followed by several hours in Slow Destain (7% (v/v) MeOH, 5% (v/v) HAc).

SYPRO Orange Protein Gel Staining: Gels stained with SYPRO Orange were electrophoresed in a running buffer containing 0.05% (w/v) SDS rather than the standard 0.1% SDS, to prevent excess background staining. After electrophoresis, gels were incubated with shaking for 30 minutes in Sypro Orange (1:5000 dilution in 7.5% (v/v) HAc), in a lightproof container. Gels were destained (7.5% (v/v) HAc) with shaking for 30 minutes. Stained gels were immediately visualized using the fluorescence mode of a Typhoon 9410 Variable Mode Imager with a 488 nm blue laser and a 580 nm filter. Gels were then silver stained.

Silver Staining: All steps took place on a bench top shaker. Gels were fixed during a 20 minute incubation with 50% (v/v) MeOH, 10% (v/v) HAc and rinsed with 15% (v/v) MeOH. Gels were then oxidized with a 10% (v/v) glutaraldehyde solution for 20 minutes and were washed with 15% (v/v) MeOH, rinsed in H_2O and stained with Silver Stain (16 mM NaOH, 0.3% (v/v) NH_4OH, 0.8% (w/v) $AgNO_3$) for 10 minutes. Gels were thoroughly washed with H_2O and incubated in developer (0.26 mM citric acid, 0.2% (v/v) formaldehyde) until the desired level of staining was reached, typically 3-6 minutes. The developer was replaced with a 1% (v/v) acetic acid solution to stop the reaction.

2.2.7.4 Western Blotting

For full-length CCT: Following electrophoresis, proteins were transferred from the SDS-PAG to PVDF membrane using a Pharmacia LKB NovaBlot

transfer apparatus at 2 mA per cm^2 of gel surface area for 1 hour in transfer buffer (39 mM glycine, 48 mM Tris, 0.037% (w/v) SDS). The membrane was then blocked, for either 1 hour at room temperature or overnight at 4°C, in Blotto (0.5% (w/v) Tween-20, 10% (w/v) skim milk powder in PBS), followed by a 1hour room temperature incubation with the primary antibody, a rabbit antibody directed against residues 256-288 of the membrane binding domain of CCT, diluted 1:1500 in Blotto. Membranes were washed 3 x 10 minutes in a 0.5% (w/v) Tween-20/PBS solution, prior to incubation with the secondary antibody: GAR-HRP, diluted 1:1500 in Blotto. They were then washed as before, followed by a 10-minute rinse in PBS. Antibody-bound protein was visualized by chemiluminescence according to the manufacturers instructions.

For CCT 236: Proteins were transferred from the gel to PVDF membrane as described above. The rest of the procedure occurred at 37°C. The membrane was blocked for 1 hour in "Gello" (1% (w/v) gelatin in Tris buffered saline (TBS) (25 mM Tris, 2.8 mM KCl, 137 mM NaCl, pH 7.4) with 0.1% (w/v) Tween-20 (TTBS)) followed by a 1 hour incubation with rabbit antibodies directed against amino acids 164-176 of the CCT catalytic domain, diluted 2000-fold in Gello. This was followed by 5 x 5 minute washes in TTBS prior to a 1h incubation of the GAR-HRP conjugated secondary antibody diluted 1:1000 in Gello. The membrane was again washed in TTBS and visualized as described above.

2.2.8 Sample Concentration And/Or Buffer Exchange

Concentration of samples or of protein stocks was sometimes necessary to obtain the smaller volumes required for certain processes such as

electrophoresis. The protocol for sample concentration is the same as for buffer exchange. Amicon Ultra-4 (30 000 MWCO) centrifugal filter devices were washed with the same buffer as the sample, by applying the buffer to the filter column and centrifuging at 3000 rpm, for 20 minutes at 4°C. The retenate was removed from the filter devices, and the sample applied (sample volumes up to 4 ml). The sample and filter were then centrifuged at 4000 rpm at 4°C for the time necessary to reduce the retenate volume to the desired volume. Laemmli buffer was added directly to samples destined for electrophoresis. For samples that required buffer exchange, the new buffer was added to the concentrated sample in the appropriate volume. The filter walls were thoroughly rinsed with the sample, which was then removed from the device by pipeting with superfine pipette tips.

2.2.9 Chemical Cross-Linking

2.2.9.1 Glutaraldehyde Cross-Linking

A 25% (v/v) glutaraldehyde stock was diluted with ddH_2O to make a 250 mM solution. This was stored at –20°C for several months. Prior to use, a working stock was diluted to 10 mM in ddH_2O. Glutaraldehyde cross-linking reactions were usually 30 μl in volume, and contained 0.4 μM CCT, 0.15 mM Triton X-100 and 20 mM phosphate buffer. Samples were prewarmed to 37°C by incubating in a shaking water bath for 2 minutes. The reaction was begun with the addition of 10 mM glutaraldehyde to a final concentration of 1.0 mM. After 15 minutes in the shaking water bath, the reactions were quenched with a final concentration of 100 mM ethanolamine. The primary amine on ethanolamine

competes with lysine for any unconjugated cross-linker. Samples greater than 30 μl were concentrated in a speed vacuum prior to gel electrophoresis.

2.2.9.2 DSP/DSS Cross-Linking

The 20 mg/ml stock of DSP was dissolved in DMSO, and stored at –20°C for several months. Prior to use, an aliquot of the stock was diluted to 0.5 mg/ml in ddH_2O. A 100 mM stock of DSS was prepared in DMSO, and stored at -20°C for several months. Immediately prior to use an aliquot of the stock was diluted to 5 mM in ddH_2O.

DSP and DSS cross-linking reactions were typically 30 μl in volume and 0.4 μM CCT, 0.15 mM Triton X-100, and 20 mM phosphate buffer. The buffer must be devoid of Tris or any other primary amines to prevent interference with the cross-linkers). The samples were placed in a 37°C shaking water bath for 2 minutes prior to the addition of cross-linker to a final concentration of 1-2 mM. The reaction was allowed to proceed for 30 minutes in the water bath before quenching. DSP and DSS reactions were quenched with excess ammonium acetate. The primary amine on NH_4Ac competes with lysine for any unconjugated cross-linker. Samples cross-linked with DSP were run on SDS-PAG without β-mercaptoethanol, as reducing agents cleave the thiol bond in the centre of the cross-linker, reversing any cross-linking that occurred. Sample volumes greater than 30 μl were concentrated in a speed vac prior to electrophoresis.

2.2.9.3 BS^3 Cross-Linking

BS^3 was prepared by dissolving a known amount of powder in DMSO to make a 100 mM stock solution. This was stored at –20°C for a maximum of one month. Immediately prior to use, an aliquot of the stock was diluted to 10 mM in ddH_2O. BS^3 cross-linking reactions were typically performed in a total volume of 30 μl and contained 0.4 μM CCT, 1 mM DTT, and 20 mM phosphate buffer (buffer must be devoid of Tris or any other primary amines to prevent interference with the cross-linker). Lipids were added to select cross-linking reactions at a concentration of at least 300 μM. Phospholipid vesicles for cross-linking experiments were made as for the CCT activity assay (section 2.2.6.1), but the dried lipids were resuspended in ddH_2O. The samples were placed in a 37°C shaking water bath for 2 minutes prior to the addition of 10 mM BS^3 to a final concentration of 1-2 mM. After 10-20 minutes in a shaking water bath the reaction was quenched with excess glycine (final concentration: 100 mM), where the primary amine on the α-carbon competes with the lysines for any unreacted BS^3. In the case where the reaction volume was greater than 30 μl, the samples were concentrated using Amicon filters, prior to gel electrophoresis.

2.2.9.4 Copper Phenanthroline Cross-Linking

A 2 mM $CuSO_4$ stock was prepared in ddH_2O. A 6 mM 1,10-phenanthroline stock was dissolved in ~80°C ddH_2O, then cooled to room temperature. Both the copper and the phenanthroline stocks were stored at –20°C for several months. Immediately prior to use, a 1:1 mixture of $Cu(Phe)_3$ was prepared. Reactions were typically 30 μl in volume: 0.4 μM CCT in a 20 mM

phosphate buffer. Buffers containing DTT and/or EDTA were avoided to maintain oxidizing conditions and to maintain free Cu^{2+}. Lipids were added to select cross-linking reactions at a concentration of at least 300 μM. The samples were placed in a 37°C shaking water bath for 2 minutes prior to the addition of the 1:1 copper:phenanthroline mix to a final concentration of 0.1 mM Cu^{2+} and 0.3 mM phenanthroline. In rare cases where extensive auto-oxidation of the purified protein had occurred, the CCT was first reduced in 2.0 mM DTT. The final concentration of DTT in the reaction was 0.16 mM and its presence was overcome by the use of double $Cu(Phe)_3$ i.e.0.2 mM Cu^{2+} and 0.6 mM phenanthroline. After 10 minutes in a shaking water bath the reaction was quenched with the addition of *N*-ethylmaleimide (NEM) to a final concentration of 10 mM. NEM alkylates free cysteines thus preventing oxidation and cystine bond formation. Sample volumes greater than 30 μl were concentrated in a speed vac prior to electrophoresis. The Laemmli buffer for electrophoresis was devoid of β-mercaptoethanol to prevent the reduction of oxidized cystine bonds.

Table 2.1 Final concentrations of all components of the cross-linking reaction mixtures
Concentrations vary depending on the volume of cross-linker or sample used.

Cross-linker:	Glutaraldehyde	1 mM
or	DSS/DSP	1 - 2 mM
or	BS^3	1 - 2 mM
or	Copper/phenanthroline	0.1/0.3 – 0.2/0.6 mM
Phosphate Buffer:		7 – 17 mM
DTT:		0 – 16 mM
Protein Sample:	CCT	0.4 μM
and	NaCl	2.5 – 33 mM
and	Triton X-100	3.75 – 50 μM
Lipids/Amphiphiles:		0 – 300 μM

3 LIPID MODULATION OF THE DIMER INTERFACE OF FULL LENGTH CCT

3.1 Introduction

CCT is known to be a dimer based on sedimentation, gel-filtration and cross-linking analyses[44,45]. Domains N and C, the region between amino acids 1-236, are sufficient for dimerization based on proteolysis and cross-linking results, showing that removal of the entire C-terminal tail (domains M and P) does not compromise the cross-linking efficiency[36,70]. The structurally homologous glycerolphosphate cytidylyltransferase (GCT) from *B. subtilis*, whose structure has been solved, is a dimer[27]. This 129 amino acid protein corresponds only to domain C of CCT. This implies that domain C of CCT may also be involved in inter-monomer contacts. However, the yeast-2 hybrid analysis of CCT domains showed clearly that domain N is critical for generating strong interactions across the CCT dimer interface[46,70]. Lastly, mutagenesis of each of the 7 cysteines in CCT followed by oxidation-induced cross-linking has shown that one portion of domain N – the region in the immediate vicinity of Cys-37 – is located with certainty in the dimer interface[46].Thus our working hypothesis is that the dimerization domain of CCT is comprised of both domains N and C.

As part of the investigation as to how membrane binding changes CCT conformation I have looked at the changes in the quaternary structure. Initial cross-linking results of CCT[46] showed that in the presence of activating lipids the

amount of covalently linked dimer is greatly reduced[46,71]. This result suggested two possible effects of membrane binding: (1) The dimer interface moves apart, or (2) the CT dimer becomes more rigid, and less likely to be cross-linked.

The work presented in this chapter had two goals: (1) to assess whether membrane binding affects the quaternary structure by perturbing the dimer interface; and (2) to identify lipid-modulated contact points within domain N. Since several amine-reactive cross-linking agents had captured dimer contacts, it was apparent that one or more lysine pairs are near the dimer interface. Furthermore these lysine-directed cross-links were not formed in the membrane-bound form of CCT, suggesting that they lie near the lipid-sensitive portions of the dimer interface. There are five lysines in domain N. To probe whether any of these lysines are at the lipid-sensitive dimer contact zones I used site-directed mutagenesis followed by lysine specific chemical cross-linking.

3.2 Results

3.2.1 Int*ra vs.* Int*er* Dimeric Cross-Linking

When lipid-free CCT was incubated with glutaraldehyde or the succinimidyl-based reagents, the 42 kDa monomer species observed on gels was converted to a diffuse molecular set between 80-110 kDa (Figure 3.1 A,B). Autoxidation of CCT during removal of DTT in preparation for $Cu(Phe)_3$ cross-linking generated species at 84 kDa and ~120 kDa, in addition to the monomeric band at 42 kDa. After incubation with $Cu(Phe)_3$ the 84 and 120 kDa bands became predominant, and the 42 kDa band disappeared (Figure 3.1 C lanes 4-6). The diffuse DSP-linked band at 80-110 kDa has been identified as heterogeneously linked homodimers by 2-D electrophoresis[34]. The identity of the 120 kDa disulfide linked species has not been resolved.

To test that cross-linked species represented bridging of monomers at their interface within a stable complex, rather than a capturing of transient collisions between monomers or dimers tumbling in solution, we examined the effect of protein dilution on the cross-linking efficiency. Diluting the protein concentration prior to cross-linking should suppress the formation of int*er*-dimer cross-linked species by eliminating the possibility for random collisions. If the cross-linked dimers we see are due to int*ra*-dimer interactions there should be no loss of intensity of the 84 kDa band because we are capturing dimers within stable complexes that would not change with the concentration of the protein. If the dimers are from int*er*-dimer interactions there will be a loss of dimer intensity

as the protein is diluted, due to fewer spurious interactions between CCT molecules (Figure. 3.2).

Figure 3.1 shows that even a 50-fold dilution in protein concentration did not reduce the intensity of the 84 kDa band/smear. While the concentration of the protein was varied, the quantity of CCT loaded on the SDS-PAG was equivalent in each lane. The dimer bands in the samples with larger volume do spread wider on the lanes of the gel due to higher salt content and therefore appear more faint; however, this is not a decrease in dimer formation, but rather a sideways diffusion of protein. Amounts of dimer at all volumes are roughly equivalent.

Additionally, higher order cross-linked oligomers were present in many samples as minor species. The oligomeric species also did not appear to be the result of transient collisions, since their prevalence was independent of sample dilution. This suggests a capacity for higher order complexes, however the functional significance of this is not known.

In summary, this data shows that cross-linking reactions across the dimer interface rather than inter-dimer collisions are captured using our conditions.

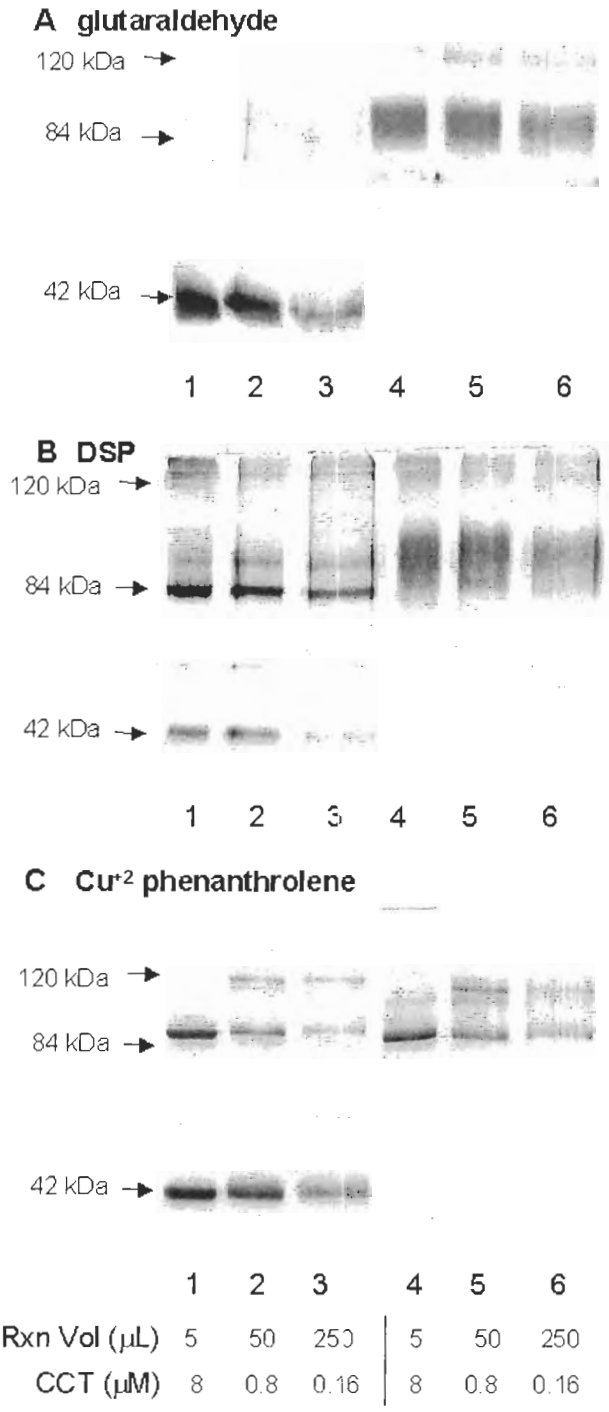

Figure 3.1 Protein dilution does not diminish cross-linking efficiency.
Purified untagged CCT was cross-linked with the indicated reagent at the indicated concentration. Lanes 1-3 were prequenched. Lanes 4-6 were quenched after (A)15 min (B) 30 min and (C) 10 min. Samples were subject to SDS-PAGE and stained with silver.

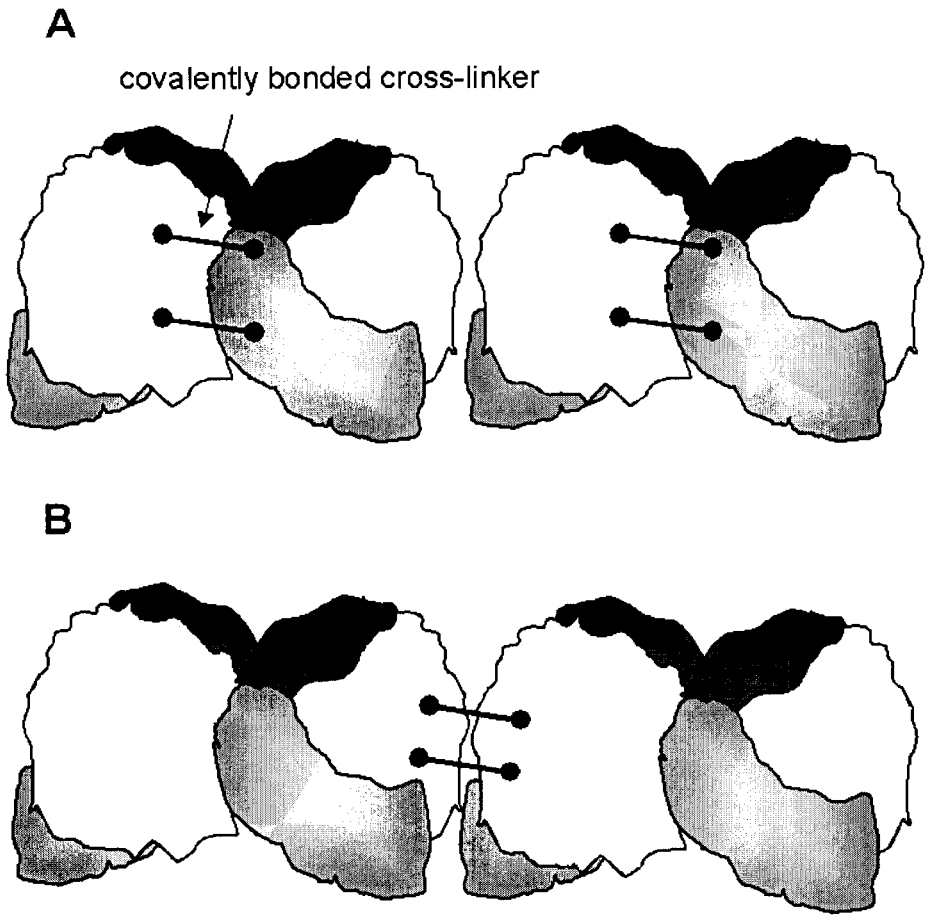

Figure 3.2 **Intra- *vs.* inter-dimer cross-linking.**
(A) Cross-linker is covalently bound across the dimer interface. (B) Cross-linker is covalently bound between subunits of two separate dimers. All interactions in the dimer interface are non-covalent; as a result, either cross-linking event would appear as an 84 kDa dimer on SDS-PAGE.

3.2.2 Lipid Binding Perturbs The Dimer Interface

A cross-linking time-course of CCT was performed with both BS^3 and glutaraldehyde, each in the presence and absence of PG vesicles. The amount of dimer species covalently cross-linked is greatly inhibited in the presence of PG (Figure 3.3 A). Fluorescent quantitation of Sypro Orange-stained monomer and dimer species of BS^3 cross-linked CCT, in the absence of lipid vesicles shows an

88% conversion to dimer, whereas there is only a 12% conversion to dimer in the presence of PG vesicles (Figure 3.3 B).

With glutaraldehyde as the cross-linker, the monomer band persisted in samples containing 400 M excess PG vesicles, with only a weak dimer band at 84 kDa appearing along with higher molecular mass oligomers (diffuse smear above 84 kDa in lanes 6-8 in Figure 3.3 C). Increasing the PG/CCT ratio from 400 to 4000 (to generate ~1 CCT/vesicle) reduced the proportion of large oligomeric species, and generated an increase in the proportion of monomer band at 42 kDa (Fig. 3.3 C, lane 9). This suggests that the higher molecular mass oligomers, prominent only at high CCT/vesicle ratios, are formed by covalent trapping of inter-dimer collisions on the surface of the vesicles, where the concentration of bound CCT molecules would be increased by ~4 orders of magnitude compared to CCT in the aqueous compartment. These results suggested that the PG vesicles were interfering with some aspect of the cross-linking reaction or were altering the structure of the dimer interface. The former possibility was ruled out by experiments showing that PG vesicles do not interfere with the BS^3 or glutaraldehyde mediated cross-linking of phosphoglycerate mutase, a non-membrane dimeric enzyme [46].

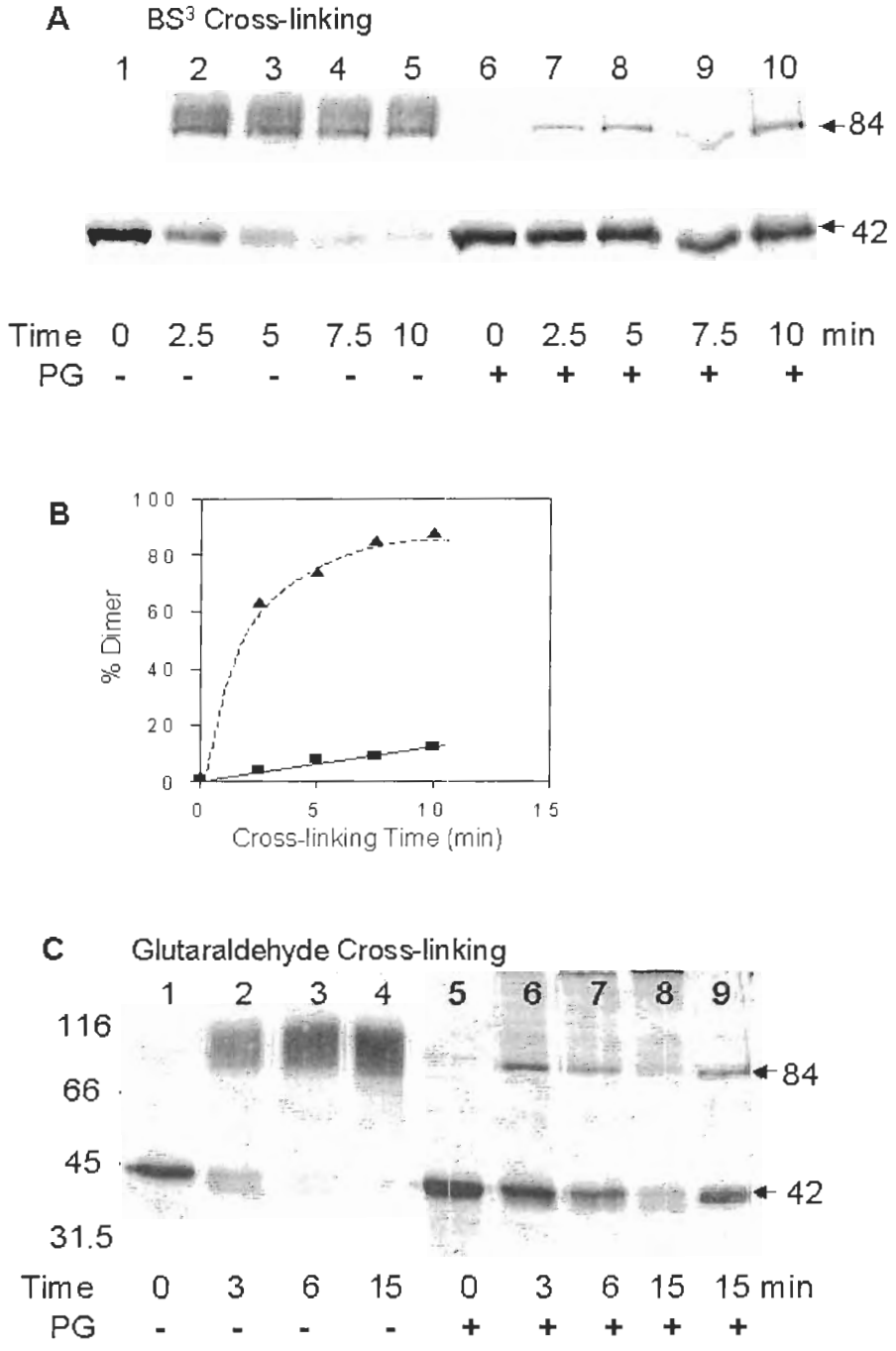

Figure 3.3 PG vesicles diminish cross-linking efficiency
(A) 0.39 μM CCT was incubated for 2 min. with or without 300 μM PG vesicles prior to cross-linking with 1 mM BS^3 for the time indicated. (B) fluorescence analysis of the Sypro Orange stained gel in (A), using Image Quant. ▲, samples without PG; ■, samples with PG. (C) 0.64 μM CCT was incubated for 5 min with or without 250 μM PG (or 2.5 mM lane 9) vesicles prior to cross-linking with 1mM glutaraldehyde for the time indicated. The experiment in (C) was performed by R. Cornell. Gel (A) was stained with Sypro Orange, then silver. Gel (C) was silver stained.

The experiment shown in Figure 3.4 explores the relationship between the membrane affinity of CCT and the reduction in cross-linking efficiency. CCT binds with highest affinity to PG and PA vesicles, which have high negative charge density, and with lower affinity to PC/OA (1:1) vesicles, and very poorly to PC vesicles[54,72]. The data shows a direct correlation between the reduction in cross-linking and the affinity of CCT for lipid vesicles.

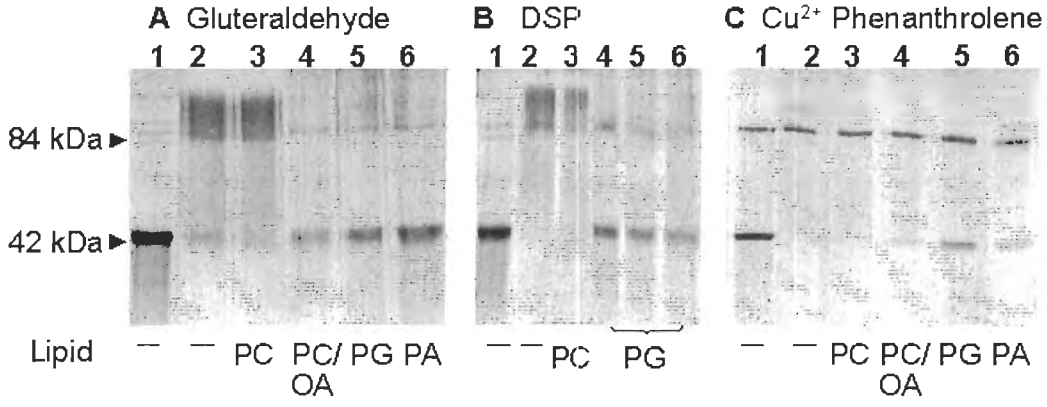

Reprinted with permission from (Xie, Smith *et al.*, 2004) Copyright © 2005 by the American Society for Biochemistry and Molecular Biology.

Figure 3.4 Anionic lipids reduce cross-linking efficiency
CCT was preincubated with the indicated lipid vesicles for 5 min prior to cross-linking with the specified cross-linker. Silver stained SDS-PAG. This experiment was performed by R. Cornell.

3.2.3 Domain N Provides A Lipid Sensitive Dimer Contact

Because CCT can form a disulfide-linked dimer under oxidizing conditions, and because membrane binding reduces the efficiency of the cross-linking, we wanted to identify the pair(s) of cysteine(s) putatively located in the dimer interface. A former member of the lab, Mingtang Xie, individually replaced each cysteine in CCT with serine (except the last two (C354, C359) which were replaced as a pair). The ability of these mutants to form disulfide-linked dimers

was tested with copper phenanthroline catalysed oxidation. Figure 3.5 shows that only CCT-C37S was present as a monomer after cross-linking. Engineering a single cysteine at position 37 in a cysteine-free CCT resulted in a reversion to dimer species after oxidation. These results proved that cysteine 37 is located in the dimer interface, but revealed nothing about the restructuring of the interface upon membrane binding.

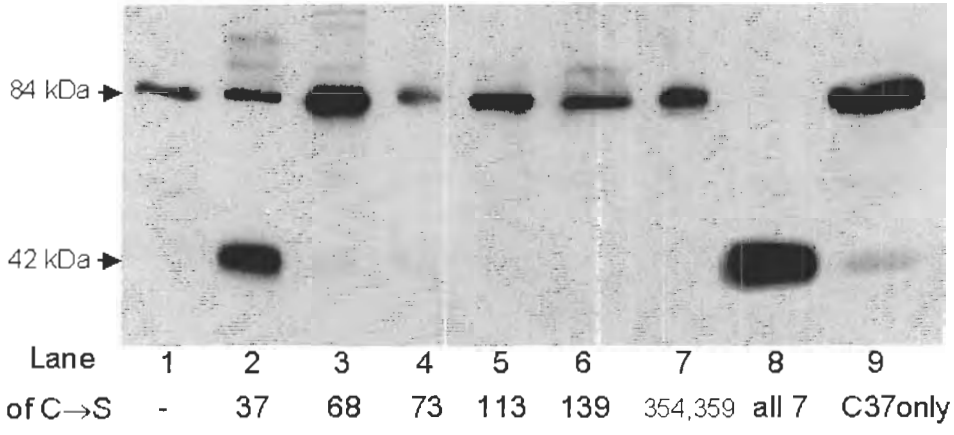

Reprinted with permission from (Xie, Smith *et al.*, 2004) Copyright © 2005 by the American Society for Biochemistry and Molecular Biology

Figure 3.5 Mapping the disulfide bond by mutagenesis.
Samples of His-tagged WT and mutant CCTs purified by Ni-agarose were cross-linked with $Cu(Phe)_3$. When cysteine 37 is mutated to a serine, disulfide cross-linking of CCT is greatly inhibited. Cross-linking is restored upon insertion of only C37 in a cysteine free CCT. Western blot with anti-domain M antibody.

I incubated CCT-C37 in buffer alone or with excess PG vesicles prior to oxidation with $Cu(Phe)_3$. In the absence of lipids, the CCT was almost fully cross-linked after 10 minutes, whereas the presence of PG vesicles resulted in the prevention of complete cross-linking (Figure 3.6). These data suggest that cys-37 is within the dimer interface and this region is restructured upon membrane binding.

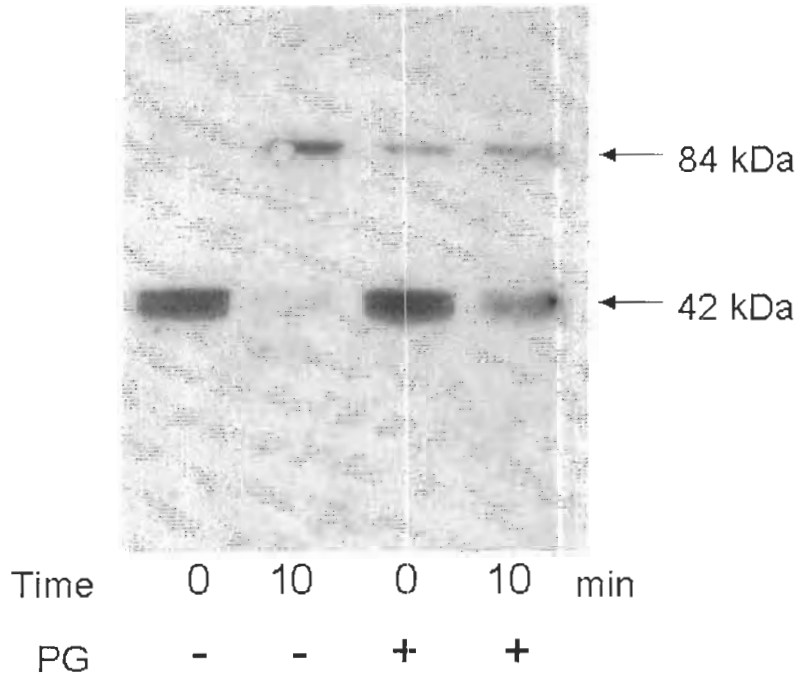

Figure 3.6 PG vesicles diminish the cross-linking efficiency of CCT-C37.
CCT C37 was cross-linked with 0.2 mM $Cu(Phe)_3$ both in the absence of lipid and in the presence of 300 μM PG vesicles. Western Blot probed with anti-domain C antibody.

3.2.4 Probing The Lipid Sensitive Contacts In Domain N

To probe whether any of the lysines in domain N contribute to lipid-sensitive cross-linking across the dimer interface we constructed mutants containing lysine substitutions at positions 8, 13 and 16 (together), and individually at positions 33 and 57. As well, a CCT mutant was constructed where all the lysines were concomitantly substituted creating a lysine-free N-terminal domain.

All the N-terminal CCT mutants were expressed in COS-1 cells (sec.2.2.4.2) at levels equivalent to wild type CCT (Figure 3.7).

The specific activity for each N-terminal CCT mutant was assayed under regular assay conditions (sec 2.2.6.2). Table 3.1 shows that the activities for His-tagged N-terminal mutant proteins are similar to equivalently expressed His-tagged WT CCT. The activities of the first expressed His WT CCT and His CCT K8R/K13R/K16R are considerably lower than the later expressions, however it is believed to be due to the fact that the transfection protocol was not optimized at that point.

The fact that expression and activity data for each N-terminal mutant are similar to wildtype figures indicates that the introduced mutations likely do not result in protein misfolding that could obscure cross-linking results.

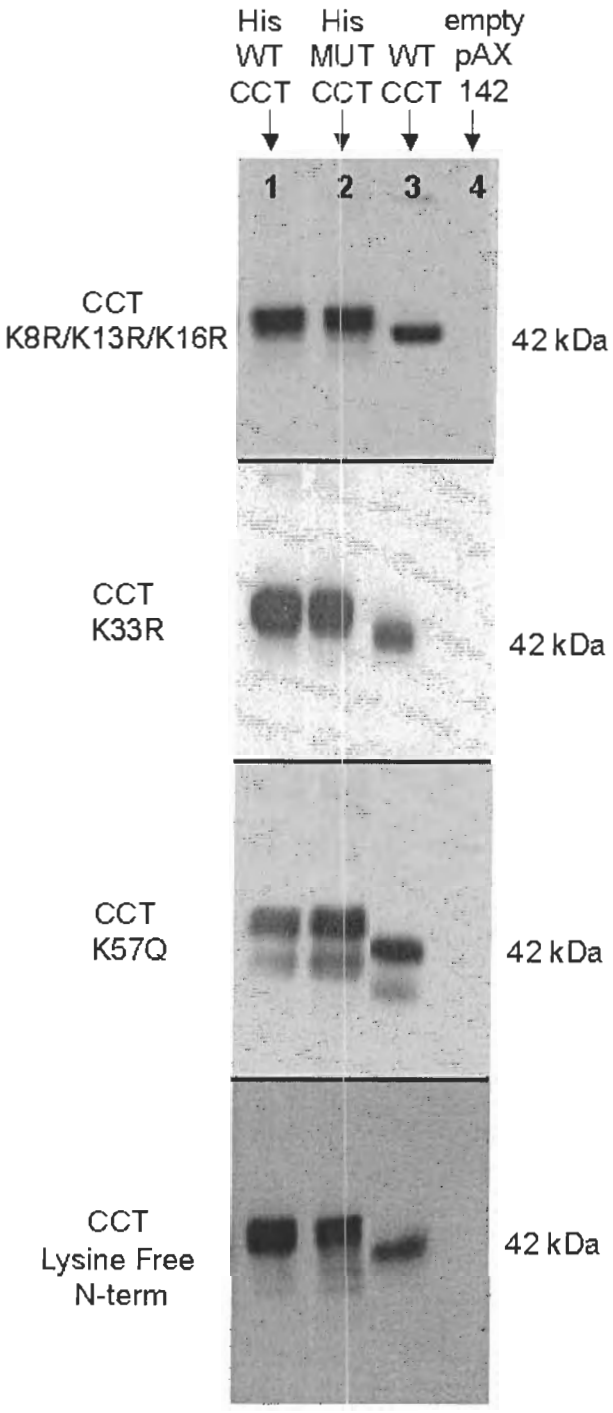

Figure 3.7 Expression of N-terminal CCT mutants
Lanes 1,2 and 4: whole cell homogenate of COS-1 cells (15μg total protein). Cells were transfected with: lane 1:His-tagged WT CCT, lane 2: His-tagged mutant construct CCT protein as indicated on the left side of the gels, lane 4: pAX142 empty vector, lane 3: purified baculovirus expressed WT CCT (1 μg total protein). Western Blot probed with anti-domain M antibody

Table 3.1 Specific activity of His-tagged WT and N-terminal mutant CCT
Assay is of whole cell homogenate from transfected COS-1 cells. 1unit = 1 nmol CDP-choline formed/min/mg protein. Results are the average of at least two activity assays.

Protein	Specific Activity (units/mg)	Transfection Protocol
His WT CCT	401 ± 7	old
His CCT K8R/K13R/K16R	380 ± 23	old
His WT CCT	1105 ±115	new
His CCT K33R	991 ± 54	new
His CCT K57Q	932 ±16	new
His CCT Lysine free N-term	923 ± 172	new

Having confirmed the expression and near-WT activity of each domain N mutant, I purified them (taking advantage of the His-tag) for cross-linking analyses. Each Ni-agarose purified N-terminal mutant was cross-linked with BS^3 in the presence of 300 μM lipid vesicles, either PC, PG or PC/O (1:1) (Figure 3.8). All mutants, including the lysine-free N-terminal mutant, were fully cross-linked in the presence of zwitterionic PC vesicles, which represents a control since CCT does not bind to these vesicles. Preincubation of CCT with anionic vesicles reduced the cross-linking efficiency of WT CCT and each mutant construct. These data suggest that none of the lysines in domain N are necessary for forging BS^3 -mediated cross-bridges across the dimer interface, and hence it is likely that they are not near points of inter-subunit contact. The manifestation of a doublet band at 42 kDa can be attributed to variations in the phosphorylation states of CCT in the pool of COS cell expressed protein.

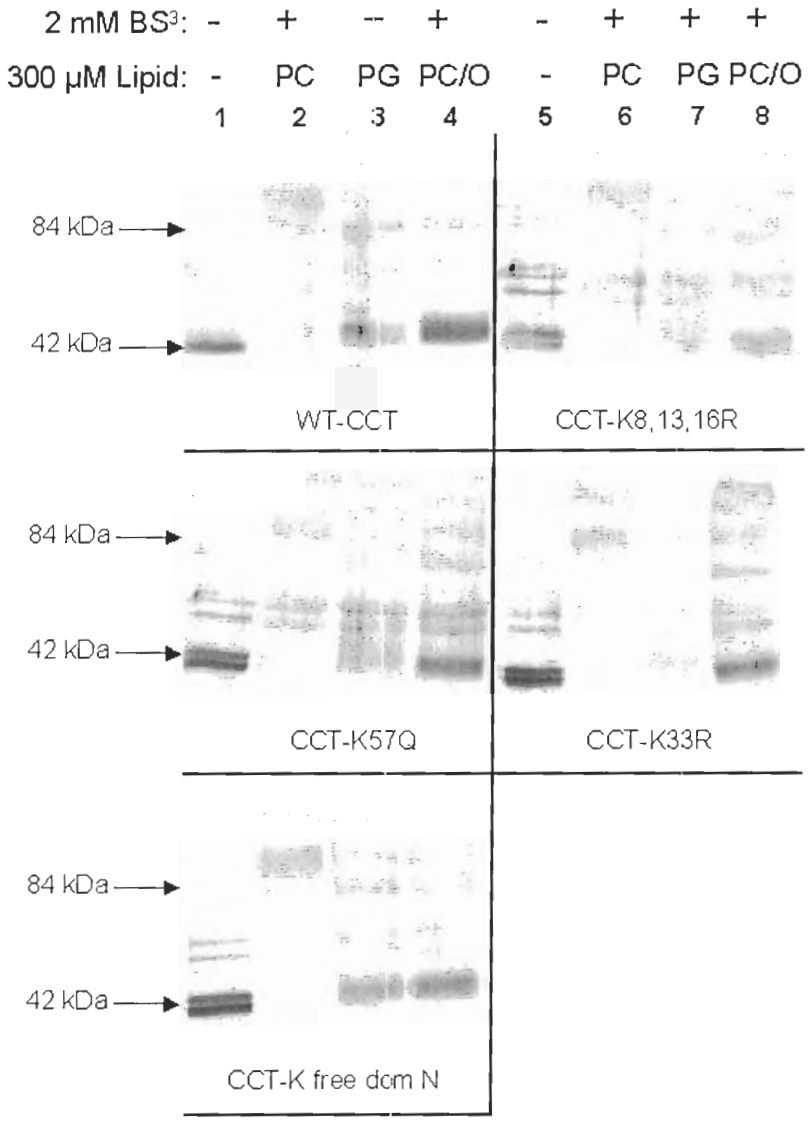

Figure 3.8 **BS^3 cross-linking of all N-terminal mutant CCT proteins.**
All N-terminal CCT mutants are fully cross-linked in the presence of non-activating PC vesicles(lanes 2 and 6). Anionic lipid vesicles reduce the efficiency of lysine cross-linking (lanes 3, 4, 7 and 8). Silver stained 10% SDS-PAG.

3.3 Discussion

3.3.1 Membrane Binding Perturbs The Dimer Interface

Phospholipid vesicles that promote CCT binding greatly reduce the efficiency of cross-linking by glutaraldehyde, the succinimidyl-based cross-linkers DSS, DSP and BS^3, and oxidation by copper phenanthroline. Because cross-linking is a non-reversible modification, the lack of dimer species indicates a significant restructuring of the dimer interface. This may result from a rigidification of the protein such that the residues in the interface are no longer flexible enough to be covalently cross-linked, or by resituating the targeted amino acids so that they are too far apart to be cross-linked. Experiments thus far have not differentiated between these two possibilities.

3.3.2 Domain N Participates In The Lipid Sensitive Dimer Interface

The strongest indication of the participation of domain N in dimerization emerged from a study of single cysteine to serine replacements at all 7 native cysteines[46]. We anticipated that the Cys-139 pair would be identified from this screen as the disulfide bonding pair because our GCT-based model shows these residues are near the dimer interface in domain C. To our surprise, this analysis instead identified the Cys-37 pair as the disulfide bridge that covalently links the two monomers under oxidizing conditions. Furthermore, the binding of CCT to membranes inhibited disulfide bond formation at this position, thus identifying one subunit contact site that is modulated by membrane binding – namely the region in the near vicinity of Cys-37. Similar cysteine mutagenesis of the CCT β

isoform has localized Cys-34, to the dimer interface (M. Dennis, unpublished data).

3.3.3 Are There Any N Terminal Lysines In The Dimer Interface?

While glutaraldehyde is a non-specific cross-linker that targets lysines, tyrosines, histidines and cysteines, DSP, DSS and BS^3 all exclusively target the ϵ-amine of lysines. Because cross-linked dimers are captured with all of the above reagents, it implies that there is at least one, if not multiple, lysines found within the dimer interface of CCT. There are 5 lysines in the N-terminal domain, 5 in the catalytic domain, 13 in the membrane binding domain and 6 in the phosphorylation domain (Figure 3.9). Domains M and P are not required for dimerization of CCT, as truncated CCT 236 can still be cross-linked to form dimers, and constructs containing just domains M and P did not score positive in yeast two-hybrid tests[46], suggesting that the dimer interface is likely within the N-terminal and/or catalytic domains. Likewise, it is known that the membrane-binding domain intercalates into the lipid bilayer and that the lysines there are probably not found in the dimer interface. Thus the dimer interface is likely within the N-terminal and/or catalytic domains.

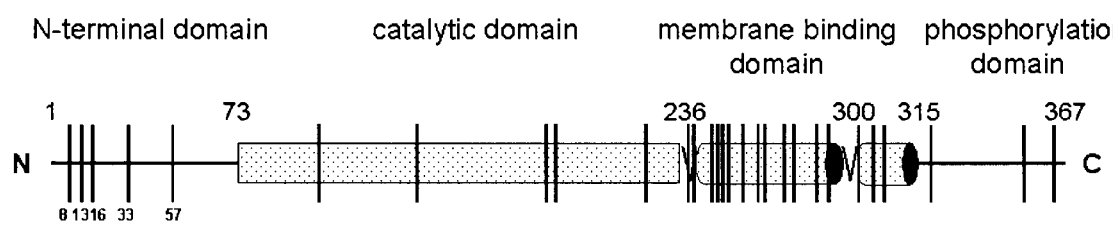

Figure 3.9 Position of the 29 lysines in CCT*α*

However, based on the proposed configuration of the CCT catalytic domain modelled on the GCT crystal structure (Figure 3.10), the lysines in the catalytic domain are too distant from each other to be conjugated by the 12 Å-spanning cross-linkers that were used. Thus, I focused on the lysines in the N-terminal domain of CCT.

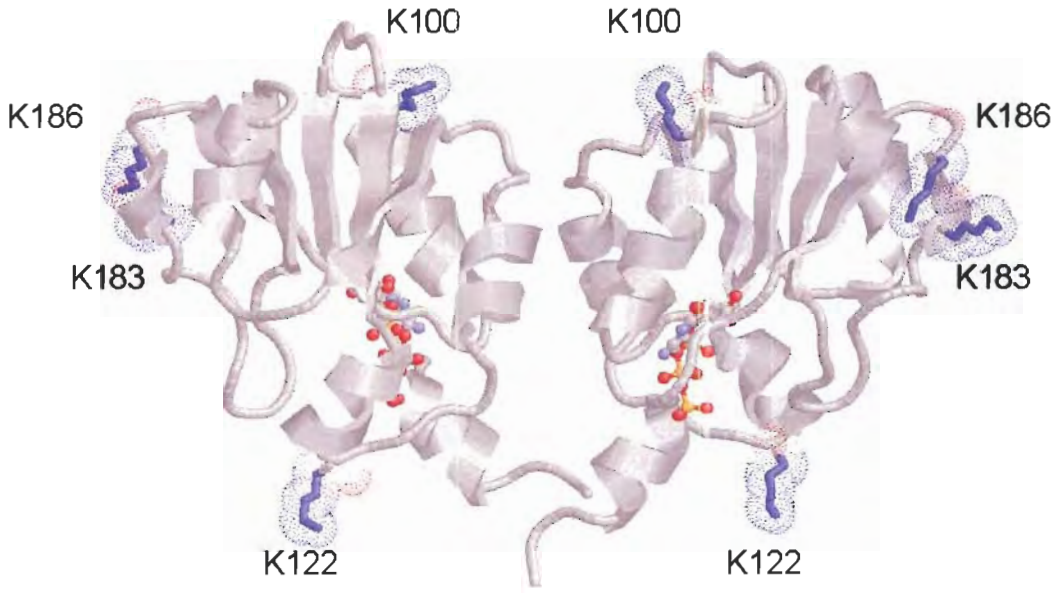

Figure 3.10 Model of CCT catalytic domain showing positions of all lysines
The lysines appear too distant to be linked across the dimer interface by a 12 Å cross-linker. Backbone and secondary structures are shown as ribbons. Lysine side chains are shown as sticks with electron filling clouds. The ball and stick in the active site is CTP. Model of CCT catalytic domain was made by Dr. Frederic Pio using Modeller and is based on the crystal structure of GCT, pdb 1coz.

Since lysine specific cross-linkers can covalently trap the dimer, I tested whether mutagenesis of individual lysines in the N-terminal domain to arginine would prevent lysine specific cross-linking, thus identifying the particular lysine(s)

in the dimer interface. Arginine was chosen as an amino acid to substitute for lysine as it has the same charge, and is roughly the same size and shape, and would therefore be less likely to result in misfolding of the protein. Arginine is not cross-linked by succinimidyl-based reagents. One exception to replacing lysine with arginine was the mutation of lysine 57 to glutamine. Arginine substitution was not tolerated at this position, evidenced by the lack of expression of this mutant in COS-1 cells (data not shown).

Since the K8R/K13R/K16R, K33R and K57Q mutants could each be completely cross-linked (Figure 3.8), it implies that none of the lysines in domain N are the sole lysines located within the dimer interface.

The theory behind these experiments was that a single pair of analogous lysines (same lysine in each half of the dimer) in domain N of CCT was situated in the dimer interface, and as such they could be chemically cross-linked. However, since full BS^3 cross-linking was observed with each eliminated lysine, it is apparent that no individual lysine in the N-terminal accounts for the cross-linking seen between monomers.

It was thought possible that there were multiple lysines in the dimer interface. Since lysines 8, 13, and 16 are not found in CCTβ (another isoform of CCT, also a homodimer) and are part of the nuclear localization signal of CCTα, we hypothesized that only K33 and K57 may be positioned in the dimer interface. The lack of inhibition of BS^3 cross-linking upon single mutations of Lys-33 or Lys-57 eliminated two possibilities: (1) that Lys-33 contacts Lys-57 in the dimer interface and (2) that only analogous lysines contact each other. However, the

results did not eliminate two other possibilities: (1) that both Lys-33:Lys-33' and Lys-57:Lys-57' forge contacts and that BS^3 reaction with either pair is sufficient to generate a covalent dimer and (2) that one or both of these domain N lysines make contacts with lysines in the catalytic domain.

3.3.4 Domain N Lysines Are Not Required For BS^3 Cross-Linking

To investigate whether *any* of the N-terminal lysines are required for cross-linking I generated a lysine free domain N mutant. It was thought that if lysine specific cross-linkers fail to trap this mutant as a covalent dimer, it would verify the involvement of multiple domain N lysines in the dimer interface. However BS^3 cross-linking using CCT devoid of all lysines in domain N was identical to the cross-linking of wild-type CCT (Figure 3.8). This result means that the covalently trapped dimer we see is not dependant on cross-linking of any of the lysines in the N-terminal region of CCT, either as an analogous pair, or by forging contacts with a lysine in another domain. The question thus remains – which lysine pair(s) are in the dimer interface that account for the cross-linking.

3.3.5 Is The Lysine In The His-Tag Interfering With Analysis?

It is feasible, but unlikely, that the His-tag is obscuring the analysis of native dimer contacts or providing false positives, as there is a single lysine residue just preceding the histidine stretch. Supposing that the folding of the His-tagged CCT allows the two His-tag lysines to come within ~12 Å of each other, the dimer may be captured by chemical cross-linking of these two residues. However, CCT expressed in the baculovirus system, which lacks a polyhistidine

tag, can be chemically cross-linked with lysine specific cross-linkers (Figures 3.2, 3.3 A ,C, and 3.4) suggesting that the lysine in the His-tag is not mediating cross-linking.

3.3.6 Is CCT Cross-Linking Between N-Terminal Amines?

Lysine specific cross-linkers react with primary amines, which on the protein level are only found on the side chain of lysines or on the α-carbon of the N-terminal amino acid. This raises the question whether the chemical cross-bridging observed is caused by the reaction of nearby N-termini of opposing subunits with the cross-linker. However, the purified CCT is acetylated on its initial methionine[25] and therefore is not accessible for reaction with the primary amine specific cross-linker. Thus, any covalently cross-linked dimer we see is most likely a result of reaction between lysines, not N-terminal amines.

3.3.7 The Effect Of Lipids On CCT And Cross-Linking

Covalent chemical cross-linking of lysines on CCT typically results in a diffuse band from 80-100 kDa (Figure 3.3 A, lanes 2-5, and C lanes 2-4), which has been identified as heterogeneously cross-linked homo-dimers[34]. There are 29 lysines in each CCT monomer and it is likely that most reside on the periphery of the protein. Lysine specific chemical cross-linkers will not only cross-link adjacent lysines in the dimer interface, but will conjugate with any lysine available. Consequently, incubation with cross-linkers can result in the modification of one, several, or all surface lysines, as well as trapping the lysines at the dimer interface. Additionally, there are several lysines in the membrane

binding domain, and as this domain has been implicated in interacting with the N-terminal domain[25] it is possible that the lysines in these two sequentially, but not necessarily spatially, separate domains are cross-linked to one another. Also possible, but not yet proven, is that the domain M from one sub-unit is cross-linked to a domain N of the opposite sub-unit. Due to the variety of molecular weight species that result, this manifests itself as smear on SDS-PAG gels.

Lysine specific cross-linking in the presence of activating lipids results in a reduction of dimer species and an increase in monomer species. The minor amount of dimer species that remains in the presence of lipids is represented as a tight band rather than a diffuse one. (Figure 3.3 A, lanes 7-10 and C, lanes 6-9). This persistent dimeric species may be less modified by the cross-linking reagent. Domain M contains many lysines that would become inaccessible to the cross-linker upon binding to the lipid vesicles (via charge interactions between the basic lysines and anionic lipid head groups). Alternatively, the sharp cross-linked dimer band that persists may be due to one dimer contact that is not disrupted upon membrane binding. The other cross-bridges giving rise to the heterogeneous smear are disrupted.

3.3.8 The Case Of The Disappearing Dimer

It was observed on some, but not all, occasions of BS^3 mediated cross-linking that the CCT dimer band appeared very faint and did not represent the amount of protein known to be in the reaction (Figure 3.8 compare lanes 1 *vs.* 2 and lanes 5 *vs.* 6). This may be due to an increase in the hydrophobicity of the protein after chemical modification by the cross-linker. The surface of CCT can

become increasingly hydrophobic as the cross-linkers conjugate to the exterior lysines, as BS^3 contains a hydrophobic chain of 6 saturated carbons. To reduce the effect of the unfavourable entropic factors, these chains may seek to remove themselves from the aqueous environment by aggregating together, thus aggregating the CCT. Aggregates of CCT cannot always be released from the walls of microfuge tubes by boiling with Laemlli buffer, and even if released from the tube, may not enter into the stacking gel due to their great size. This phenomenon has since been rectified by the addition of the detergent OG (n-octyl-β-D-glucopyrannoside) to samples to facilitate their removal from surfaces such as microfuge tubes (H. Huang unpublished data).

4 INVESTIGATION INTO LIPID MODULATION OF CCT 236

4.1 Introduction

CCT 236 is a truncation mutant of CCT, ending after residue 236; therefore, it contains only the N-terminal and catalytic domains, and lacks the membrane binding domain and domain P. CCT 236 is a good mimic of domains N and C of wild-type CCT as chymotrypsin digestion of both CCT 236 and full length CCT result in the same fragmentation pattern[25,26]. This implies that the secondary and tertiary structures do not differ between full length and truncated CCT. Both gel filtration and chemical cross-linking studies have shown that CCT 236 is a homodimer[67] suggesting that domain M is not an essential part of the dimerization domain, and that the dimerization interface is composed of either domain N or C, or both. Activity assays have revealed that CCT 236 is constitutively active, even in the absence of activating lipids, supporting the proposal that the membrane binding domain acts as an inhibitor of CCT activity in the soluble state[67]. However, the K_m for CTP is elevated from 1.2 mM in WT CCT to 4.4 mM in CCT 236[67]. Circular dichroism studies showed that the addition of lipids to CCT 236 does not result in any change to the secondary structure[26]; and Friesen *et al.* [67] found that PC/O (1:1) lipid vesicles do not alter activity. Timed chymotrypsin digests followed by Maldi-MS revealed that the tertiary structure of CCT 236 more closely resembles membrane bound than soluble CCT 367, as the peptide bond accessibility maps were most comparable

between those two[25]. With that knowledge in mind, it was anticipated that the cross-linking efficiency of CCT 236 by BS^3, in the absence of lipids, should be similar to that of membrane bound full length CCT, where cross-linking is greatly reduced.

The goals of this chapter were to explore, through chemical cross-linking in the absence and presence of lipids, whether CCT 236 is in the same conformation as membrane bound full length CCT with respect to contacts between subunits. Much to our surprise I found that CCT 236, although missing the membrane-binding domain, forms stable chemically cross-linked dimers and, even more surprising, undergoes conformational rearrangements at the dimer interface in the presence of activating lipids. This led me to investigate whether there was a second membrane-binding domain in CCT.

4.2 Results

4.2.1 CCT 236 Can Be Covalently Cross-Linked

His-tagged CCT 236 was expressed in COS-1 cells, and was purified on a nickel-agarose column. Figure 4.1 shows that BS^3, $Cu(Phe)_3$, and glutaraldehyde all cross-link CCT 236 in the absence of lipid. In the absence of cross-linking reagent, CCT 236 appeared as a 27 kDa monomer (lanes 1,3,5). With cross-linkers, CCT 236 was almost completely in the 55kDa dimer state (lanes 2,4,6). Thus, CCT 236 does not resemble membrane bound CCT 367 in this regard.

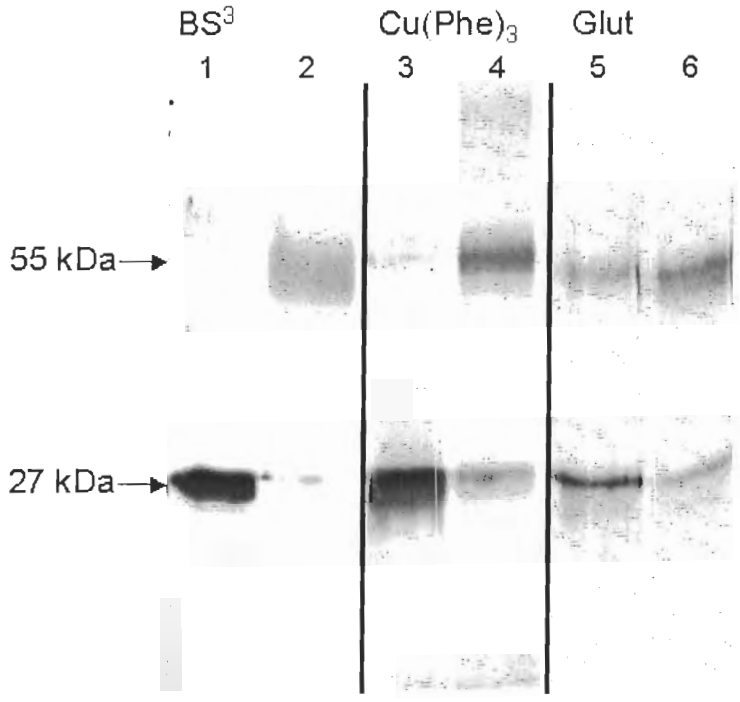

Figure 4.1 CCT 236 is cross-linked in the absence of lipid.
Purified untagged CCT 236 (0.39 μM) was cross-linked with 2 mM BS^3, 0.2/0.6 mM mM $Cu(Phe)_3$ or 1 mM glutaraldehyde as described in the Methods. Lanes 1,3,5: samples were prequenched (see methods). Silver stained 10 % SDS-PAG.

4.2.2 CCT 236 Cross-Linking Is Lipid Sensitive

I next investigated the effects of lipid vesicles on CCT 236 cross-linking efficiency. In agreement with the results shown in Figure 4.1, CCT 236 was trapped in the dimer state by BS^3 cross-linking or oxidation with $Cu(Phe)_3$. The addition of activating lipids (PG, PC/O (1:1)) resulted in a decrease in the efficiency of cross-linking. (lanes 4,5,9,10). There is a correlation between the negative charge on the lipids (PG>PC/O (1:1)>PC) and the reduction in cross-linking efficiency.

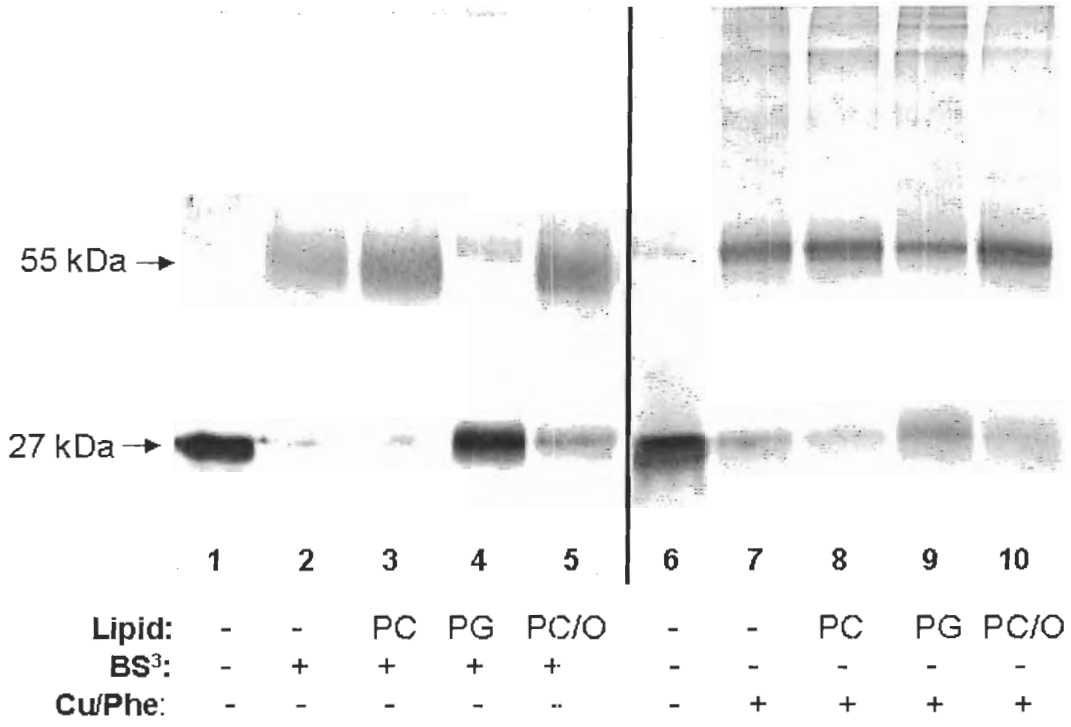

Figure 4.2 CCT 236 cross-linking is diminished with anionic lipids.
Purified untagged CCT 236 was cross-linked with 2 mM BS^3 or 0.2/0.6 mM $Cu(Phe)_3$ as described in the Methods. Silver stained 10% SDS-PAG.

4.2.3 CCT 236 Δ12-16 Cross-Linking Is Lipid Sensitive

The sensitivity of CCT 236 to lipids, despite the truncation of the membrane binding domain, suggested that there may be a second lipid interacting region within the N-terminal or catalytic domains of CCT. The most obvious candidates were residues 8-16 in the polybasic region in the nuclear localization signal, located in the N-terminal domain (^{8}KVNSRKRRK^{16}). Polybasic domains act as electrostatic membrane binding motifs in several proteins such as MARCKS and Src[73].

I constructed CCT 236 with residues 12-16 deleted, which was expressed in COS-1 cells at levels similar to His CCT 236. The activity was also similar to

COS-1 expressed His CCT 236, implying that the deletion of the polybasic region was not detrimental to the folding of the protein (data not shown).

CCT 236 Δ12-16 was cross-linked with 2 mM BS^3 alone, and in the presence of PC/O or PG vesicles. BS^3 cross-linking of CCT 236 Δ12-16 was virtually identical to wild-type CCT cross-linking, both in the absence and presence of lipid vesicles (Figure 4.3). This result suggested that the N-terminal polybasic region is not acting as a lipid responsive element.

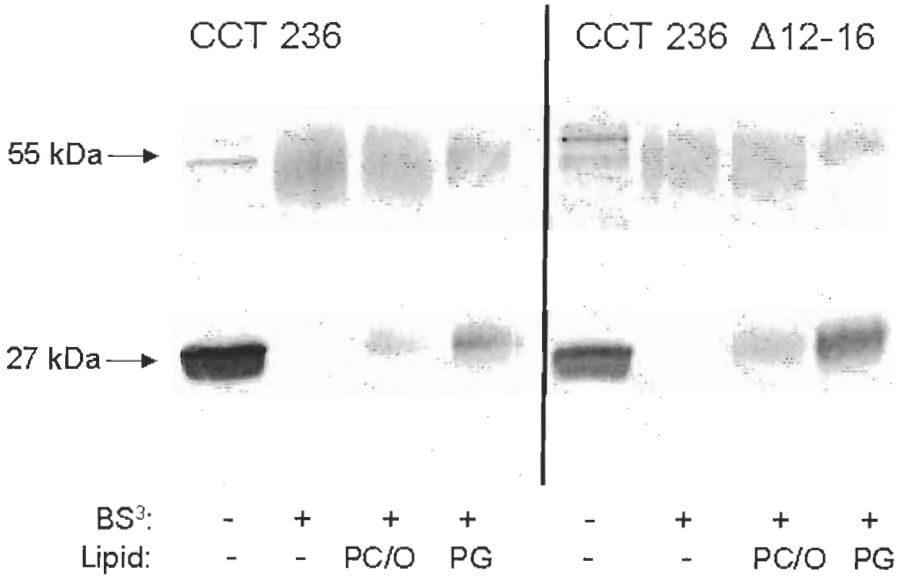

Figure 4.3 **BS^3 cross-linking of CCT 236 and CCT 236 Δ12-16**
His-tagged purified CCTs (0.39 μM) were cross-linked with 2 mM BS^3 alone or in the presence of 300 μM PC/O (1:1) or PG vesicles as described in the methods. Silver stained 10% SDS-PAG.

4.2.4 Is A Protonated His-Tag Binding To Anionic Membranes?

The histidine tag attached to all the CCT mutants for expression purposes contains a stretch of 6 histidines that, if protonated, could possibly be attracted to the negative charge of anionic lipid head groups. A strong attraction of the most

N-terminal region of CCT to the lipid bilayer could potentially result in changes to the structure of CCT that would reduce the efficiency of cross-linkers to capture the dimer state. To make certain that this was not the case, cross-linking conditions were optimised to ensure all histidines would be in a non-protonated state (i.e. at pH 8.2).

Figure 4.4 indicates that even at pH 8.2 the presence of PG vesicles still results in reduction of dimer species. Under conditions where the histidines possess no positive charge, CCT 236 remains responsive to lipid vesicles. Thus the poly-histidine tag is not the lipid responsive element.

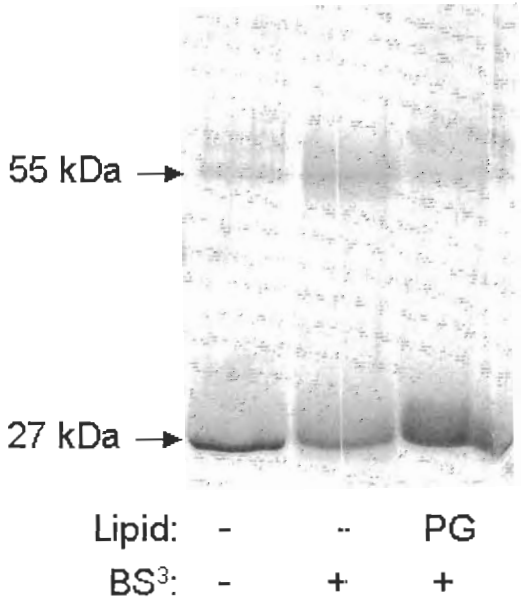

Figure 4.4 BS^3 cross-linking of CCT 236 at pH 8.2
Purified His-tagged CCT 236 (0.39 μM) was cross-linked with 2 mM BS^3 at pH 8.2. alone, or with 300 μM PG vesicles as described in the Methods.

4.2.5 Cross-Linking CCT 236 With Lipid And Detergent Monomers

The experiments above ruled out the N-terminal polybasic motif and the His-tag as determinants of the lipid modulation of cross-linking efficiency. To explore further the mechanism of the lipid effects on cross-linking of CCT 236 we tested the response to lipids/amphiphiles of varying structure and potential for forming micelles *vs.* vesicles. I hypothesized that the lipids might be binding as monomers directly to the hydrophobic dimer interface. The lipids tested included lyso PG, a negatively charged micellar lipid (CMC = 18 μM)[74]; lyso PC, a zwitterionic micellar lipid (CMC = 20 - 200 μM)[75]; SDS, a strongly negatively charged micellar detergent (CMC = ~4.5 mM)[76]; and CTAB, a positively charged micellar detergent (CMC = ~1 mM)[77]. The concentration range I used encompassed the CMC, going from well below CMC where the monomeric form dominates to above the CMC, where micelles dominate.

I found that anionic amphiphiles lyso PG and SDS (Figures 4.5 A and 4.6 A), like diacyl PG, disrupted the cross-linking efficiency, whereas zwitterionic and positively charged amphiphiles had very little effect (lyso PC) (Figure 4.5 B) or no effect (CTAB) (Figure 4.6 B). For samples with CTAB, the gel electrophoresis was complicated by the presence of high concentrations of positively charged amphiphile, which likely antagonized the effect of SDS. Nevertheless, it is evident that CTAB did not lead to increased monomer *vs.* dimer.

It appears that in the absence of amphiphile, or when it was present in very low concentrations, that less protein is visible in each lane of the gel compared to the lanes with high(er) amphiphile concentration. This is thought to

be a result of the increasing hydrophobicity and aggregation of the CCT due to the conjugation of the cross-linker with surface lysines on the protein, and thus the aggregates could not enter the gel. This phenomenon has since been rectified by the addition of the detergent OG (n-octyl-β-D-glucopyrannoside) to samples to facilitate their removal from surfaces such as microfuge tubes (H. Huang unpublished data).

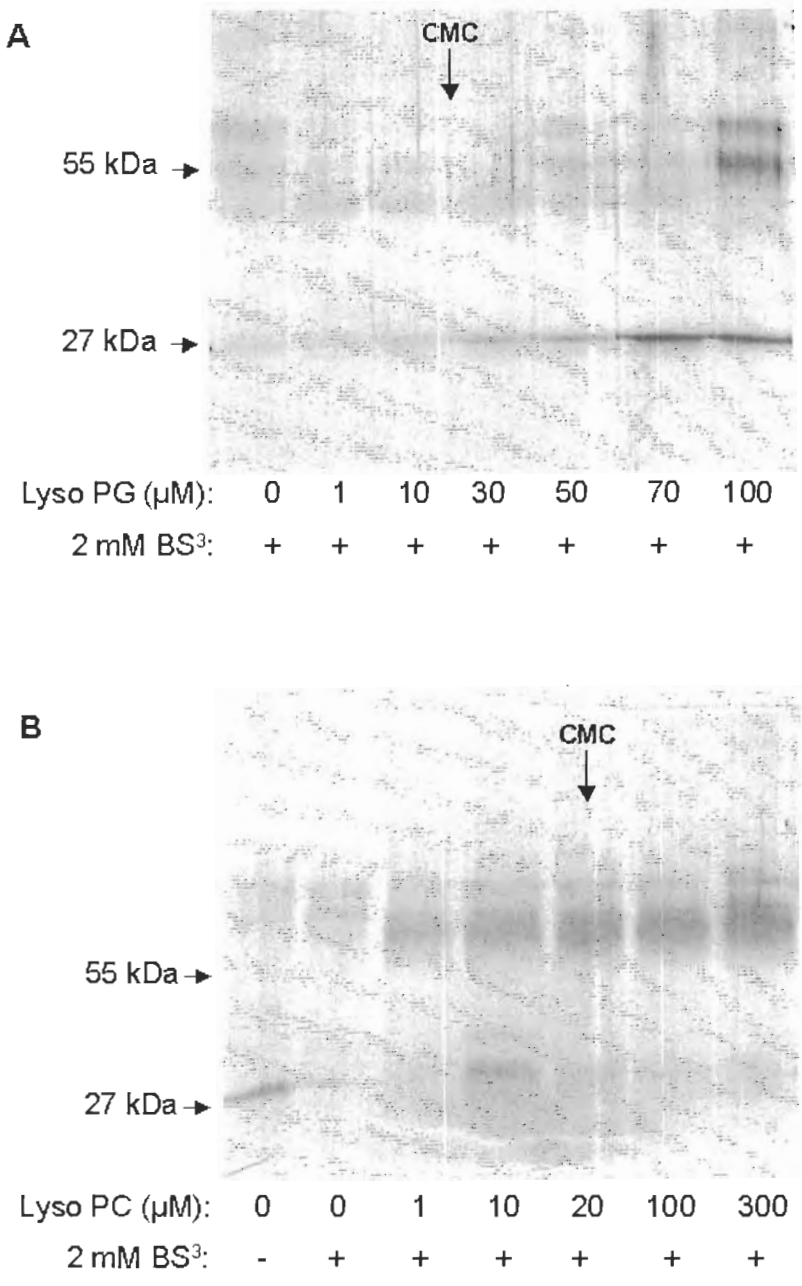

Figure 4.5 BS^3 cross-linking of CCT 236 in the presence of lyso lipids
Purified untagged CCT 236 (0.39 μM) was cross-linked with 2 mM BS^3 in the indicated concentrations of (A) lyso-PG or (B) lyso PC as described in the Methods. Silver stained 10% SDS-PAG.

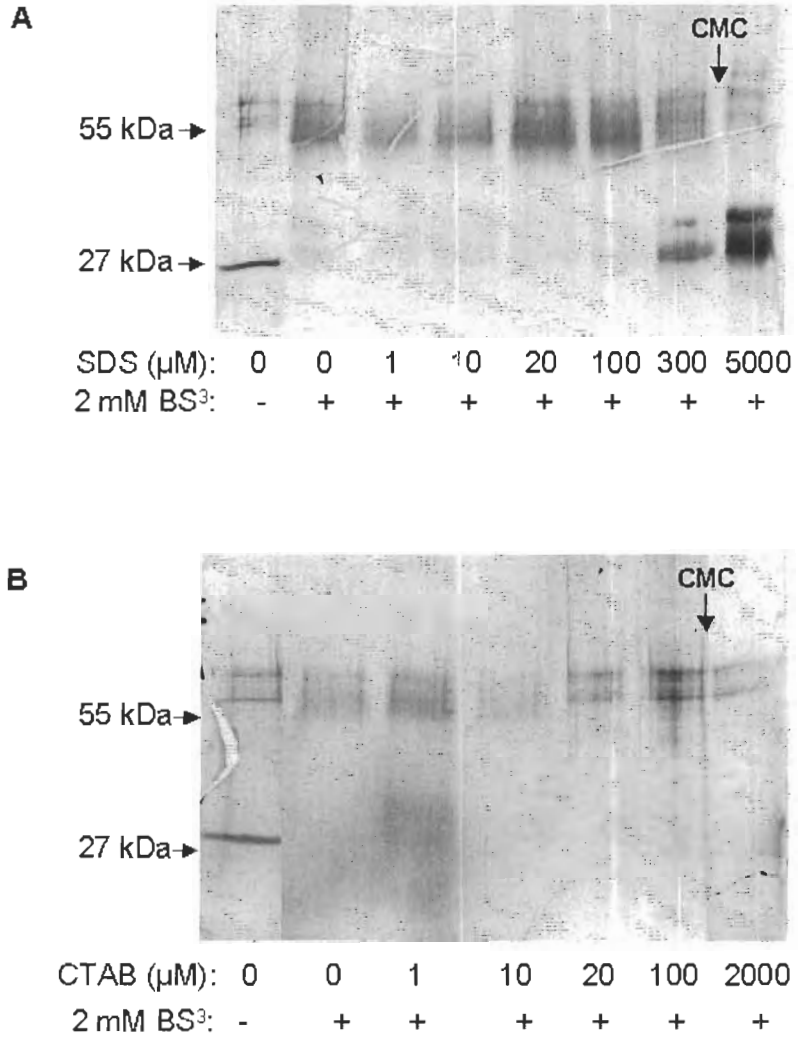

Figure 4.6 BS^3 cross-linking of CCT 236 in the presence of detergent amphiphiles
Purified untagged CCT 236 (0.39 μM) was cross-linked with 2 mM BS^3 in the indicated concentrations of (A) SDS or (B) CTAB as described in the Methods. Silver-stained 10% SDS-PAG.

4.2.6 The Effect Of Amphiphiles On The Activity Of CCT 236

The activity of CCT 236 was assayed under non-standard conditions (Section 2.2.6.3) in the absence of lipid and in the presence of vesicles composed of PG, PC or PC/O (1:1), or the micellar amphiphiles lyso-PC, lyso-PG or CTAB. The results show that CCT 236 activity is modulated ≤3-fold by lipids

(Figure 4.7). Although thorough concentration curves were not carried out, based on the preliminary experiments the order of potency is PC > lyso PC > PC/O > CTAB > lyso PG > PG. CTAB activated only at low concentrations below its CMC. At or above its CMC it was inhibitory. Concentration curves for lyso PC also showed that this lipid activated CCT 236 below and above its CMC (data not shown). These data suggest that the monomeric form of the amphiphile can affect CCT 236 activity.

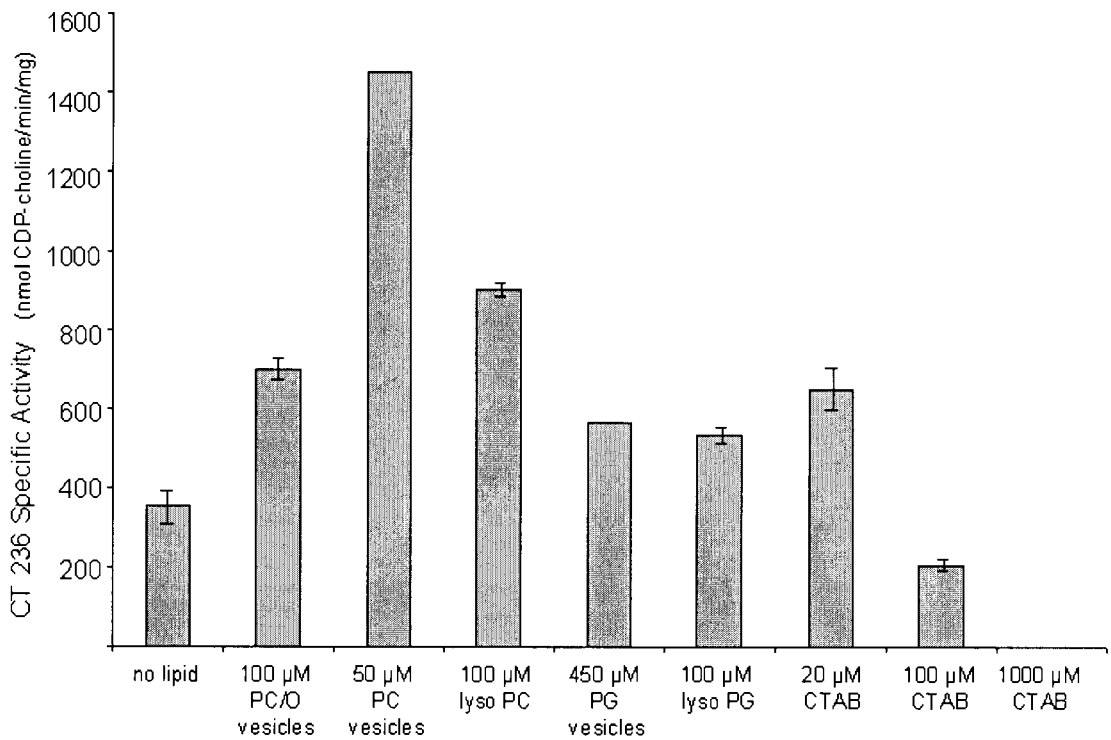

Figure 4.7 The effect of lipid vesicles and monomeric amphiphiles on CCT 236 activity
Purified untagged CCT 236 was assayed under non-standard conditions as described in the Methods. Data are averages of at least two activity assays. Data for PC and PG vesicles was from S. Taneva.

The activity of full length CCT was assayed in the presence of lyso PC and lyso PG, in addition to PC/O (1:1), PC and PG vesicles. The most effective activators are the anionic vesicles, PC/O and PG, although lyso PG and lyso PC do activate CCT to a lesser extent. PC vesicles are the least potent activators of full length CCT (Figure 4.8). It is apparent that there are significant differences between the lipid response of CCT 236 and full length CCT with respect to the magnitude of activation, the selectivity for anionic *vs.* zwitterionic lipids, and the amphiphile aggregation requirement. CCT 236 prefers zwitterionic amphiphiles and is activated at most by 3-fold. Full length CCT is activated by anionic lipids in a vesicle form, at concentrations above their CMCs[26] and exhibits a 50-fold increase in activation.

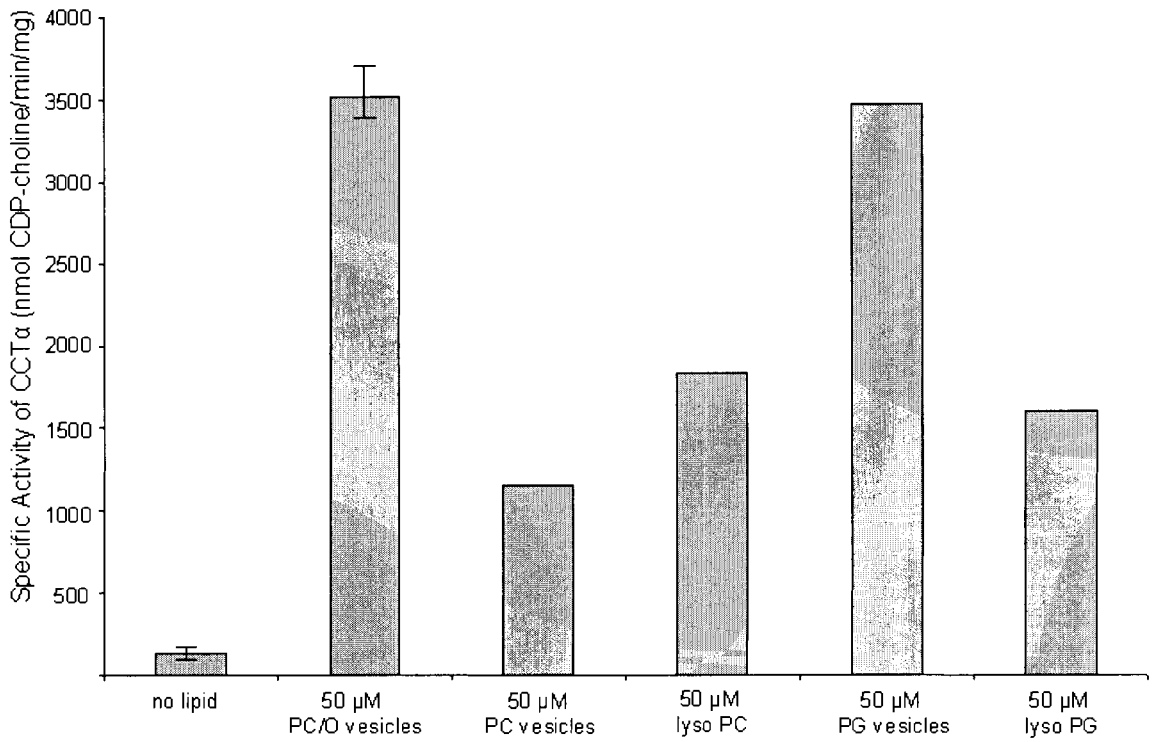

Figure 4.8 The effect of lipid vesicles and monomers on full length CCT activity
Purified untagged CCT was assayed under standard conditions as described in the Methods. Data are averages of at least two activity assays. Data for lyso PC and lyso PG and PC and PG vesicles was from S. Taneva.

4.3 Discussion

4.3.1 The Dimer Interface Organization Of CCT 236 Is Not Identical To Membrane Bound Full Length CCT

Although other experimental results probing tertiary structures, i.e. similarities in accessibility to proteases[25], suggest otherwise, efficient covalent cross-linking of the CCT 236 dimer implies that the conformation of the dimer interface of CCT 236 does not resemble that of membrane bound CCT.

This leaves open the possibility that the dissociation of domain M from its interactions with the rest of the protein during its intercalation into the membrane

bilayer results in conformational changes at dimer interface, pulling the subunits apart. In the absence of the membrane binding domain, these conformational changes do not occur in CCT 236, and thus it can be captured as a dimer. Full length CCT dimers have been shown to link at least two anionic vesicles in a cross-bridging mode, implying that the two M domains are situated on opposite poles of the domain N/C dimer. The domain M–lipid interaction may thus exert tension on the dimer interface[72].

4.3.2 Anionic Phospholipid Vesicles Reduce The Cross-Linking Efficiency Of CCT 236

Surprisingly, the cross-linking efficiency of CCT 236 was greatly reduced in the presence of highly anionic PG vesicles, somewhat reduced in the presence of PC/OA vesicles, and barely reduced in the presence of zwitterionic PC vesicles. This suggested that lipids may induce a conformational change in CCT through either domain N or the catalytic domain, in addition to the membrane binding domain, and that the charge on the lipid head group may be implicated in this structural rearrangement.

As observed with full length CCT 367, the cross-linked dimer species of CCT 236 is a smear in the absence of phospholipid vesicles, yet appears as a tight band in their presence. Since the membrane-binding domain, domain M, is absent in this construct, this implies that at least some of the remaining lysines in the N and catalytic domains are being modified by the cross-linker, and that these sites are protected from conjugation with BS^3 in the presence of lipid vesicles.

4.3.3 There Is No Secondary Lipid Binding Domain In CCT

The sensitivity of CCT 236 to lipids, despite the lack of membrane binding domain, suggested that there may be another discrete region of CCT that interacts with anionic lipid head groups, thus resulting in conformational changes to CCT. This led to the hypothesis that the polybasic region of the nuclear localization signal in the N-terminal domain (residues 8-16) (^{8}KVNSRKRRK^{16}) may interact with negatively charged lipids, thus resulting in conformational changes to CCT[73].

To test this, I made mutant CCT 236 and CCT 367 where the N-terminal basic residues (amino acids 12-16) were deleted, which was followed by chemical cross-linking in the absence and presence of lipids. It was thought that if attraction of the polybasic region to anionic lipids does result in conformational changes to CCT thus preventing full chemical cross-linking, this lipid response should be ablated in the mutants and we should see full cross-linking of CCT 236 in the presence of anionic lipids.

BS^3 cross-linking of CCT 236 Δ12-16 was virtually identical to wild-type CCT cross-linking, both in the absence and presence of lipid vesicles. This result implies that there is no secondary lipid-binding domain in the polybasic region of the N-terminus of CCT.

4.3.4 The His-Tag Does Not Interact With Anionic Membranes

It should be noted that the removal of residues 12-16 was concurrent with the addition of an N-terminal His-tag that brings an additional two positively charged amino acids, lysine and arginine. They alone are probably insufficient to

cause a conformational change in CCT due to an attraction to anionic lipids, however the His-tag itself is a stretch of 6 histidines. Cross-linking was undertaken at pH 7.4 and as the pKa of histidine is 6.5, it is unlikely that the His-tag is protonated and thus is probably not attracted to the anionic membrane. To eliminate a role for protonated histidines in the event that the local environment results in such a species, BS^3 cross-linking was repeated in a more basic environment (pH ~8.2) and quenched with glycine at pH 7.4, rather than pH 6.5 as in the standard protocol I had used. I found that at an alkaline pH where histidines are most certainly unprotonated there was no change in the CCT 236 cross-linking efficiency, or in its response to lipid vesicles. This means that the conformational changes occurring in the CCT dimer interface in the presence of lipids are not a result of a protonated His-tag distorting the protein structure in an effort to bind/interact with anionic lipid head groups.

4.3.5 Amphiphilic Molecules May Disrupt The Dimer Interface Of CCT 236 Via Binding As Monomers

Because histidine charge is ruled out as an explanation for the effect of lipids on cross-bridging of CCT 236 dimers, we are left with two unanswered questions: (1) what is the basis of the lipid/amphiphile interaction with CCT 236 that leads to a reduction in cross-linking with BS^3, glutaraldehyde and $Cu(Phe)_3$; and (2), is it different from the lipid interaction with full-length CCT that reduces cross-linking efficiency? One hypothesis was that free phospholipid monomers exchanging out of the vesicles could bind to and disrupt the dimer interface. The hydrophobic tails may interact with hydrophobic patches in the dimer interface

disrupting van der Waals contacts across the dimer interface, while the charged head groups break salt-bridges and electrostatic interactions across the interface. This would replace stable protein-protein interactions with protein-amphiphile contacts. To test the theory that amphiphile monomers are disrupting the dimer interface I cross-linked CCT 236 in the presence of phospholipids containing a single chain such as lyso PG (negatively charged head group) and lyso PC (zwitterionic head group) as well as in the presence of single chain detergents such as SDS (anionic head group) and CTAB (cationic head group). The concentration of these lipids was varied from below the CMC, where they would exist as monomers, to above the CMC, where they would be found in micelle form. The results showed that CCT 236 cross-linking efficiency with BS^3 was disrupted only by the anionic amphiphiles lyso PG and SDS beginning at concentrations near the CMC. This implies that only anionic phospholipids have the physical characteristics necessary to perturb the dimer interface of CCT 236. Since CCT 236 contains no obvious exposed hydrophobic surface for binding a micelle or vesicle, the simplest rationalization to explain the effects near the CMC is that at this concentration the monomeric amphiphiles will be driven entropically to interact with another amphiphile – including CCT 236. The putative dimer interface is the only hydrophobic surface on CCT 236. Hence it is reasonable that amphiphile monomers will insert into that interface at concentrations near CMC leading to disruption of some protein-protein contacts.

4.3.6 Lipid Interaction With CCT 236 Is Different Than That With Full Length CCT

There are significant differences between the lipid response of CCT 236 and full length CCT. Firstly, the degree of activation of CCT 236 with lyso PC, the most potent activator, is at best 3-fold, whereas the activation of full-length CCT by the strongest activators, anionic lipid vesicles, is approximately 50-fold. Secondly, the set of activating lipids differs. CCT 236 is most responsive to PC and lyso PC, while full-length CCT activation is selective for the anionic PG and PC/O vesicles. Thirdly, preliminary results suggest that while CCT 236 appears to be activated by sub-CMC concentrations of lyso-lipids, full-length CCT responds only to lipids in a micellar or vesicular organization. The discrepancy between the levels of activation of full length CCT and CCT 236, combined with the difference in lipid activators, suggest that the methods in which these two versions of the same protein interact with lipids is vastly different. We hypothesize that the primary interaction of lipids with CCT 236 is via monomer interactions at the dimer interface, whereas full length CCT interaction with lipids is primarily via domain M

There is a poor association between the lipids that activate CCT 236 and those that affect cross-linking (Table 4.1). For example, lyso PG is the strongest disruptor of cross-linking efficiency, nearly eradicating all dimer formation, whereas it has the least influence on the activity of the enzyme. The opposite is true for lyso PC – it is the most potent activator of CCT 236, but has no effect on the intra dimer contacts, as seen by its inability to disrupt cross-linking. These

findings suggest that the interactions between the lipids and the protein that influence cross-linking have different modes than those that affect activation.

Table 4.1 Comparing the effect of lipids on cross-linking efficiency and activity of full-length CCT and CCT 236

Lipid	Full Length CCT		CCT 236	
	Cross-linking	Activity	Cross-linking	Activity
Lyso PG	n/a	↑	↓↓	↑
PG	↓	↑↑	↓↓	↑
Lyso PC	n/a	↑	↓	↑↑
PC	-	↑	-	↑↑

5 CONCLUDING DISCUSSION

My thesis work contributed to the discovery that the dimer interface of CCT is modulated upon membrane binding. The insertion of domain M, the membrane-binding domain, into a lipid bilayer causes the dimer interface of full length CCT to undergo a conformational restructuring that increases the *distance* or *rigidity* of cross-linkable residues. These two possible mechanisms have not yet been distinguished. My work showed that the Cysteine 37 pair in the N-terminal domain (N) resides in the membrane-sensitive dimer interface. This discovery prompted an evaluation of other contact sites within domain N, by targeting lysines by mutagenesis for participation in NHS-ester cross-linking.

There was evidence that only domains N and C are required for dimerization, and the position of lysine residues in the domain C model suggested that none of the domain C lysines are in the dimer interface. Consequently, the most probable candidates for lysine mediated cross-linking were the 5 lysines in the N-terminal domain. Yet, a lysine-free N-terminal CCT cross-linked with an NHS-ester resulted in the complete conversion of CCT to covalently trapped dimer. Thus it can be concluded that the lysine meditating NHS-ester cross-linking must be located somewhere other than the N-terminal domain.

It may be that there is a single analogous pair of lysines elsewhere in CCT that can be covalently cross-linked, or perhaps even a non-analogous pair.

Based on the positions of the lysine residues in the domain C model, it is unlikely to be a pair of lysines in the catalytic domain. However, there is a lysine at position 228 in the C-terminal end of the catalytic domain in the hinge region between the catalytic and membrane binding domains, which does not appear on the model and thus does not have a presumed location. It may well be found in the dimer interface. If so, it may mediate the cross-linking of both full length CCT and CCT 236. It has been shown through cross-linking, cyanogen bromide fragmentation and mass spec analysis that lysine 228 can be conjugated to an NHS-ester, revealing it is accessible, but there is not yet any evidence for cross-linking with any lysine, analogous or otherwise (H. Huang - unpublished data). Alternatively, any of the 13 lysines in the membrane-binding domain or 5 lysines in the phosphorylation domain may be positioned in the dimer interface. This is possible, but would not constitute the only lysines found in the dimer interface because a truncation mutation of CCT missing these regions (CCT 236) can still be trapped in the dimer state by lysine specific cross-linkers.

Work in this thesis also demonstrates that membrane-binding of CCT to anionic lipids results in a perturbation of the dimer interface and consequently a sharp reduction in the amount of CCT covalently trapped as a homodimer. The greatest reduction in cross-bridging is seen with the most anionic lipid membranes, and cross-bridging is reduced by a lesser degree with less anionic membranes. It was originally thought that secondary structure conformational changes that occur in domain M upon membrane-binding and lipid activation, ripple through the surrounding domains resulting in subtle quaternary

conformation changes that rigidify or restructure the dimer interface such that it can no longer be covalently cross-linked with 12 Å NHS-ester based cross-linker. The discovery that CCT 236 also showed perturbation in the dimer interface only in the presence of anionic lipids, despite lacking a membrane-binding domain, was surprising and led to further investigation of the effect of anionic and zwitterionic lipids in both monomer, micellar or vesicular form and their effects on cross-linking efficiency.

Both CCT 236 and CCT 367 interact with anionic lipids in a manner that restructures the dimer interface or realigns/masks specific protein side-chains involved in chemical cross-linking. However, the mechanism of the interaction differs. CCT 367 primarily interacts with membranes through the membrane binding domain. CCT 236, on the other hand is lacking the membrane binding domain, yet still displays a sensitivity to lipids. We hypothesized that monomers of anionic and possibly zwitterionic, but not cationic, lipids bind to discrete sites on the interface at concentrations around the critical micelle concentration where entropic effects are sufficient to drive the formation of CCT 236 amphiphile complexes. Unlike CCT 367, this interaction is non-activating as lyso-PG has the biggest effects on cross-linking but has no effect on activity or activation. Conversely, lyso PC has negligible effects on cross-linking, but the biggest effect on enzyme activity. For full length CCT there is better correlation between lipids that activate the enzyme and lipids that reduce cross-linking efficiency.

The impact of the restructuring of the CCT dimer interface on the remodelling of the active site is still a black box. Portions of the HXGH loop that

contact CTP reside in the dimer interface and the repositioning of this loop to make productive interactions with CTP may result in poorer contacts across the interface. In the future this hypothesis could be tested by disulfide engineering at strategic positions along the dimer interface and analysis of the consequences on enzyme activation by membrane binding.

APPENDICES

Appendix A: PCR And Thermocycling Reaction Conditions

pBS-His K8R/K13R/K16R PCR

Table A 1 PCR Reaction Components

Template DNA	PBS-His WTCT	100 ηg
Forward Primer	T7	100 ηg
Reverse Primer	CL34	100 ηg
dNTPs	dATP, dTTP dCTP,dGTP	250 μM each (final)
10X Reaction Buffer		5 μl
ddH_2O		to 50 μl
polymerase	*Pfu* Turbo	2.5 U

Table A 2 pBS-His K8R/K13R/K16R PCR conditions

95°C	2 min	
94°C	1 min	x 30 cycles
52°C	1 min	
72°C	1 min	
72°C	5 min	
4°C	∞	

QuikChange Site Directed Mutagenesis

Table A 3 QuikChange Site Directed Mutagenesis Reaction Components

Template DNA	Various	50 ηg
Forward Primer	Various	125 ηg
Reverse Primer	Various	125 ηg
dNTPs	dATP,dTTP dCTP, dGTP	2.5 mM each (final)
10x Reaction Buffer		5 µl
DdH_2O		to 50 µl
DNA polymerase	*PfuTurbo*	2.5 U

Table A 4 QuikChange Site Directed Mutagenesis Thermocycling Conditions

95°C	30 sec	
95°C	30 sec	x 16 cycles
55°C	1 min	
68°C	2 min/kb template length	
4°C	∞	

Appendix B: Oligonucleotide Primers

T_M: 81.5 +0.41(%GC)-(675/N)-% mismatch N=primer length in bases

NAME:	DESCRIPTION:
CL36	Reverse primer for CCT K 8,13,16R mutations

↓mutated K→R ↓mutated K→R ↓mutated K→R

G P V E **R** R R **R** R S N V **R** A S S Q

5' CCA GGT ACC TCT **C**TC CTC CTC **C**TC CTT GAA TTG ACT **C**TA GCT GAA CTC TGT GC 3'

20 19 18 17 16 15 14 13 12 11 10 9 8 7 6 5 4

# OF BASES: 53	GC CONTENT: 53%	MISMATCH: 5.7%	T_M: 85°C

NAME:	DESCRIPTION:
T7	Forward primer complementary to T7 region of pBS

5' GTA ATA CGA CTC ACT ATA GGG C 3'

# OF BASES: 22	GC CONTENT: 46%	MISMATCH: 0%	T_M: 70°C

NAME:	DESCRIPTION:		
CL41F	Forward primer for CCT K33R mutation		

↓mutated lys→arg

E D G I P S **R** V Q R C

5' G GAA GAT GGA ATC CCT TCC A**G**A GTG CAG CGC TGT GC 3'

27 28 29 30 31 32 33 34 35 36 37

↑ abolished EcoRI site (isoleucine is conserved)

# OF BASES: 36	GC CONTENT: 58%	MISMATCH: 5.6%	T_M: 81°C

NAME:	DESCRIPTION:		
CL41R	Reverse primer for CCT K33R mutation		

↓mutated lys→arg

C R Q V **R** S P I G D E

5' GC ACA GCG CTG CAC T**C**T GGA AGG GAT TCC ATC TTC C 3'

37 36 35 34 33 32 31 30 29 28 27

↑ abolished EcoRI site

# OF BASES: 36	GC CONTENT: 58%	MISMATCH: 5.6%	T_M: 81°C

NAME:	DESCRIPTION:		
CL44F	Forward primer for CCT K57Q mutation		

↓ mutated Lys → Gln

E I E V D F S **Q** P Y V R V

5' GAA ATT GAA GT**G** GAC TTT AGT **C**AG CCC TAT GTC AGG GTG 3'

50 51 52 53 54 55 56 57 58 59 60 61 62

↑ abolished HincII site (valine is conserved)

# OF BASES: 39	GC CONTENT: 46%	MISMATCH: 5.1%	T_M: 78°C

NAME:	DESCRIPT ION:
CL44R	Reverse primer for CCT K57Q mutation

↓ mutated Lys → Gln

V R V Y P **Q** S F D V E I E

5' CAC CCT GAC ATA GGG CT**G** ACT AAA GTC **C**AC TTC AAT TTC 3'

62 61 60 59 58 57 56 55 54 53 52 51 50

↑ abolished HincII site

# OF BASES: 39	GC CONTENT: 46%	MISMATCH: 5.1%	T_M: 78°C

NAME:	DESCRIPTION:
CL51F	Forward primer for CCT Δ12-16 deletion

S A K V N S E V P G P N

5' GT TCA GCT AAA GTC AAT TCA GAG GT**G** CCT GGC CCT AAT 3'

6 7 8 9 10 11 17 18 19 20 21 22

↑ abolished KpnI site
(valine is conserved)

# OF BASES: 38	GC CONTENT: 47%	MISMATCH: 2.6%	T_M: 80°C

NAME:	DESCRIPTION:
CL51R	Reverse primer for CCT Δ12-16 deletion

N P G P V E S N V K A S

5' ATT AGG GCC AGG **C**AC CTC TGA ATT GAC TTT AGC TGA AC 3'

22 21 20 19 18 17 11 10 9 8 7 6

↑ abolished KpnI site

# OF BASES: 38	GC CONTENT: 47%	MISMATCH: 2.6%	T_M: 80°C

Appendix C: Fluorescent Labelling Of CCT Lysines

A 100 mM stock of Alexa Fluor 532 succinimidyl ester was prepared in DMSO and stored at -80°C. Immediately prior to use, an aliquot of the stock was diluted to 10 mM in DMSO. Lysine labelling was done in a volume of 60 μl and contained 0.4 μM CCT, 0.15 mM Triton X-100, and 20 mM phosphate buffer. Lipids were added to select labelling reactions at a final concentration of 300 μM. Phospholipid vesicles for fluorescent labelling experiments were made as for the CCT activity assay. The samples were placed in a 37°C shaking water bath for 2 minutes prior to the addition of the Alexa Fluor 532 probe, which ranged in final concentration from 0 to 2.4 mM. Samples were incubated for 1 hour in the water bath prior to quenching with 0.1 M hydroxylamine. 30 μl of each sample was run on 12% SDS-PA gels and the fluorescence of the conjugated probe was assessed immediately using the fluorescence mode of a Typhoon 9410 Variable Mode Imager with a 532 nm green laser and a 555 nm filter. Gels were then silver stained.

We wanted to examine whether the reduced efficiency of lysine specific cross-linking could be explained by a loss of lysines on CCT available for reaction with the cross-linkers. This was done by comparing the labelling of lysines with an Alexa Fluor 532 succinimidyl ester in the presence and absence of excess PG vesicles.

Figure C1 shows that fluorescent labelling of lysines with the Alexa Fluor 532 succinimidyl ester results in a molecular weight shift of the CCT band with and without 300 μM PG vesicles. Calculation of the number of lysines labelled

with the Alexa Fluor 532 probe reveals that only a small fraction of the 29 lysines in CCT were conjugated with the probe, and that fluorescent labelling did not reach saturation in the protein.

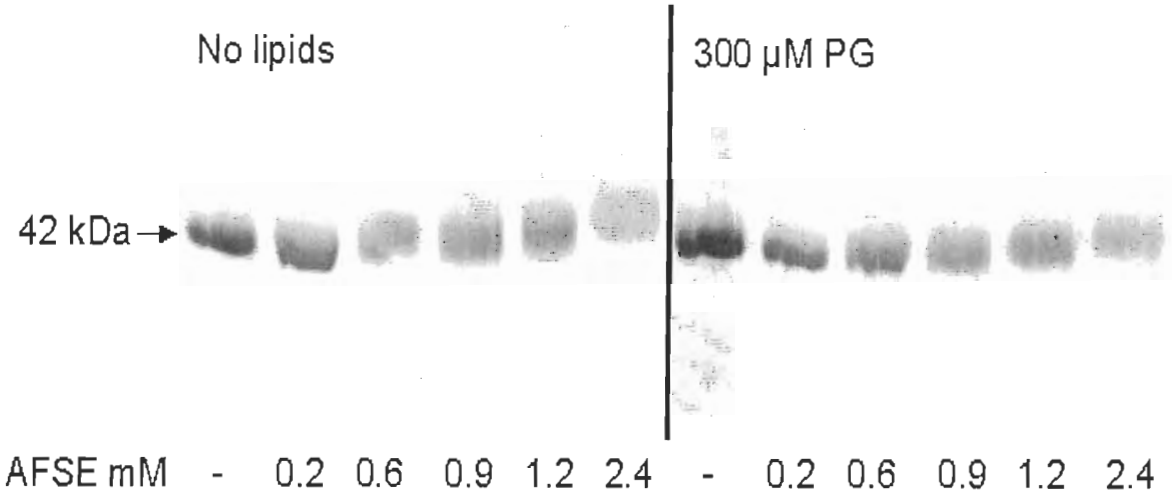

Figure C 1 Alexa Fluor labelling of lysines in CCT
Purified untagged CCT (0.39 μM) was incubated with or without 300 μM PG vesicles prior to reaction with the indicated concentrations of AFSE probe. Silver stained 10% SDS-PAG.

Analysis of the fluorescence emitted from the conjugated probe shows that as the concentration of AFSE is increased, fluorescence is decreased, indicating self-quenching of the probe (Figure C2).

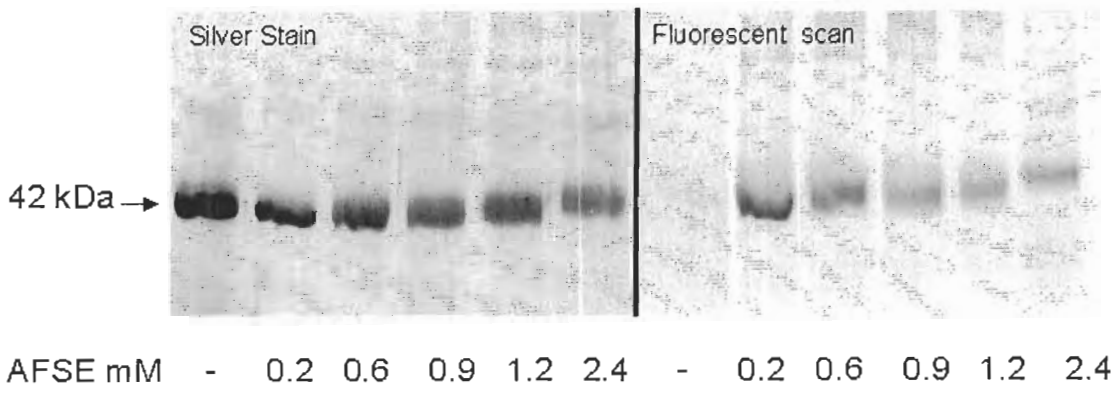

Figure C 2 Alexa Fluor labelling of lysines in CCT results in self-quenching
The same gel of AFSE labelled CCT with 300 μM PG as shown in Figure C1. (A) Silver Stained SDS-PAG. (B) Fluorescent image scanned on Typhoon Imager shows self-quenching of AFSE probe at higher concentrations.

Alexa Fluor Fluorescent Labelling Of CCT Is Inconclusive

I attempted to compare labelling of lysines with the succinimidyl ester of Alexa Fluor 532 in the presence and absence of PG vesicles. However, the presence of 29 lysines in CCT complicates interpretation of any changes in labelling. Changes in accessibility of only a few sites, which could impact on the cross-linking results, would be hard to detect. In fact, the labelling of CCT caused self-quenching of the Alexa Fluor probe. The extent of lysine labelling had to be determined from the molecular weight shift of the labelled CCT *vs.* non-labelled CCT, rather than by quantitating the fluorescent emission of the probe. Self-quenching of the fluorescent probe, combined with low efficiency of lysine labelling, made pursuit of this project futile.

Table C 1 Data for calculating the number of Alexa Fluor probes bound per CCT based on the molecular weight shift of conjugated CCT

NO LIPID

gel length (migration distance) LHS = 54 mm, RHS = 55 mm, AVG = 54.5 mm

MW STD (Da)	log of MW STD	L - ladder migration (mm)	L - ladder Rf	R - ladder migration (mm)	R - ladder Rf	avg ladder migration	avg ladder Rf
200000	5.30	2.50	0.05	3.50	0.06	3.00	0.06
116250	5.07	7.00	0.13	8.00	0.15	7.50	0.14
97400	4.99	9.50	0.18	10.00	0.18	9.75	0.18
66200	4.82	16.00	0.30	17.00	0.31	16.50	0.30
45000	4.65	30.50	0.56	32.00	0.58	31.25	0.57
31000	4.49	46.00	0.85	47.50	0.86	47.50	0.87

CT Band (mM Alexafluor)	CT Band migration (mm)	LHS Rf	RHS Rf	AVG Rf	avg log MW (from graph)	avg MW (Da)	MW of Bound Probes (Da)	~ # of Probe Molecules Bound	~ # of Probe Molecules Bound (Normalized to Prequenched)
preq	28.5	0.53	0.52	0.52	4.68	48194.78	5694.78	9.38	0.00
0.2	29	0.54	0.53	0.53	4.68	47315.13	4815.13	7.93	-1.45
0.6	28.5	0.53	0.52	0.52	4.68	48194.78	5694.78	9.38	0.00
0.9	29	0.54	0.53	0.53	4.68	47315.13	4815.13	7.93	-1.45
1.2	28	0.52	0.51	0.51	4.69	49158.66	6658.66	10.97	1.59
2.4	26.5	0.49	0.48	0.49	4.70	50118.72	7618.72	12.55	3.17

300 uM PG

gel length (migration distance) LHS = 53 mm, RHS = 54 mm, AVG = 53.5 mm

MW STD (Da)	log of MW STD	L - ladder migration (mm)	L - ladder Rf	R - ladder migration (mm)	R - ladder Rf	avg ladder migration	avg ladder Rf
200000	5.30	3.00	0.06	3.00	0.05	3.00	0.06
116250	5.07	8.00	0.15	8.00	0.15	8.00	0.15
97400	4.99	10.50	0.19	10.50	0.19	10.50	0.19
66200	4.82	17.50	0.32	17.50	0.32	17.50	0.32
45000	4.65	32.00	0.59	31.00	0.56	31.50	0.58
31000	4.49	49.00	0.91	47.50	0.86	48.25	0.89

CT Band (mM Alexafluor)	CT Band migration (mm)	LHS Rf	RHS Rf	AVG Rf	avg log MW (from graph)	avg MW (Da)	MW of Bound Probes (Da)	~ # of Probe Molecules Bound	~ # of Probe Molecules Bound (Normalized to Prequenched)
preq	30.00	0.56	0.55	0.55	4.67	46773.51	4273.51	7.04	0.00
0.2	30.50	0.56	0.55	0.56	4.66	45972.70	3472.70	5.72	-1.32
0.6	30.75	0.57	0.56	0.56	4.66	45708.82	3208.82	5.29	-1.75
0.9	30.00	0.56	0.55	0.55	4.67	46773.51	4273.51	7.04	0.00
1.2	29.75	0.55	0.54	0.55	4.68	47315.13	4815.13	7.93	0.89
2.4	27.50	0.51	0.50	0.50	4.70	49831.05	7331.05	12.08	5.04

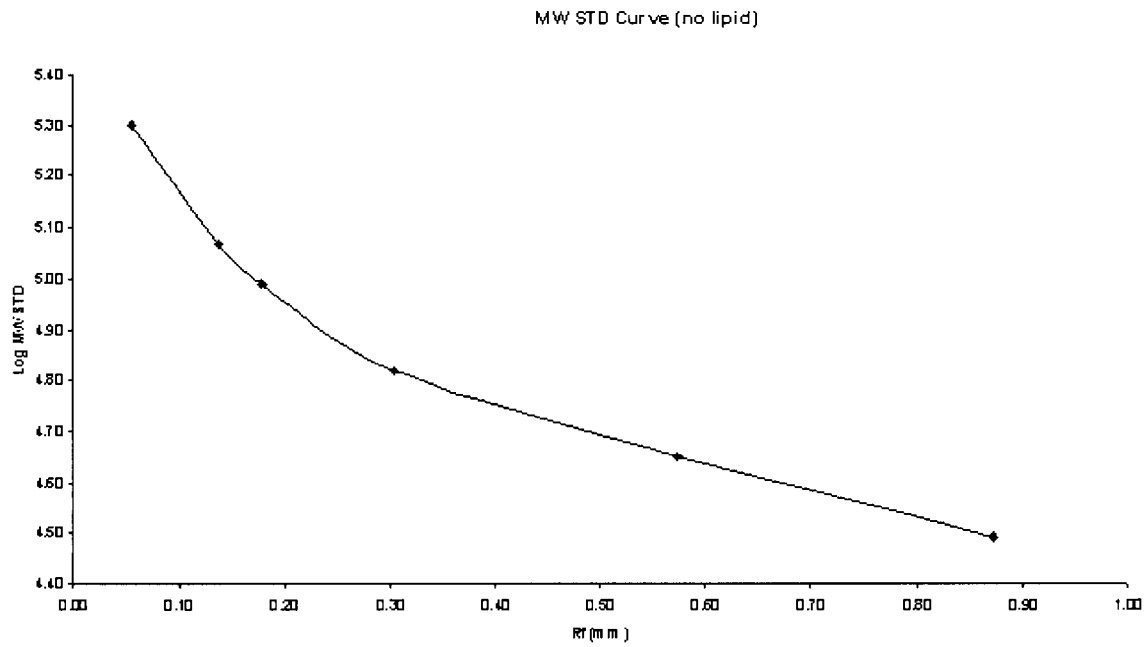

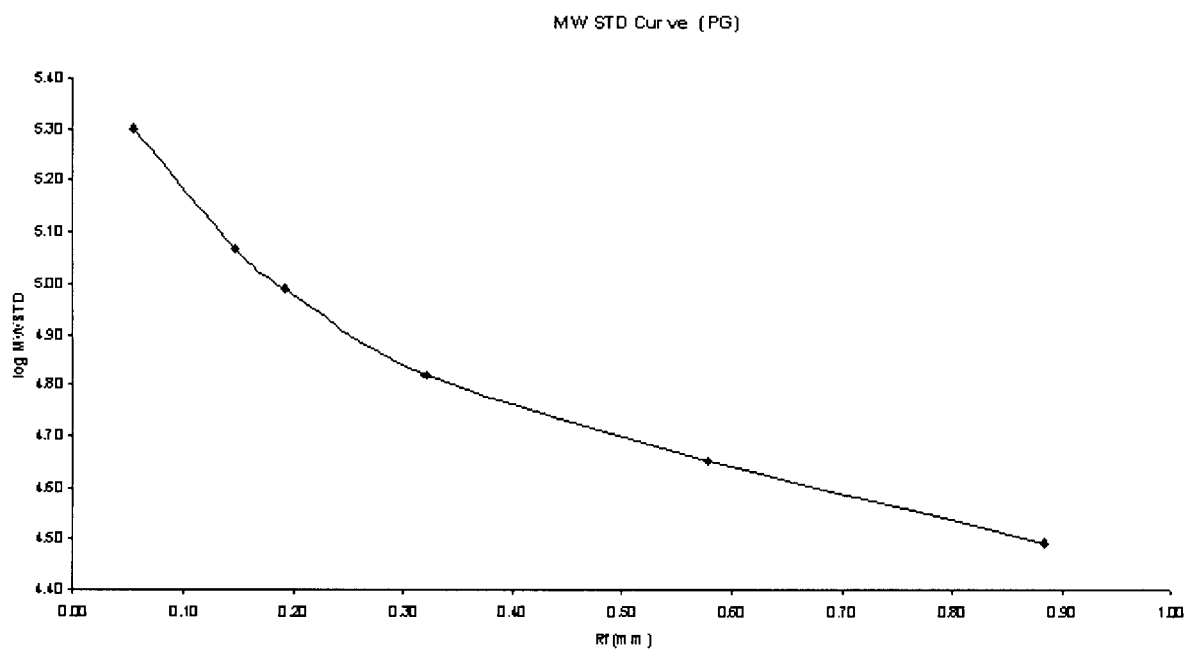

Figure C 3 Standard Curve For The Migration Of Molecular Weight Standards

REFERENCE LIST

1. Vance, D. E. Phosphatidylcoline metabolism: masochistic enzymology, metabolic regulation and lipoprotein assembly. *Biochem Cell Biol* **68**, 1151-1165 (1990).

2. Cui, Z. et al. A Genetic Defect in Phosphatidylcholine Biosynthesis Triggers Apoptosis in Chinese Hamster Ovary Cells. *J Biol Chem* **271**, 14668-14671 (1996).

3. Pelech, S. L. & Vance, D. E. Signal transduction via phosphatidylcholine cycles. *Trends Biochem Sci* **14**, 28-30 (1989).

4. Exton, J. Phosphatidylcholine breakdown and signal transduction. *Biochim Biophys Acta* **1212**, 26-42 (1994).

5. Kennedy, E. P. & Weiss, S. B. Function of Cytidine Coenzymes in the Biosynthesis of Phospholipids. *J Biol Chem* **222**, 193-215 (1956).

6. Ridgway, N. D. (ed. Vance, D. E.) 121-142 (CRC Press, Boca Raton, Florida, 1989).

7. George, T. P. et al. Phosphatidylcholine biosynthesis in cultured glioma cells: evidence for channelling of intermediates. *Biochim Biophys Acta* **1004**, 283-291 (1989).

8. Cornell, R. B. & Northwood, I. C. Regulation of CTP:phosphocholine cytidylyltransferase by amphitropism and relocalization. *Trends Biochem Sci* **25**, 441-7 (2000).

9. Kent, C. CTP:phosphocholine cytidylyltransferase. *Biochim Biophys Acta* **1348**, 79-90 (1997).

10. Weinhold, P. A., Rounsifer, M. E. & Feldman, D. A. The Purification and Characterization of CTP:Phosphorylcholine Cytidylyltransferase from Rat Liver. *J Biol Chem* **261**, 5104-5110 (1986).

11. Tsukagoshi, Y., Nikawa, J. & Yamashita, S. Molecular cloning and characterization of the gene encoding cholinephosphate cytidylyltransferase in *Saccharomyces cerevisiae*. *Eur J Biochem* **169**, 477-486 (1987).

12. Kalmar, G. B., Kay, R. J., Lachance, A., Aebersold, R. & Cornell, R. B. Cloning and expression of rat liver CTP: phosphocholine cytidylyltransferase: an amphipathic protein that controls

phosphatidylcholine synthesis. *Proc Natl Acad Sci U S A* **87**, 6029-33 (1990).

13. Kalmar, G. B., Kay, R. J., LaChance, A. C. & Cornell, R. B. Primary structure and expression of a human CTP:phosphocholine cytidylyltransferase. *Biochim Biophys Acta* **1219**, 328-34 (1994).

14. Rutherford, M. S. et al. The Gene for Murine CTP:Phosphocholine Cytidylyltransferase (*ctpct*) is Located on Mouse Chromosome 16. *Genomics* **18**, 698-701 (1993).

15. Sweitzer, T. D. & Kent, C. Expression of wild-type and mutant rat liver CTP: phosphocholine cytidylyltransferase in a cytidylyltransferase-deficient Chinese hamster ovary cell line. *Arch Biochem Biophys* **311**, 107-16 (1994).

16. Choi, S., Lee, K. & Cho, S. Cloning of CTP:Phosphocholine Cytidylyltransferase cDNA from *Arabidopsis thaliana*. *Mol Cells* **7**, 58-63 (1996).

17. Nishida, O., Swinhoe, R., Slabas, A. R. & Murata, N. Cloning of *Brassica napus* CTP:phosphocholine cytidylyltransferase cDNAs by complementation in a yeast *cct* mutant. *plant Mol. Biol.* **31**, 205-211 (1996).

18. Helmink, B. A. & Friesen, J. A. Characterization of a lipid activated CTP:phosphocholine cytidylyltransferase from *Drosophila melanogaster*. *Biochim Biophys Acta* **1683**, 78-88 (2004).

19. Wilson, R. et al. 2.2 Mm of contiguous nucleotide sequence from chromosome III of *C. elegans*. *Nature* **368**, 32-38 (1994).

20. Friesen, J. A., Liu, M. F. & Kent, C. Cloning and characterization of a lipid-activated CTP:phosphocholine cytidylyltransferase from Caenorhabditis elegans: identification of a 21-residue segment critical for lipid activation. *Biochim Biophys Acta* **1533**, 86-98 (2001).

21. Karim, M., Jackson, P. & Jackowski, S. Gene structure, expression and identification of a new CTP:phosphocholine cytidylyltransferase beta isoform. *Biochim Biophys Acta* **1633**, 1-12 (2003).

22. Lykidis, A., Murti, K. G. & Jackowski, S. Cloning and characterization of a second human CTP:phosphocholine cytidylyltransferase. *J Biol Chem* **273**, 14022-9 (1998).

23. Lykidis, A., Baburina, I. & Jackowski, S. Distribution of CTP:phosphocholine cytidylyltransferase (CCT) isoforms. Identification of a new CCT beta splice variant. *J Biol Chem* **274**, 26992-7001 (1999).

24. Wang, Y., MacDonald, J. I. & Kent, C. Identification of the nuclear localization signal of rat liver CTP:phosphocholine cytidylyltransferase. *J Biol Chem* **270**, 354-60 (1995).

25. Bogan, M. J., Agnes, G. R., Pio, F. F. & Cornell, R. B. Inter-domain and membrane interactions of CTP: Phosphocholine cytidylyltransferase revealed via limited proteolysis and mass spectrometry. *J Biol Chem* **280**, 19613-19624 (2005).

26. Taneva, S., Johnson, J. E. & Cornell, R. B. Lipid-induced conformational switch in the membrane binding domain of CTP:phosphocholine cytidylyltransferase: a circular dichroism study. *Biochemistry* **42**, 11768-76 (2003).

27. Yeo, H.-J., Sri Widada, J., Mercereau-Puijalon, O. & Vial, H. J. Molecular cloning of CTP:phosphocholine cytidylyltransferase from *Plasmodium falciparum*. *Eur J Biochem* **233**, 62-72 (1995).

28. Park, Y. S., Sweitzer, T. D., Dixon, J. E. & Kent, C. Expression, purification, and characterization of CTP:glycerol-3-phosphate cytidylyltransferase from Bacillus subtilis. *J Biol Chem* **268**, 16648-54 (1993).

29. Veitch, D. P. & Cornell, R. B. Substitution of serine for glycine-91 in the HXGH motif of CTP:phosphocholine cytidylyltransferase implicates this motif in CTP binding. *Biochemistry* **35**, 10743-50 (1996).

30. Veitch, D. P., Gilham, D. & Cornell, R. B. The role of histidine residues in the HXGH site of CTP:phosphocholine cytidylyltransferase in CTP binding and catalysis. *Eur J Biochem* **255**, 227-34 (1998).

31. Park, Y. S. et al. Identification of functional conserved residues of CTP:glycerol-3-phosphate cytidylyltransferase. Role of histidines in the conserved HXGH in catalysis. *J Biol Chem* **272**, 15161-6 (1997).

32. Weber, C. H., Park, Y. S., Sanker, S., Kent, C. & Ludwig, M. L. A prototypical cytidylyltransferase: CTP:glycerol-3-phosphate cytidylyltransferase from bacillus subtilis. *Structure Fold Des* **7**, 1113-24 (1999).

33. Helmink, B. A., Braker, J. D., Kent, C. & Friesen, J. A. Identification of lysine 122 and arginine 196 as important functional residues of rat CTP:phosphocholine cytidylyltransferase alpha. *Biochemistry* **42**, 5043-51 (2003).

34. Dunne, S. J., Cornell, R. B., Johnson, J. E., Glover, N. R. & Tracey, A. S. Structure of the membrane binding domain of CTP:phosphocholine cytidylyltransferase. *Biochemistry* **35**, 11975-84 (1996).

35. Johnson, J. E., Aebersold, R. & Cornell, R. B. An amphipathic alpha-helix is the principle membrane-embedded region of CTP:phosphocholine cytidylyltransferase. Identification of the 3-(trifluoromethyl)-3-(m-[125I]iodophenyl) diazirine photolabeled domain. *Biochim Biophys Acta* **1324**, 273-84 (1997).

36. Craig, L., Johnson, J. E. & Cornell, R. B. Identification of the membrane-binding domain of rat liver CTP:phosphocholine cytidylyltransferase using chymotrypsin proteolysis. *J Biol Chem* **269**, 3311-7 (1994).

37. Yang, W., Boggs, K. P. & Jackowski, S. The association of lipid activators with the amphipathic helical domain of CTP:phosphocholine cytidylyltransferase accelerates catalysis by increasing the affinity of the enzyme for CTP. *J Biol Chem* **270**, 23951-7 (1995).

38. Wang, Y. & Kent, C. Identification of an inhibitory domain of CTP:phosphocholine cytidylyltransferase. *J Biol Chem* **270**, 18948-52 (1995).

39. Cornell, R. B. et al. Functions of the C-terminal domain of CTP: phosphocholine cytidylyltransferase. Effects of C-terminal deletions on enzyme activity, intracellular localization and phosphorylation potential. *Biochem J* **310 (Pt 2)**, 699-708 (1995).

40. Johnson, J. E. & Cornell, R. B. Membrane-binding amphipathic alpha-helical peptide derived from CTP:phosphocholine cytidylyltransferase. *Biochemistry* **33**, 4327-35 (1994).

41. Watkins, J. D. & Kent, C. Phosphorylation of CTP:phosphocholine cytidylyltransferase in vivo. Lack of effect of phorbol ester treatment in HeLa cells. *J Biol Chem* **265**, 2190-7 (1990).

42. Wieprecht, M., Wieder, T., Paul, C., Geilin, C. C. & Orfanos, C. E. Evidence for Phosphorylation of CTP:Phosphocholine Cytidylyltransferase by Multiple Proline-directed Protein Kinases. *J Biol Chem* **271**, 9955-9961 (1996).

43. Arnold, R. S., DePaoli-Roach, A. A. & Cornell, R. B. Binding of CTP:phosphocholine cytidylyltransferase to lipid vesicles: diacylglycerol and enzyme dephosphorylation increase the affinity for negatively charged membranes. *Biochemistry* **36**, 6149-56 (1997).

44. Weinhold, P. A., Rounsifer, M. E., Charles, L. & Feldman, D. A. Characterization of cytosolic forms of CTP:choline-phosphate cytidylyltransferase in lung, isolated alveolar type II cells, A549 cell and Hep G2 cells. *Biochim Biophys Acta* **1006**, 299-310 (1989).

45. Cornell, R. B. Chemical Cross-linking Reveals a Dimeric Structure for CTP:Phosphocholine Cytidylyltransferase. *J Biol Chem* **264**, 9077-9082 (1989).

46. Xie, M., Smith, J. L., Ding, Z., Zhang, D. & Cornell, R. B. Membrane binding modulates the quaternary structure of CTP:phosphocholine cytidylyltransferase. *J Biol Chem* **279**, 28817-25 (2004).

47. Bakovic, M., Waite, K. & Vance, D. E. Oncogenic Ha-Ras transformation modulates the transcription of the CTP:phosphocholine cytidylyltransferase alpha gene via p42/44MAPK and transcription factor Sp3. *J Biol Chem* **278**, 14753-14761 (2003).

48. Banchio, C., Schang, L. M. & Vance, D. E. Phosphorylation of Sp1 by cyclin-dependant kinase 2 modulates the role of Sp1 in CTP:phosphocholine cytidylyltransferase alpha regulation during the S phase of the cell cycle. *J Biol Chem* **279**, 40220-40226 (2004).

49. Sugimoto, H. et al. Sp1 is a co-activator with Ets-1, and Net is an important repressor of the transcription of CTP:Phosphocholine cytidylyltransferase alpha. *J Biol Chem* **e-print ahead of publication** (2005).

50. Watkins, J. D. & Kent, C. Immunolocalization of membrane-associated CTP:phosphocholine cytidylyltransferase in phosphatidylcholine-deficient Chinese hamster ovary cells. *J Biol Chem* **267**, 5686-92 (1992).

51. Northwood, I. C., Tong, A. H., Crawford, B., Drobnies, A. E. & Cornell, R. B. Shuttling of CTP:Phosphocholine cytidylyltransferase between the nucleus and endoplasmic reticulum accompanies the wave of phosphatidylcholine synthesis during the G(0) --> G(1) transition. *J Biol Chem* **274**, 26240-8 (1999).

52. Lagace, T. A. & Ridgway, N. D. The rate-limiting enzyme in phosphatidylcholine synthesis regulates proliferation of the nucleoplasmic reticulum. *Mol Biol Cell* **16**, 1120-1130 (2005).

53. Henneberry, A. L., Wright, M. M. & McMaster, C. R. The major sites of cellular phospholipid synthesis and molecular determinants of fatty acid and head group specificity. *Mol Biol Cell* **13**, 3148-3161 (2002).

54. Arnold, R. S. & Cornell, R. B. Lipid regulation of CTP: phosphocholine cytidylyltransferase: electrostatic, hydrophobic, and synergistic interactions of anionic phospholipids and diacylglycerol. *Biochemistry* **35**, 9917-24 (1996).

55. Cornell, R. B. How cytidylyltransferase uses an amphipathic helix to sense membrane phospholipid composition. *Biochem Soc Trans* **26**, 539-44 (1998).

56. Cornell, R. B. Regulation of CTP:phosphocholine cytidylyltransferase by lipids. 1. Negative surface charge dependence for activation. *Biochemistry* **30**, 5873-80 (1991).

57. Drobnies, A. E., van Der Ende, B., Thewalt, J. L. & Cornell, R. B. CTP:phosphocholine cytidylyltransferase activation by oxidized phosphatidylcholines correlates with a decrease in lipid order: a 2H NMR analysis. *Biochemistry* **38**, 15606-15614 (1999).

58. Johnson, J. E., Rao, N. M., Hui, S. W. & Cornell, R. B. Conformation and lipid binding properties of four peptides derived from the membrane-binding domain of CTP:phosphocholine cytidylyltransferase. *Biochemistry* **37**, 9509-19 (1998).

59. Houweling, M., Jamil, H., Hatch, G. M. & Vance, D. E. Dephosphorylation of CTP:Phosphocholine Cytidylyltransferase is not Required for Binding to Membranes. *J Biol Chem* **269**, 7544-7551 (1994).

60. Hatch, G. M., Jamil, H., Utal, A. K. & Vance, D. E. On the Mechanism of the Okadaic Acid-induced Inhibition of Phosphatidylcholine Biosynthesis in Isolated Rat Hepatocytes. *J Biol Chem* **267**, 15751-15758 (1992).

61. Wang, Y. & Kent, C. Effects of altered phosphorylation sites on the properties of CTP:phosphocholine cytidylyltransferase. *J Biol Chem* **270**, 17843-9 (1995).

62. Yang, W. & Jackowski, S. Lipid activation of CTP:phosphocholine cytidylyltransferase is regulated by the phosphorylated carboxyl-terminal domain. *J Biol Chem* **270**, 16503-6 (1995).

63. Agassandian, M. et al. Oxysterols Inhibit Phosphatidylcholine Synthesis via ERK Docking and Phosphorylation of CTP:Phosphocholine Cytidylyltransferase. *J Biol Chem* **280**, 21577-21587 (2005).

64. Habeeb, A. F. S. A. & Hiramoto, R. Reaction of proteins with glutaraldehyde. *Arch Biochem Biophys* **126**, 16-26 (1967).

65. Kay, R. & Humphries, R. K. New Vectors and Procedures for Isolating cDNAs Encoding Cell Surface Proteins by Expression Cloning in COS Cells. *Methods in Molecular and Cellular Biology* **2**, 254-265 (1991).

66. Gluzman, Y. SV40-Transformed Simian Cells Support the Replication of Early SV40 Mutants. *Cell* **23**, 175-182 (1981).

67. Friesen, J. A., Campbell, H. A. & Kent, C. Enzymatic and cellular characterization of a catalytic fragment of CTP:phosphocholine cytidylyltransferase alpha. *J Biol Chem* **274**, 13384-9 (1999).

68. Bradford, M. A rapid and sensitive method for the quantitation of microgram quantities of protein utilizing the principle of protein-dye binding. *Anal Biochem* **72**, 248-253 (1976).

69. Laemmli, U. K. Cleavage of Structural Proteins during the Assembly of the Head of BacteriophageT4. *Nature* **227**, 680-685 (1970).

70. Ding, Z. in *Institute of Molecular Biology and Biochemistry* 91 (Simon Fraser University, Burnaby, BC, 1999).

71. Zhang, D. in *Institute of Molecular Biology and Biochemistry* (Simon Fraser University, Burnaby, 1997).

72. Taneva, S., Patty, P. J., Frisken, B. J. & Cornell, R. B. CTP:phosphocholine cytidylyltransferase binds anionic vesicles in a cross-bridging mode. *Biochemistry* **44**, 9382-9393 (2005).

73. Murray, D., Ben-Tal, N., Honig, B. & McLaughlin, S. Electrostatic interaction of myristoylated proteins with membranes: simple physics, complicated biology. *Structure* **5**, 985-9 (1997).

74. Stafford, R. E., Fanni, T. & Dennis, E. A. Interfacial properties and critical micelle concentration of lysophospholipids. *Biochemistry* **28**, 5113-5120 (1989).

75. Saunders, L. Molecular aggregation in aqueous dispersions of phosphatidyl and lysophosphatidyl cholines. *Biochim Biophys Acta* **125**, 70-74 (1966).

76. Lad, M. D., Ledger, V. M., Briggs, B., Green, R. J. & Frazier, R. A. Analysis of the SDS-Lysozyme Binding Isotherm. *Langmuir* **19**, 5098-5103 (2003).

77. Bhairi, S. M. *Detergents: A guide to the properties and uses of detergents in biological systems* (Calbiochem-Novabiochem Corporation, 2001).